
# ACCESS 2012

The Third International Conference on Access Networks

ISBN: 978-1-61208-205-9

June 24-29, 2012

Venice, Italy

**ACCESS 2012 Editors**

Alessandro Bogliolo, Università di Urbino, Italy

Abdulrahman Yarali, Murray State University, USA

# ACCESS 2012

# Foreword

The Third International Conference on Access Networks [ACCESS 2012], held between June 24-29, 2012 - Venice, Italy, continued a series of conferences dealing with access networks, services and technologies based on the previous NEUTRAL and HOWAN workshop treating particular access aspects. ACCESS 2012 aimed to provide an international forum by researchers, students, and professionals to present recent research results on advances in networking access, including the newest emerging access technologies, broadband access, wireless access, copper access, optical access, mobility aspects, as well as optical/wireless combination and neutrality.

Hybrid Optical and Wireless Access Networks (HOWANs) consist of a multi-hop wireless mesh network (WMN) at the front-end and an optical access network, e.g., a passive optical network (PON) at the back-end. PONs use inexpensive and passive optical splitters to divide a single fiber into separate strands feeding individual subscribers. EPON is based on the Ethernet standard, which comes with the added benefit of the economies-of-scale of Ethernet, and provides simple and easy-to-manage connectivity both at the customer premises and at the central office.

Granting positive externalities to the shared access infrastructure in order to enhance digital inclusion and broadband penetration by triggering a positive feedback loop among users, service providers, network operators, and investors is an option. The access infrastructure can be considered as a network per see, called "neutral access network" (NAN), which provides internal services and possibly exploits its territorial dimension in order to overcome the dichotomy between "on-line" and "off-line" people. While in a traditional access network, people who are not registered with any ISP are left out from the so called "information society", NANs can provide an intermediate area, which is logically placed "before the Internet", where on-line services and applications can be made available to residential and nomadic users who are not yet registered with any ISP.

We take here the opportunity to warmly thank all the members of the ACCESS 2012 Technical Program Committee, as well as the numerous reviewers. The creation of such a high quality conference program would not have been possible without their involvement. We also kindly thank all the authors who dedicated much of their time and efforts to contribute to ACCESS 2012. We truly believe that, thanks to all these efforts, the final conference program consisted of top quality contributions.

Also, this event could not have been a reality without the support of many individuals, organizations, and sponsors. We are grateful to the members of the ACCESS 2012 organizing committee for their help in handling the logistics and for their work to make this professional meeting a success.

We hope that ACCESS 2012 was a successful international forum for the exchange of ideas and results between academia and industry and for the promotion of progress in networking access.

We are convinced that the participants found the event useful and communications very open. We also hope the attendees enjoyed the charm of Venice, Italy.

**ACCESS 2012 Chairs:**

Alessandro Bogliolo, Università di Urbino, Italy
Mark Perry, University of Western Ontario/Faculty of Law/ Faculty of Science - London, Canada
Abdulrahman Yarali, Murray State University, USA
Manuel Villen-Altamirano, Technical University of Madrid, Spain
Mark Perry, University of Western Ontario/Faculty of Law/ Faculty of Science - London, Canada
Ljiljana Trajkovic, Simon Fraser University - Burnaby, Canada

# ACCESS 2012

# Committee

**ACCESS Advisory Committee**

Alessandro Bogliolo, Università di Urbino, Italy
Mark Perry, University of Western Ontario/Faculty of Law/ Faculty of Science - London, Canada
Abdulrahman Yarali, Murray State University, USA
Manuel Villen-Altamirano, Technical University of Madrid, Spain

**ACCESS Special Area Chairs**

**Technical/Legal**
Mark Perry, University of Western Ontario/Faculty of Law/ Faculty of Science - London, Canada

**Wireless**
Ljiljana Trajkovic, Simon Fraser University - Burnaby, Canada

**ACCESS 2012 Technical Program Committee**

Hojjat Adeli, The Ohio State University, USA
Konstantin Avratchenkov, INRIA, France
Michael Bahr, Siemens AG - Munich, Germany
Andrzej Beben, Warsaw University of Technology, Poland
Alessandro Bogliolo, Università di Urbino, Italy
Fernando Boronat Seguí, Polytechnic University of Valencia - Gandia, Spain
Alejandro Cordero, Amaranto Consultores, Spain
Istvan Frigyes, Budapest University of Technology and Economics, Hungary
Emiliano Garcia-Palacios, Queens University - Belfast, UK
Vanessa Gardellin, University of Pisa, Italy
Tauseef Jamal, Universidade Lusofona de Humanidades e Tecnologias (ULHT) - Lisbon, Portugal
Georgios Karagiannis, University of Twente, The Netherland
Deepak Kataria, IPJunction Inc. - Bridgewater, USA
George Korinthios, COSMOTE - Mobile Telecommunications S.A. - Athens, Greece
Trung-Thanh Le, Hanoi University of Natural Resources and Environment, Vietnam
Gyu Myoung Lee, Institut Telecom / Telecom SudParis, France
Yunxin (Jeff) Li, IP Australia, Australia
Enjie Liu, University of Bedfordshire, UK
Olaf Maennel, Loughborough University, UK
Zoubir Mammeri, IRIT - Paul Sabatier University - Toulouse, France
Elsa María Macías López, University of Las Palmas de Gran Canaria, Spain
Jon Matias, University of the Basque Country (UPV/EHU), Spain
Jogesh K. Muppalla, The Hong Kong University of Science and Technology, Hong Kong
Armando Nolasco Pinto, Instituto de Telecomunicações / Universidade de Aveiro, Portugal

George Oikonomou, University of Bristol, UK
Mark Perry, University of Western Ontario/Faculty of Law/ Faculty of Science - London, Canada
Serena Elisa Ponta, SAP Lab - Mougins, France
Zsolt Saffer, Budapest University of Technology and Economics (BUTE) - Hungary
Bruno Sericola, INRIA, France
Dimitrios Serpanos, ISI / University of Patras, Greece
Xu Shao, Institute for Infocomm Research, Singapore
Eduardo James Pereira Souto, UFAM, Brazil
Álvaro Suárez Sarmiento, University of Las Palmas de Gran Canaria, Spain
Ljiljana Trajkovic, Simon Fraser University - Burnaby, Canada
Rob van der Mei, CWI - Amsterdam, The Netherlands
Dario Vieira, EFREI, France
Manuel Villen-Altamirano, Technical University of Madrid, Spain
Zuqing Zhu, University of Science and Technology of China, China

**Copyright Information**

For your reference, this is the text governing the copyright release for material published by IARIA.

The copyright release is a transfer of publication rights, which allows IARIA and its partners to drive the dissemination of the published material. This allows IARIA to give articles increased visibility via distribution, inclusion in libraries, and arrangements for submission to indexes.

I, the undersigned, declare that the article is original, and that I represent the authors of this article in the copyright release matters. If this work has been done as work-for-hire, I have obtained all necessary clearances to execute a copyright release. I hereby irrevocably transfer exclusive copyright for this material to IARIA. I give IARIA permission or reproduce the work in any media format such as, but not limited to, print, digital, or electronic. I give IARIA permission to distribute the materials without restriction to any institutions or individuals. I give IARIA permission to submit the work for inclusion in article repositories as IARIA sees fit.

I, the undersigned, declare that to the best of my knowledge, the article is does not contain libelous or otherwise unlawful contents or invading the right of privacy or infringing on a proprietary right.

Following the copyright release, any circulated version of the article must bear the copyright notice and any header and footer information that IARIA applies to the published article.

IARIA grants royalty-free permission to the authors to disseminate the work, under the above provisions, for any academic, commercial, or industrial use. IARIA grants royalty-free permission to any individuals or institutions to make the article available electronically, online, or in print.

IARIA acknowledges that rights to any algorithm, process, procedure, apparatus, or articles of manufacture remain with the authors and their employers.

I, the undersigned, understand that IARIA will not be liable, in contract, tort (including, without limitation, negligence), pre-contract or other representations (other than fraudulent misrepresentations) or otherwise in connection with the publication of my work.

Exception to the above is made for work-for-hire performed while employed by the government. In that case, copyright to the material remains with the said government. The rightful owners (authors and government entity) grant unlimited and unrestricted permission to IARIA, IARIA's contractors, and IARIA's partners to further distribute the work.

**Table of Contents**

# Radio-over-Fibre Transmission of Multiple Wireless Standards for Digital Cities: Exploiting the New Tramway Infrastructure

Rabiaa Guemri, Hexin Liu, Irina Jäger, Daniel Bourreau, Camilla Kärnfelt and Frédéric Lucarz
Telecom Bretagne, Brest, France
Email: {rabiaa.guemri, hexin.liu, daniel.bourreau, camilla.karnfelt, Frederic.lucarz}@telecom-bretagne.eu,
ira_jaeger@yahoo.de

*Abstract* — **The present paper aims at the specific application of Radio-over-Fibre to provide dedicated Wi-Fi access to tramway passengers. The challenge here is to provide wireless services in densely populated city areas based on a real-case scenario targeting public transport. The proposed system targets 2.4 GHz Wi-Fi access at 1 Mbps per user inside a tram, with a wireless bridge at 5 GHz along the track. A chosen design will finally be implemented and evaluated in terms of WiFi coverage, BER and power consumption. Lessons learned will be interpolated for 60 GHz RoF for Wi-Fi access. Replacing the 5-GHz track site solution by a 60 GHz wireless link will bring a significant increase in data throughput (>1 Gbps). We report here performances of running experiments on 2.4 and 5 GHz RoF systems and results on photonic 60 GHz generation for existing fibre backbone between the stations.**

***Keywords - radio-over-fibre applications; multiple standards; running experiments.***

## I. INTRODUCTION

There is a growing demand for high-speed wireless access by the end users while they are on the move using trains, buses, planes, ships, etc [1-3]. Yet, train operators offer limited radiofrequency-based wireless network solutions to passengers on their intercity high-speed trains. Such solutions are mainly based on mobile (UMTS, LTE-4G) and/or satellite communications but are limited in terms of bandwidth, resulting in slow access even under the best conditions. One attractive way to overcome these limitations is to employ Radio-over-Fibre (RoF) transmissions to transport data-carrying radio-frequency (RF) signals optically to/from a set of wireless access points distributed along the track. Ongoing project CapilRTram (2011-2012) aims at developing a fibre-supported wireless system to provide high speed and seamless Wi-Fi connectivity along the new tramway line (under deployment) in Brest (France). One key advantage is that all stations are interconnected by an optical distribution network.

Section II of this paper presents the general system architecture of the Tram infrastructure. As will be shown, this system deals with different frequencies: Section III deals with the frequency 2,4 GHz to provide Wi-Fi for the passengers waiting in the tram station. In section IV, we focus on the frequency of 5 GHz to provide Wi-Fi connectivity between the Tram station and passengers inside the tram. Finally, Section V deals with the mm wave generation as 60 GHz band is an alternative to the 5 GHz link discussed in Section IV.

## II. OVERALL SYSTEM ARCHITECTURE


Figure 1. General system architecture

As depicted in Fig. 1, the proposed system comprises, at each station, an optical node (5) including a bidirectional optoelectronic transceiver (O/E; E/O) adapted to convert RF signals into the optical domain and vice-versa. This transceiver is coupled to a first wireless module (3) which is adapted to communicate with at least one RF transceiver (1; 2) installed on top of each tramway carriage, thereby forming a high-speed wireless bridge between the tram and the stations. For that purpose, the antennas are selected and positioned to ensure continuous link availability between the station and the tram. A second wireless module (4) coupled to the optical node (5) provides wireless coverage to passengers waiting on the station platform. The first and second modules (3; 4) may be combined in a single module. The proposed system is Wi-Fi compliant (IEEE 802.11 a/g/b) and adapted to operate simultaneously on two distinct RF bands (i.e. 2.4 GHz and 5 or 60 GHz). Microwave links (e.g. 5 GHz) or millimetre-wave links (e.g. 60 GHz) will be deployed using commercially available equipment all along the tramway line to connect tram carriages to stations. Inside the tram, Wi-Fi coverage is provided at the conventional 2.4 GHz band by a commercially available wireless access point (1). Wi-Fi access points (4) at 2.4 GHz

 ISBN: 978-1-61208-205-9 

will also be provided to passengers on the station platform. The proposed solution is a flexible (easily upgradeable) and low-cost for a dedicated wireless access with high speed connections based on mature technology (IEEE 802.11a, 54 Mbps for 5 GHz). Thanks to its fibre base, it is transparent to wireless protocols and future-proof. There will be no need to replace the whole infrastructure in case higher throughputs are needed or other frequency bands need to be used. Replacing the 5-GHz link by a 60 GHz wireless link will bring a significant increase in data throughput [4] using existing standards at 57-66 GHz (ECMA-387, IEEE 802.15.3c or IEEE 802.11ad).

## III. BI-DIRECTIONAL ROF/ DAS LINK AT 2.4 GHZ (IEEE 802.11B/G)

Radio-over-fibre techniques used to interconnect optically wireless access points over Distributed Antenna Systems (DAS) could provide sustainable solutions for delivering high data rates to mobile end-users in public transport. In RoF systems, both the carrier and the data signals are transmitted from a central office via an optical fibre feed network to the remote antenna units from where they are distributed to the mobile end-users via wireless links. With RoF DAS, the transmitted signals can be easily shared amongst a large set of cells to provide improved coverage with reduced power levels. DAS was shown to be a flexible, bandwidth-efficient and cost-effective option for fibre-radio access infrastructure [5-6]. The use of RoF in moving vehicles is a novel application of RoF and more particularly for trains.

A Wi-Fi DAS demonstrator adapted to operate at 2.4 GHz will provide wireless coverage for mobile users, waiting for the tramway on the station platform. With reference to the overall system architecture illustrated in Fig. 1, the optical node at each station is connected to the optical distribution network by means of silica single-mode fibres (SMF) that transport the data-carrying RF signals on an optical carrier up to the individual roadside antenna units. As depicted in Fig. 2, the proposed DAS demonstrator comprises a conventional wireless router adapted to distribute Wi-Fi signals (IEEE 802.11b/g) to a set of four wideband omni-directional antennas, through a wired infrastructure based on fibre and coaxial cable. A circulator is used at each end of the loop to isolate the signals on the uplink and on the downlink. The circulators with an isolation of 23 dB could be replaced by switches showing an isolation level of 30-40 dB. An optical transmission link was introduced between the router and the antennas by means of two bidirectional RoF transceivers (E/O; O/E) with an output optical power of - 4.56 dBm and connected to each other by a 500-m single-mode fibre span. This length of fibre corresponds to the average distance between two adjacent stations in Brest.

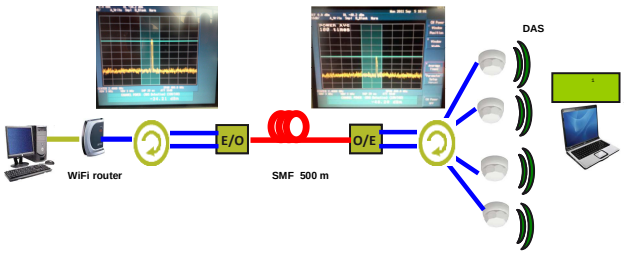


Figure 2. Bi-directional RoF-DAS demonstrator based on commercially-available components (Buffalo Wi-Fi router Model WHR-HP-G54) at 2.4 GHz; 2 RF Circulators; 2 FiberSpan bidirectional Transceivers (O/E; E/O) for 2.4 - 2.5 GHz with 1.5µm and 1.3µm optical sources; 1 Power supply for the two FiberSpan modules (HAMEG HM8040-3 (12V) – not shown here; 500m SMF (Corning); 4 Omni-directional Antennas 2.4/5 GHz (Hyperlink HG2458CU)

Power measurements (see Fig. 2) showed an attenuation of 18 dB between the RF output of the router and the output of the 2nd circulator. The optical link composed of the two RoF transceivers and the optical fibre span was characterised in terms of gain (-25 dB), non-linearity (Input Interception Point Order 3: 0 dBm <IIP3< 25 dBm), noise performance (Noise Figure: 50 dB <NF<55 dB) and frequency response (bandwidth: 2.4 GHz). Due to the low optical IIP3 and high NF of the optical link, the dynamic range (DR) of the RF signals must be reduced in order to meet the SNR requirements (minimum level of output signal power > noise + SNR) and to avoid the nonlinearities (maximum level of output signal power < OIP3 – 20 dB). DR is an important parameter for mobile cellular communications because the power received by the antenna from the endpoint varies widely (e.g. DR = 52 dB: -82 dBm to -30 dBm for WLAN 802.11g,). Automatic Gain Control techniques can be used to adapt the RoF system to various signal levels as described in the Wi-Fi standard.

The system performance has been assessed through bi-directional transmission of High Definition (HD) videos between two computers as shown in Fig. 2. Free software VLC 1.1.9 was used in broadcast mode to transmit 1360x768 HD video signals with an average data rate of 17.66 Mbps and maximum possible 20 Mbps.

## IV. ROF LINK AT 5 GHZ (IEEE 802.11A/N)

According to the proposed system architecture, tram stations are interconnected by an optical distribution network and each station is connected to the tram by a 5 GHz Wi-Fi link.
For demonstration purposes, we tested the architecture as shown in Fig. 3 towards the 60 GHz RoF approach. This approach becomes essential to provide high data rates >10Gbps with high available bandwidth (7 GHz) to the end-user.

 ISBN: 978-1-61208-205-9 

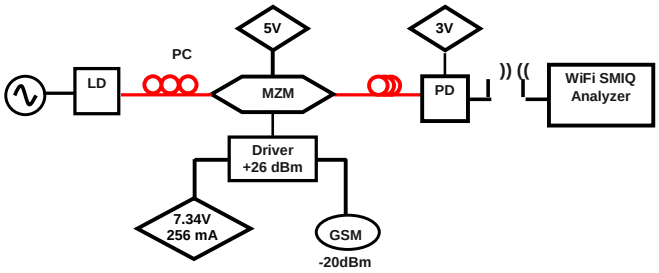


Figure 3. System setup showing the photonic mmw generation, data modulation, photonic wireless transmitter and SMIQ06 software as the wireless receiver. Laser Diode (LD): EMCORE [10341A] with FC/APC Optical Connector, Mach-Zehnder Modulator (MZM): LiNbO3 40 Gbps Photline MXAN-LN-40 at 1550 nm, 2.5 Gbps with FC/APC connectors; RF driver amplifier; Photodiode (PD): U2t 70 GHz photodetector, 0.57 A/W

Photonic RF generation was performed by means of a DFB Laser Diode (LD), operating at 1309 nm with an optical output power of 9.28 dBm directly modulated by 5 GHz RF signal at -10 dBm . Applying a direct modulated laser (DML) at frequency $f_0$ and a RF source with a frequency $f_{RF}$, the generated first-order sidebands are located at a frequencies $f_0 + f_{RF}$ and $f_0 - f_{RF}$. The same DSL technique can be applied at much higher frequencies in the millimetre-wave range.

Broadband modulation in the optical domain was carried out using a $LiNbO_3$ 40 Gbps Mach-Zehnder modulator (MZM). The modulator acts here as an optical mixer, multiplying the optical RF carrier with the data signal. As shown on Fig. 3 the transmitter is followed by a polarisation controller (PC) to adjust and maintain the polarisation state of the light for the MZM, which is extremely polarisation sensitive. The maximum RF power that can be possibly applied directly to the RF input port of the MZM is 28 dBm (i.e. 2 dBm delivered to the input of its driver amplifier which has a gain of 26 dB). We used -20 dBm GSM /IEEE 802.11.b signal at 5 GHz. The modulator is driven by a driver amplifier (bias 7.34 Volt corresponding to 256 mA) and biased at $V_\pi$, here 6.5 Volt and modulated first with a GSM data signal, generated by a R&S *vector signal generator* with a level of -20dBm maximum output power of 64 dBm for 2.4 GHz (GSM) with demodulation rate 270 kHz; symbol rate 270 ksym/s and GSM modulation 1bit/sym. The optical power measured at the output of MZM was -6 dBm.

The RoF unit is adapted to transmit the RF signal at 5 GHz in free space to the end user terminal. This RoF unit consists of a photodetector (PD) that converts the received optical signal to an electrical 5 GHz signal, a power amplifier that boosts this electrical signal and an antenna adapted to operate up to 5.8 GHz. The PD ($U^2t$ Photonics XPDV3120R-FC-VF) has a bandwidth of 70 GHz and a responsivity of 0.57 A/W. The gain of the photodetector equals to -42 dB as measured by connecting it to the directly modulated laser diode LD (9.28 dBm optical LD output, -52 dBm electrical PD output).

The performance of the modulation procedure has been evaluated. The power of the optical signal measured at the output of the MZM was equal to -11.8 dBm with an input RF signal power level of -20 dBm. With a PD gain of -42 dB, the output signal should be -63.8 dBm as compared to its measured value: -64 dBm). Eye diagram for this signal is wide open with EVM = 6.5%, Peak EVM=15%, Mean Power = -62.3 dBm and SNR = 24 dB. Changing the level of the input signal up to -10 dBm shows corresponding results: satisfactory error-vector magnitude EVM = 2.5%, Peak EVM = 6%, Mean Power = -53.5 dBm, SNR = 32 dB.

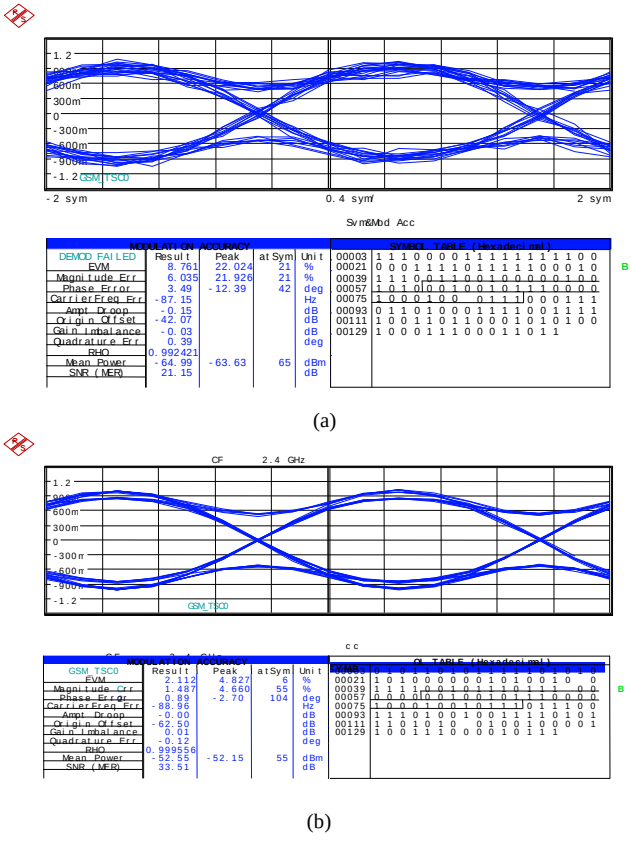


Figure 4. Eye diagram characterisations, corresponding to GSM modulating signal with data rate of 30-40 Kbps with low noise amplification. GSM modulation is 1 bit/sym and demodulation rate is 270 ksym/sec (a) Signal at level -20 dBm, EVM = 6.5% (b) Signal at level -10dBm, EVM=2.5%

Clearly open eye diagrams were observed for GSM transmission experiment (Figs. 4a and 4b). It shows that the signal has little noise and the amplitude is sufficient to be clearly "recognized". Adding a low noise RF amplifier (MAXIM-MAX2649) with an electrically-controlled variable gain (not shown in Fig. 3) used as a Trans-

 ISBN: 978-1-61208-205-9

Impedance Amplifier (TIA) after the photodiode can improve corresponding values to EVM = 1%, Peak EVM = 2.5%, Mean Power = -45 dBm (compared to -62 dBm before), SNR = 40 dB (compared to 24 dB before).

To analyse the link performance, we have used *Rhode& Schwarz OFDM Software* working as a vector signal analyser. This Software synchronises and demodulates the modulated signal. For this purpose, we have chosen a standard WLAN A – 64 QAM demodulation and both cyclic and pilot aided synchronisations. EVM vs. Carrier diagram (showing peak, average, minimum performance) and selected constellation diagram, taken by choosing digital standard GSM-EDGE (GSM LNB) are displayed in Fig. 5 and Fig. 6. EVM analysis shows that multiple standard wireless access signals such as GSM and WLAN 802.11g can be successfully transmitted with no errors. With input Wi-Fi signal of -10 dBm, EVM is about 10% worse than with the GSM signal of the same power. In fact, as the envelope of Wi-Fi signals is no longer constant, it is possible that the peaks of signal exceed the maximum RF input level allowed by the MZM. In order to improve EVM and constellation, the input signal power of the driver should be less than – 20 dBm.

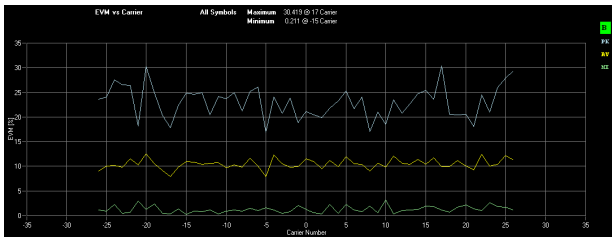


Figure 5. EVM vs carrier

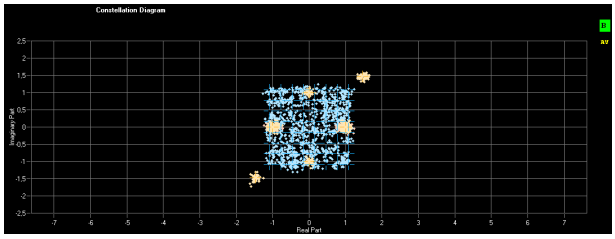


Figure 6. Constellation diagram

## V. PHOTONIC 60 GHZ GENERATION (IEEE 802.11AD) BASED UPON EXTERNAL MODULATION

With the use of the IEEE 802.11ad standard, higher throughputs could be achieved - at least 3 Gbps within 4 m and 1 Gbps up to 25 m [7]. Such speed becomes mandatory to deliver future applications. The standard takes advantage of large continuous blocks of unlicensed spectrum at 60 GHz. As signal bandwidth and carrier frequencies keep on increasing, there is an urgent need to define the full potential of RoF technology for the transport of various wireless signals and protocols to meet the demand for new wireless services with enhanced data throughputs in moving vehicles. With the implementation of 60 GHz RoF, more than 1 Gbps could be delivered on wireless links between the tram carriages and the stations. Rather than generating the local oscillator signal electrically at each station, it is optically generated from a central point and distributed to the stations. Optical heterodyning was used to generate the 60 GHz carrier according to the schematics as shown in Fig.7. Some of the equipment listed in the previous paragraph was used in combination with a high power laser diode (ILX Lightwave). The DFB laser diode operating at 1550 nm was driven by a precision current source (LDX-3545B) and stabilised by a temperature controller (LDT-5412). The operating point was fixed at 18 dBm, corresponding to $\lambda_0$ = 1548 nm. The laserdiode is again followed by a polarisation controller, slightly reducing the optical power to 17.7 dBm.

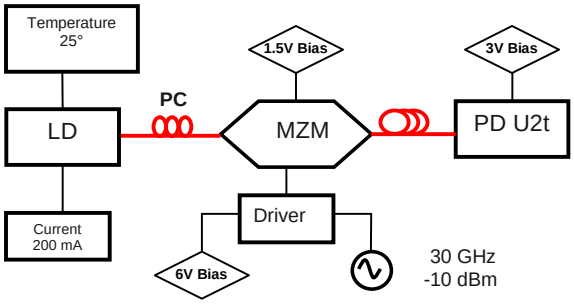


Figure 7. Photonic millimeter-wave generator based on external modulation. Components additional to Fig. 3: ILX Lightwave LDT-5412 temperature controller; Precision Current Source: ILX Lightwave LDX-3545B

Using the driver amplifier, the modulator (MZM) was biased at a minimum transmission point (MITP, here 1.5V), in order to suppress the optical carrier at central wavelength $\lambda_0$, and modulated with a millimetre-wave signal at a frequency of 30 GHz, provided by the signal generator Anritsu MG-364A. The power of the 30 GHz input signal was set to -10 dBm. If bias is set to MITP with respect to the optical carrier, the carrier is cancelled out as the phase shift between both arms is set to $\pi$. While applying an electrical signal at half the desired mm-wave frequency, i.e. 30 GHz (= 0.5 x $f_{LO}$) to the RF electrode of the modulator, the total frequency difference between both sidebands is now $f_{LO}$ = 60 GHz. Two optical signals with a wavelength separation of 0.5 nm at 1550 nm generate the desired beat frequency upon detection by the photodiode: $\delta f = f_2 - f_1 = \tilde{c}/\lambda_2 - \tilde{c}/\lambda_1$ with $\lambda_1 = 1562.5$ nm and $\lambda_2 = 1562$ nm. Applied

 ISBN: 978-1-61208-205-9 

signal generation technique is called double-sideband with carrier-suppression (DSB-CS) (see [8-9]).

Simulations under VPI Transmission Maker™, based on the schematics shown on Fig. 8 demonstrate that sidebands suppression contrast here is about 36 dB (see Fig. 9). The output optical field from the modulator consists now of the suppressed optical carrier and two optical sidebands (lower and upper sidebands). Additionally, Fig. 10a illustrates that the maximum output power at 60 GHz that can be obtained with this material is equal to -35 dBm. From Fig. 10b, it is also clear that -35 dBm is the highest measured power value for the discussed system.

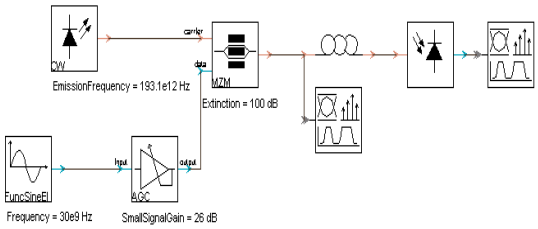


Figure 8. VPI scheme for setup, depicted on Fig. 7

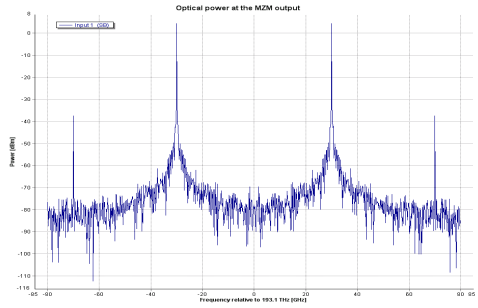


Figure 9. Optical spectrum while applying fLO/2 and biased at MITP

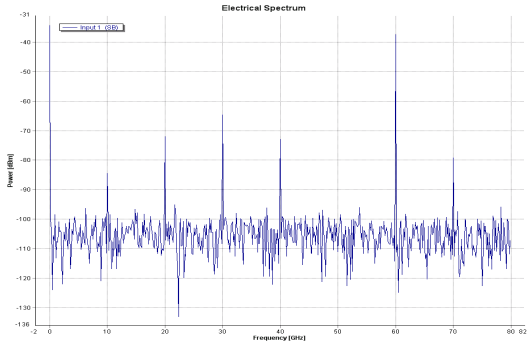


(a)

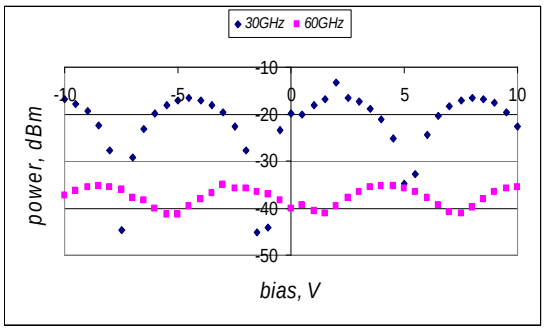


(b)

Figure 10. VPI simulations (a) and power measurements of 30 GHz and 60 GHz signals at the output of the PD (b)

## VI. CONCLUSION AND FUTURE WORKS

In this paper, we have proposed track side solutions to provide Wi-Fi to tram passengers. Different scenarios, based on RoF were simulated and tested, in order to demonstrate their performance for tram installations and to make an insight into the limits of existing RoF components. Through careful application of bias, the linear and nonlinear domains of the MZM transfer function are successfully used for 60 GHz generation and for broadband modulation. VPI simulations were proved to be reliable and will be required in the future for the implementation of multiple standard solutions. Thanks to the broadband operation characteristics of the MZM and the PD, the proposed system can advantageously accommodate a large range of frequencies. System validations will follow by identification of critical components and optimization of energy consumption on 3 (out of 28) tramway stations in Brest and 2 carriages.

## ACKNOWLEDGMENT

The authors acknowledge the financial support of Institut Carnot and Université Européenne de Bretagne (UEB) within the context of the International SISCom Chair (2011-2012), without which this work could not have been carried out. The authors are grateful to the members of the Optics and the Microwaves Department of Telecom Bretagne and in particular to the joint CapilR™ and PERDYN teams specializing respectively in radio-over-fibre technologies for wireless and mobile access and optical access networks. Special thanks are addressed to Brest Métropole Océane for supporting ongoing project CapilTram.

## REFERENCES

[1] B. Lannoo et al., “Business Model for Broadband Internet on the Train”, in Proc. 46th Federation of Telecommunications Engineers of the European Community Congress (FITCE 2007), Warsaw, Poland, July, pp. 241-248, 2007

[2] H. B. Kim, M. Emmelmann, B. Rathke, and A. Wolisz., A Radio over Fiber Network Architecture for Road Vehicle Communication Systems“, in Proc. Of IEEE Vehicular Technology Conference, VTC, Spring 2005

 ISBN: 978-1-61208-205-9 

[3] B. Lannoo, D. Colle, M. Pickavet, and P. Demeester “Radio-over Fiber-Based Solution to Provide Broadband Internet Access to Train Passangers”, IEEE Communications Magazine, pp. 56-62, February, 2007

[4] A. Stöhr et al., “60 GHz Radio-over-Fiber Technologies for Broadband Wireless Services”, OSA Journal of Optical Networking, vol.8, no.5, pp. 471-487, Aug, 2009 (invited)

[5] H. Al-Raweshidy and S. Komaki., “Radio over Fiber Technologies for Mobile Communication Networks”, Artech House, 2002

[6] D. Wake et al., “Optically powered Remote Units for Radio-over-Fiber Systems”, JLT, vol. 26, No. 15, 2008

[7] S. Kato, et al, “Single Carrier Transmission for Multi-gigabit 60-GHz WPAN Systems”, IEEE Journa l on Selected Areas in Communications, vol. 27, No. 8, pp. 1466-1478, October 2009.

[8] Yu.Z. Jia, et al., "Optical millimeter-wave generation or up-conversion using external modulators”, IEEE Photon. Technol. Lett., vol. 18, p.265, 2006.

[9] M. G. Larrode, A. M. J. Koonen, J. J. Vegas Olmos, and A. Ng’Oma., "Bidirectional radio-over-fiber link employing optical frequency multiplication", IEEE Photon. Technol. Lett., vol. 18, p. 241, 2006.

 ISBN: 978-1-61208-205-9 

# WTFC to TCP Flow Control Proxy

Vesna Pekic, Ante Kristic, Julije Ozegovic
Faculty of Electrical Engineering, Mechanical Engineering and Naval Architecture
University of Split
Split, Croatia
e-mail: vesna.pekic@fesb.hr, ante.kristic@fesb.hr, julije.ozegovic@fesb.hr

***Abstract*—Integration of different kinds of traffic on the Internet can be resolved by employing QoS policies on access networks. One possible solution is to use WTFC (Window-Time Flow Control) flow control algorithm on access network. In this paper, the WTFC-TCP flow control proxy is introduced in order to exploit the ability of WTFC to estimate the optimal working point for the available capacity and to keep on average empty node buffers. A basic proxy model is defined and elementary congestion signaling algorithms for flows directed to and from access network are applied. Simulation experiments have shown potential successfulness of the concept.**

***Keywords-access network; WTFC; QoS; Flow Control Proxy***

## I. INTRODUCTION

WTFC (Window-Time Flow Control) [12] was designed to keep a network at the optimal working point, using its fair share of the available capacity and keeping node buffers empty. This makes it suitable for integrated services implementation. The problem is the coexistence of WTFC with the more aggressive TCP (Transport Control Protocol). On the other hand, TCP is the prevailing technology that will be hard to replace in the near future. One possible solution is to introduce new technologies on access network without changing TCP/IP protocol stack on the rest of the network.

The idea of this paper is that the cooperation of WTFC on access network and TCP on the rest of the network would be beneficial for deployment of integrated services. For that purpose, a special gateway or proxy node is needed to transfer packets from one protocol to the other, and to map their flow controls. We explore the possibility of interconnecting WTFC with TCP and show some simulation results using WTFC-TCP flow control gateway/proxy.

In Section 2, an overview of related work on improving TCP performance via a proxy and on mapping TCP to another protocol is given. A brief description of TCP and WTFC flow control is given in Section 3. Section 4 introduces a model used for WTFC-TCP interconnection, highlights the problems encountered when mapping the two protocols' flow control and proposes basic algorithms to successfully perform the mapping. Simulation results are given in Section 5 and conclusions with future work in Section 6.

## II. RELATED WORK

Intensive work has been done on improving TCP performance over a combination of wireless access and fixed transport network. The dominant technology, if fixed side TCP client is not to be altered, is using PEPs (Performance Enhancing Proxies). A survey of existing performance enhancing proxy schemes is given in [4]. PEP schemes in the literature include modifying acknowledgment (ACK) spacing [3], generating local acknowledgments for large bandwidth-delay products (BDP) [14], variable bandwidth [7], or wireless links [9], specifically negative acknowledgments, and performing local retransmission [1][3][9], as well as ACK filtering and reconstruction [2].

The accent in the above schemes is on error recovery and hiding errors caused by unreliable nature of wireless links from TCP on the fixed side, so that standard TCP congestion control wouldn't unnecessarily trigger and reduce congestion window. Proposals concerning actual flow control are receiver window signaling according to free space in proxy buffers [1][14], ACK spacing [3] and changing window according to congestion measurements [13]. Aggregating flows that pass through the same Base Station to the same mobile host and using aggregate state variables instead of per-flow state variables is explored in [5].

Several approaches, like [1], suggest splitting connection between fixed host and mobile host at the Base Station. A protocol optimized for wireless links is employed on the wireless part of the network. Our work follows a similar idea of using different protocols for different parts of the network. However, even though applying WTFC-TCP connection on heterogeneous wired-cum-wireless networks looks promising, due to WTFC flow and error control being decoupled, in this paper a general type of link is considered. Interconnecting congestion controls of TCP and another protocol is described in [6]. An XCP-TCP gateway is used that interconnects XCP (eXplicit Control Protocol) and TCP networks. It maps the congestion control functions between TCP and XCP by mapping incipient congestion of XCP domain into drop event of TCP domain.

## III. TCP AND WTFC FLOW CONTROL MECHANISMS

### A. TCP Flow Control

Transport Control Protocol (TCP) uses window flow control consisting of four main mechanisms: slow start (SS), congestion avoidance (CA), fast retransmission and fast

 ISBN: 978-1-61208-205-9 

recovery, although many more have been proposed in the literature.

TCP sender maintains two variables that determine window size and the rate of its increment: congestion window and slow start threshold [8]. Congestion window (*cwnd*) represents the amount of data bytes that can be transmitted at a given time before receiving an acknowledgment (ACK) from the receiver. Slow start threshold (*ssthresh*) serves as a boundary that determines if slow start or congestion avoidance mechanism is used to control data transmission. *Ssthresh* can be recognized as the sender's estimation of optimal packet window.

Slow start mechanism is used while *cwnd*<*ssthresh*, i.e. at the beginning of a transfer, or after detecting network congestion. Packet loss or ECN (Explicit Congestion Notification) serve as congestion indication. Initially, TCP sender sets *ssthresh* to receiver's advertised window and *cwnd* to 1 packet and increases it by 1 for each ACK received, effectively doubling *cwnd* every round trip time (RTT). After packet loss, *ssthresh* is set to half the current *cwnd* value and slow start begins again from its initial *cwnd*.

When *cwnd* value exceeds *ssthresh*, TCP sender transits from slow start to congestion avoidance mechanism. During congestion avoidance, *cwnd* is incremented by approximately 1 segment per RTT. Congestion avoidance continues until a packet loss is detected.

Basic indication of packet loss is the occurrence of retransmission timeout (RTO). RTO is dynamically computed based on RTT value and its variance. Fast retransmission algorithm shortens the time needed to detect packet loss. After receiving an out-of-order packet, TCP receiver sends a duplicate ACK to inform the sender of a possible packet loss. When the sender receives three duplicated ACKs, it concludes that the packet has been lost. Sender can then perform a retransmission of what appears to be the missing packet, without waiting for RTO to expire.

To benefit from fast retransmission, fast recovery mechanism was introduced. After a packet loss detection and fast retransmission, values of *ssthresh* and *cwnd* are set to cwnd/2 and ssthresh+3, respectively. This takes into account packets that have left the network and have generated three duplicated ACKs. After receiving an ACK for the retransmitted packet, the sender sets *cwnd* to *ssthresh*.

### *B. Window Time Flow Control*

Window Time Flow Control (WTFC) uses window and RTT measurements to calculate optimal window and packet sending rate [12]. *WT* (window-time) space is used for analysis. *W*,*T* plane is determined by the network optimal working point ($W_0$, $T_0$), $T_0$ and $W_0$ being minimal RTT and optimal window in case of only one user, respectively. This point represents the total capacity of the network from the packet transmitter's point of view. $\mu=W_0/T_0$ would then be the optimal sending rate.

When more users share the network, each should acquire a proportional part of the network capacity, $\mu_j = \alpha\mu$, under the assumption that $\alpha \in (0,1)$ is equal for all users. Optimal working point ($W_0(\alpha)$, $T_0(\alpha)$) of each transmitter, that now observes reduced capacity $\mu_j$, depends on ($W_0$, $T_0$) and the parameter $\alpha$. The pair ($W_0(\alpha)$, $T_0(\alpha)$) also determines delay for each transmitter:

$$T = \begin{cases} T_0(\alpha) & ,W \le W_0(\alpha) \\ W\dfrac{T_0(\alpha)}{W_0(\alpha)} & ,W > W_0(\alpha) \end{cases} \quad (1)$$

Parameter $\alpha$ defines a set of delay response curves in WT space. Their breaking points, being at the same time optimal working points, are placed along the hyperbola-like curve defined by constant bandwidth delay product; see Figure 1.

When packet acknowledgment arrives, transmitter measures new coordinates in *W*,*T* plane, which allows it to compute $\alpha$. Then it calculates the optimal working point C, i.e. optimal sending period $t_0(\alpha)$ and window $W_0(\alpha)$, reducing the packet rate from the point A according to

$$t_0(\alpha) = \frac{T}{W} \quad , \quad W_0(\alpha) = T_p \frac{W}{T} + 1 \quad (2)$$

or increasing it from the point B according to:

$$t_0(\alpha) = T - T_p \quad , \quad W_0(\alpha) = \frac{T_p}{T - T_p} + 1. \quad (3)$$

$T_p$ in the above expressions is the propagation delay. WTFC transmitter requires information about the total network capacity ($W_0$, $T_0$) for WTFC to function. Network nodes can signal parameters needed to compute the capacity of the bottleneck link using special fields in packet headers. Alternatively, transmitter can estimate the capacity [11]. Experimental simulations in [11] have shown that signaling yields better fairness. A special Fast-Start algorithm is used for sending packets before the first acknowledgment arrives and optimal working point can be computed.

WTFC does not use packet loss to detect congestion and simulation measurements have shown that WTFC algorithm can provide high network utilization with on average empty node buffers [12].

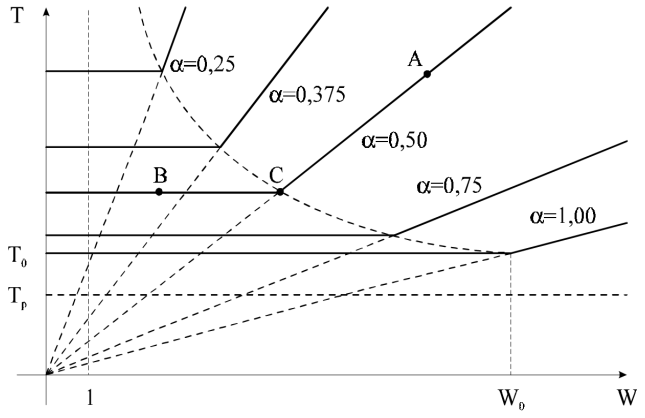


Figure 1. Delay curves depending on α in WT space (from [10])

## IV. CONNECTING TCP WITH WTFC

The goal of our concept is to exploit the ability of WTFC to estimate the optimal working point for its share of the available capacity, while keeping the property of TCP to compete for its share of the total capacity.

### A. Basic connecting architecture

Model of the access network connected to the Internet provider network and core Internet is used as the basic connecting architecture. The model is further developed using packet queues abstraction; see Figure 2. On both WTFC and TCP domains, WTFC and TCP sender packet queues are considered. Of the four, two are located on the proxy node. The WTFC and TCP flows are interconnected through the interconnection queues located on the proxy node. Interconnection queues, called proxy buffers, are available for manipulation.

The WTFC-TCP flow control proxy is a stateful (per flow) proxy and all the traffic of an access network is supposed to pass through it. Its placement could be in DSL Access Multiplexers or in Base Stations of cellular networks. Those are highly distributed devices placed relatively near the end-user, with moderate several hundred flows passing through at a given time.

We consider four main scenarios:

- TCP to WTFC domain flow; congestion on the TCP sender domain.
- TCP to WTFC domain flow; congestion on the WTFC receiver domain.
- WTFC to TCP domain flow; congestion on the WTFC sender domain.
- WTFC to TCP domain flow; congestion on the TCP receiver domain.

In case of congestion on the sender side, it is enough to simply translate the packet from one protocol to the other on the proxy and forward it immediately, since the proxy buffer will not be saturated. Intervention is needed when congestion is on the receiver side. In that case, packets will begin to accumulate in the proxy buffer and some sort of mechanism should slow the sender down, while at the same time keeping the efficiency high.

Since both WTFC and TCP protocols use acknowledgments (ACKs) to estimate network condition, ACK manipulation is the first choice to achieve desired performance. Three different possibilities are detected, to close acknowledgments loopback at the near-end (e.g. proxy TCP receiver to TCP sender), at the far-end (e.g. WTFC receiver to the TCP sender), and on the proxy buffer (e.g. proxy WTFC receiver to WTFC sender after a packet is removed from the WTFC-TCP proxy buffer).

Proxy buffer packet losses are acceptable with far-end ACK loopback, because those buffers are included in the normal queue chain of the packet trajectory. However, with near-end and buffer ACK policies, proxy buffer packet loss is unacceptable, because it is not covered with the packet loss recovery in either WTFC or TCP domain.

### B. Basic algorithms for TCP to WTFC domain flows

In case of TCP to WTFC domain flow, TCP sender is located at the distant node and TCP receiver at the proxy node, while WTFC sender is located at the proxy node and WTFC receiver at the distant node. In case of congestion in TCP domain, TCP should react normally to packet loss. When congestion arises in WTFC domain, proxy WTFC sender should reduce its sending rate using normal WTFC mechanisms. However, TCP sender continues to use its current congestion window and TCP-WTFC proxy buffer tends to overflow.

When far-end ACK loopback is used, ACKs in TCP domain are sent after corresponding ACKs from WTFC domain are received at the proxy, so that TCP sender can have accurate overall RTT information.

Proxy WTFC sender can calculate optimal sending interval and window for WTFC domain using either capacity estimation or explicit signaling. TCP-WTFC proxy buffer is used between TCP and WTFC domain to forward packets with the optimal interval computed. ACKs are forwarded directly between WTFC and TCP domain. Their spacing paces TCP sender to optimal sending interval. Still, TCP sender increases its *cwnd*, either doubling it per RTT if in SS phase, or incrementing it by one per RTT if in CA phase. Consequently, packets start accumulating in the TCP-WTFC proxy buffer.

Despite the reason for TCP-WTFC proxy buffer overflow, it is obvious that some kind of WTFC to TCP congestion signaling is needed. TCP reacts to packet losses, so packets are intentionally discarded from the TCP-WTFC proxy buffer. The algorithm is triggered when TCP-WTFC proxy buffer reaches two times the proxy WTFC sender

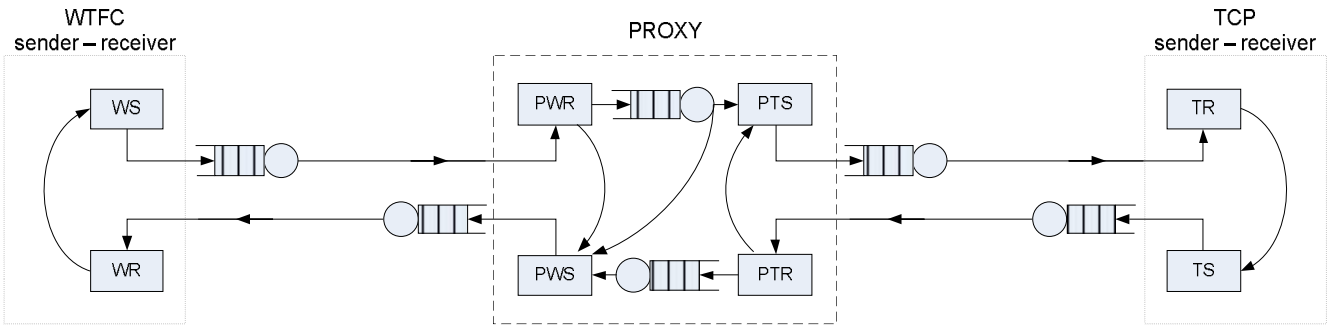


Figure 2. WTFC-TCP flow control proxy model

 ISBN: 978-1-61208-205-9

congestion window.

Simulation results show acceptable performance of the proposed far-end ACK policy with the induced packet losses algorithm, so near-end and buffered ACK policies are left for future research.

### C. Basic algorithms for WTFC to TCP domain flows

In case of WTFC to TCP domain flow, WTFC sender is located at the distant node and WTFC receiver at the proxy node, while TCP sender is located at the proxy node and TCP receiver at the distant node. In case of congestion in WTFC domain, WTFC should react normally by calculating the optimal packet rate and window. When congestion arises in TCP domain, proxy TCP sender should reduce its sending rate as a reaction to packet losses. However, WTFC sender continues to use its current congestion window and WTFC-TCP proxy buffer tends to overflow.

All three ACK loopback policies are considered in this case: far-end, near-end and proxy buffer loopback.

Further, proxy TCP sender can be a full or modified TCP sender. Near-end ACK loopback requires a full TCP sender to be used, to let it compete with other TCP flows in TCP domain. Far-end ACK loopback provides some feedback for WTFC sender from TCP domain as well as WTFC domain, so modified proxy TCP sender can be used.

Far-end ACK policy was at first considered with proxy TCP forwarder, a simple process that sends whatever packet is received at the WTFC-TCP proxy buffer. The performance of this combination was unpredictable, because both path capacity estimation and load estimation mechanisms of WTFC were influenced by TCP domain network load. This resulted in poor fairness, where WTFC used less than its fair share when congestion in TCP domain was low, and more than its fair share during heavy congestion in TCP domain.

To compensate for the TCP domain influence, TCP forwarder was then replaced with the full TCP sender. This had further effects on WTFC estimation processes due to the proxy TCP sender slow start mechanism.

Finally, a variant of TCP sender without initial slow start phase was included, but acceptable performance could not always be obtained.

As expected, near-end ACK loopback suffered from lack of flow control between WTFC and TCP domains. In this case, full proxy TCP sender was the only choice. Obviously, some signaling from TCP to WTFC domain is indispensable.

At this point, the proxy buffer ACK loopback was considered, with full TCP sender. Proxy WTFC receiver sends ACK to proxy WTFC sender after a packet is removed from WTFC-TCP proxy buffer. This way, if packets are accumulated at the WTFC-TCP proxy buffer, flow of WTFC acknowledgments is delayed, thus signaling possible congestion in TCP domain.

However, early simulations did not achieve acceptable performance. The reason was the proxy TCP sender algorithm that builds up its *cwnd* despite the constrained number of packets available from WTFC domain. When congestion in TCP domain finally occurs, proxy TCP sender continues to transfer incoming WTFC packets as allowed by high *cwnd*, despite the lack of TCP acknowledgments.

To limit *cwnd* build up on proxy TCP sender, a simple limiting algorithm is introduced: if *cwnd* tends to excess the current window (number of packets in flight) plus packets in the WTFC-TCP proxy buffer, *cwnd* is limited to that value plus some additive value (5 packets in simulations performed).

The combination of the proxy buffer ACK loopback with *cwnd* limiting policy provided acceptable performance in the simulation environment.

## V. SIMULATIONS

Simulations were conducted using ns2 simulator (version 2.34) on the simplistic topology with seven nodes, node n2 being WTFC-TCP proxy, shown in Figure 3. Link capacity of 10 Mb/s between nodes n2 and n3 emulates a possible ADSL connection to the Internet which is often of restricted capacity. 10 Mb/s capacity between nodes n2 and n1 emulates often scarce resources in parts of an Internet provider network. In order to present the induced packet loss algorithm, Figure 6 was taken from a simulation conducted on the same topology, but with 100 Mb/s capacity between nodes n1 and n2.

In simulations presented, a flow under observation between nodes n0 and n4 starts at t=0s and ends at t=16s, which is the duration of simulation. In Section A, results for a TCP to WTFC domain flow from node n0 to node n4 are presented, and in Section B, results for a WTFC to TCP domain flow from node n4 to node n0. From t=2s to t=6s ten competing TCP Reno flows are active in TCP domain between nodes n0 and n2, and from t=10s to t=14s ten competing WTFC flows are active in WTFC domain between nodes n2 and n4. Competing flows use the same direction as the flow observed. Drop Tail algorithm is used on links in the WTFC domain and ARED (Adaptive RED) on links in the TCP domain.

To examine the effects of WTFC-TCP flow control proxy on QoS sensitive applications additional simulations were conducted on the same topology. In those simulations a UDP/CBR (User Datagram Protocol / Constant Bit Rate) flow is active in the WTFC domain between nodes n6 and n5 from t=1s to t=16s. The rate used is 64 kb/s, which is the VoIP standard. The UDP/CBR flow is placed in the WTFC domain rather than in the TCP domain, so as not to let TCP influence it. The assumption here is that QoS would be otherwise provided (enforced) in the provider network by

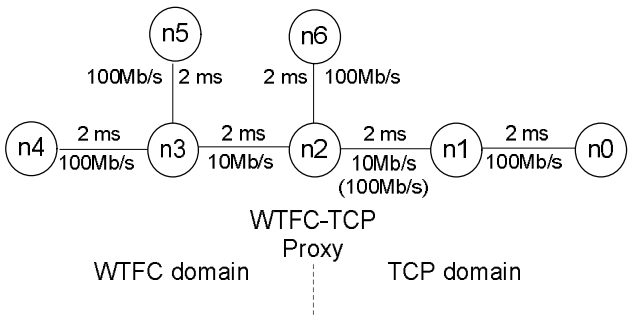


Figure 3. Simulation network topology.

Traffic Engineering (TE) under DiffServ paradigm.

### A. TCP to WTFC domain flows

Packet flow dynamics for a TCP to WTFC domain flow with the induced packet loss algorithm on TCP-WTFC proxy buffer is shown in Figure 4. Slow start algorithm of the TCP sender causes losses and disrupted flow of packets in the first second of simulation time. In time intervals when the competing flows are active the slope of the curve, representing throughput, is reduced as expected. Calculated throughput is shown in Figure 9 and discussed in Section C.

Window for TCP sender and proxy WTFC sender, as well as TCP-WTFC proxy buffer occupancy are shown in Figure 5. The value of the TCP sender window going to 240 packets at the beginning of the simulation is not shown in the figure in order to limit the scale of the y-axis. TCP sender window follows the additive increase-multiplicative decrease (AIMD) rule of the TCP Reno algorithm, while proxy WTFC sender keeps its window steady according to the calculated optimal working point. Low TCP-WTFC proxy buffer occupancy shows the efficiency of the applied algorithm.

Packet dynamics in the event of an induced packet loss is

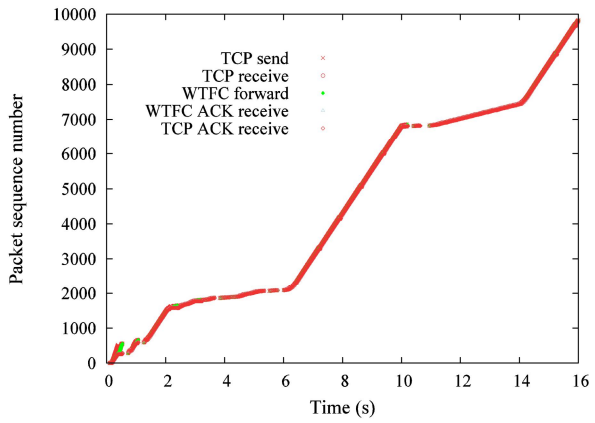


Figure 4. TCP to WTFC domain flow packet dynamics.

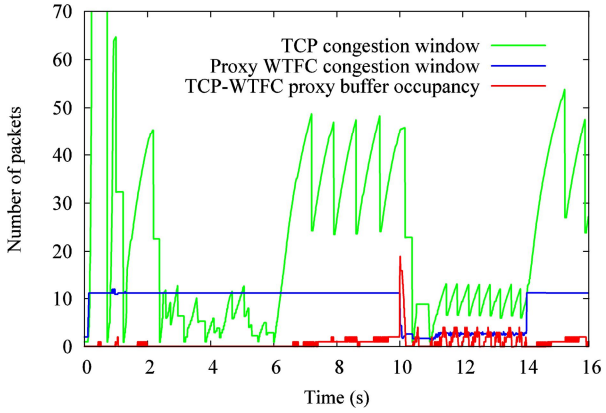


Figure 5. TCP to WTFC domain flow windows and proxy buffer occupancy.

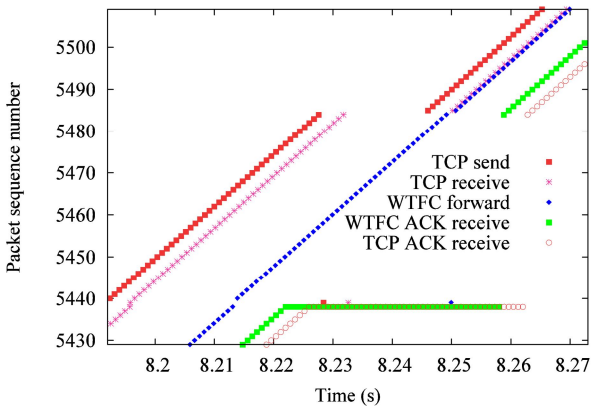


Figure 6. Packet dynamics in the event of induced packet loss.

shown in Figure 6. The increasing latency between TCP receive event and WTFC forward event on the proxy is due to the increasing proxy buffer occupancy, eventually resulting in induced packet loss and duplicated ACKs. After the packet loss, the TCP window is halved by the TCP Reno flow control algorithm. Consequently, there is a pause in sending new packets. TCP-WTFC proxy buffer deque, regulated by Proxy WTFC sender, remains steady.

### B. WTFC to TCP domain flows

Packet flow dynamics for a WTFC to TCP domain flow with WTFC-TCP proxy buffer ACK loopback and the proxy TCP sender *cwnd* limiting algorithm is shown in Figure 7. Performance observed is similar to that of Figure 4. The first slope is smoother then in Figure 4 because WTFC sender does not use the aggressive slow start algorithm. Optimal working point is computed upon the arrival of the first ACK.

Window for WTFC sender and TCP proxy sender, as well as WTFC-TCP proxy buffer occupancy are shown in Figure 8. Low WTFC-TCP proxy buffer occupancy shows the efficiency of the applied algorithm. Proxy TCP sender window growth is limited to the number of packets in flight plus the number of packets in proxy buffer plus 5. Therefore, proxy TCP sender window is steady and following the change of WTFC window when there is no congestion in

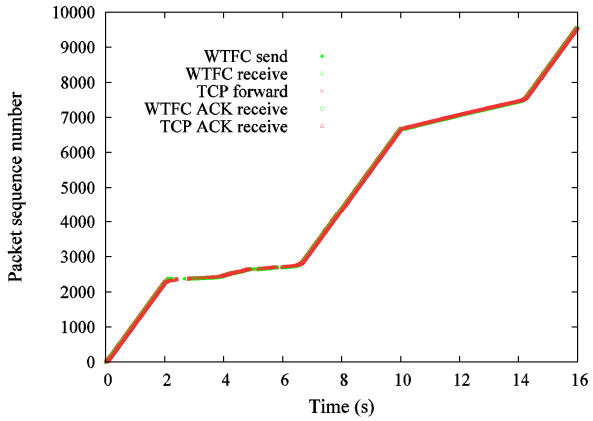


Figure 7. WTFC to TCP domain flow packet dynamics.

 ISBN: 978-1-61208-205-9

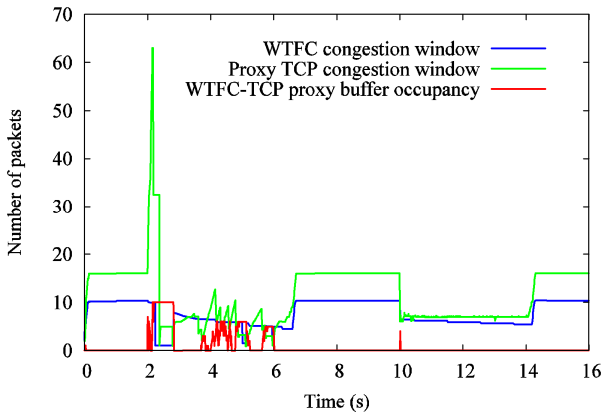


Figure 8. WTFC to TCP domain flow windows and proxy buffer occupancy.

TCP domain. Otherwise it follows the TCP Reno AIMD rule. The *cwnd* spike at t=2s shows that *cwnd* limiting algorithm should be improved.

### C. *Throughput, delay and jitter*

Simulation results presented in this section were obtained with TCP to WTFC domain flows. Results with WTFC to TCP domain flows are similar. Comparison is made with results obtained when traditional TCP flow control is deployed on the entire network. Topology used is the same as with the WTFC-TCP proxy. Competing flows in this TCP-all network are TCP Reno flows in both the time interval from t=2s to t=6s and the time interval from t=10s to t=14s. Additional simulations were conducted on the TCP-all network with ARED algorithm on all links.

Throughput achieved by the TCP to WTFC domain flow under observation is comparable to that of a standard TCP Reno flow on the same topology, as well as on the topology with only ARED; see Figure 9. It shows good channel utilization when there is no competing traffic and fair reaction when competing flows are present.

The property of WTFC to estimate the optimal working point and to keep on average empty node buffers is expected to result in some QoS metric improvements when using WTFC to TCP flow control proxy, in comparison with results using only traditional TCP flow control. For verification, delay and jitter of VoIP traffic, represented by a UDP/CBR flow between node n6 and node n5, are observed.

As expected, delay when using the WTFC-TCP flow control proxy is generally smaller than delay on the equivalent TCP-all network, both with just ARED and with the combination of Drop Tail and ARED algorithms; see Figure 10. Peak delay with the proxy is 60 ms and without the proxy about 125 ms. While competing flows between nodes n2 and n4 are active, delay with the proxy is stabilized below 30 ms. In the same interval, delay of the TCP flow with ARED has almost 10 times greater jitter and the delay of the TCP flow with ARED and Drop Tail is near the peak value.

Jitter estimator MAPDV2 according to ITU-T G.1020 Recommendation is used to compute the jitter. Results are shown in Figure 11. Peak jitter value with the WTFC-TCP flow control proxy is 20 ms, while the same value for TCP-all flows exceeds 100 ms. The proxy reduces jitter in general as well as the fluctuation of jitter values. While competing

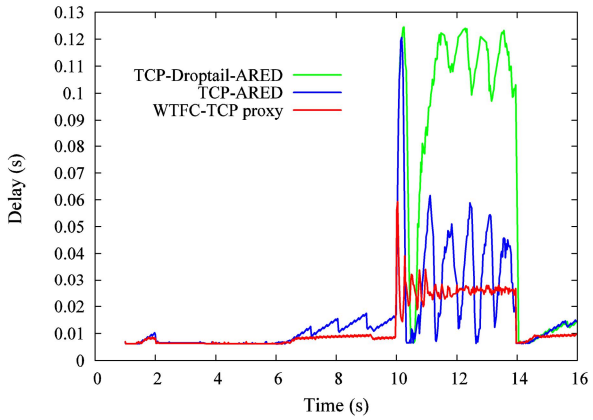


Figure 10. Delay of a CBR flow using WTFC-TCP flow control proxy and using standard TCP flow control.

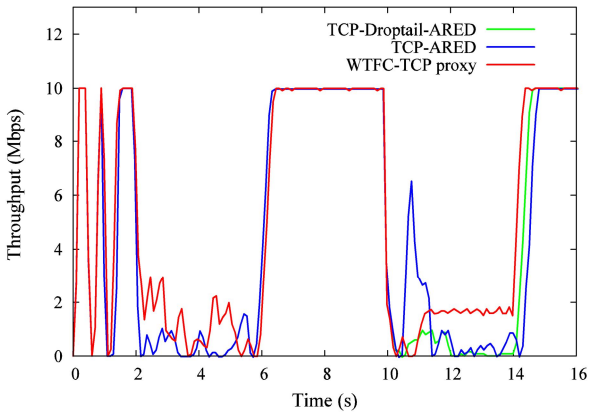


Figure 9. Throughput using WTFC-TCP flow control proxy and using standard TCP flow control.

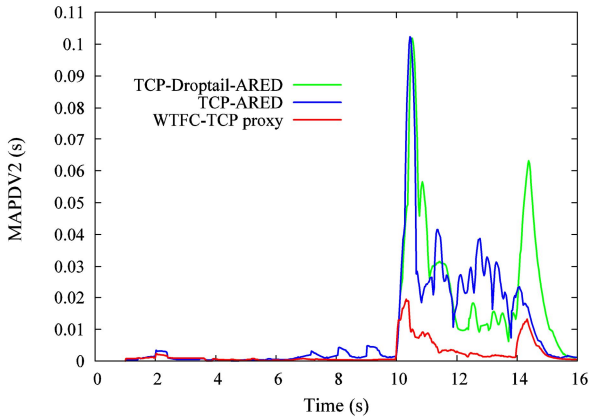


Figure 11. Jitter (MAPDV2) of a CBR flow using WTFC-TCP flow control proxy and using standard TCP flow control.

 ISBN: 978-1-61208-205-9 

flows in WTFC domain are active, jitter drops from peak value to below 5 ms.

The UDP/CBR flow passes through the link between nodes n2 and n3 together with the TCP to WTFC domain flow and competing WTFC flows, or together with equivalent TCP flows. Both delay and jitter have the lowest values in the time interval from t=10s to t=14s when competing flows in TCP domain are active. Congestion is then present in the TCP domain, thus leaving the link between nodes n2 and n3 unsaturated.

## VI. CONCLUSION AND FUTURE WORK

In this paper, the concept of resolving the QoS at the edge between access network and the Internet is explored using WTFC flow control on the access network and standard TCP on the Internet. The WTFC-TCP flow control proxy is introduced in order to exploit the ability of WTFC to estimate the optimal working point for the available capacity and to keep on average empty node buffers.

A basic proxy model is defined, consisting of packet queues in both WTFC and TCP domains. WTFC and TCP flows are interconnected through proxy buffers located on the proxy node.

In this scenario main flow control problems arise when congestion is present on the receiver side of the model. In this case some kind of flow control signalization is needed between WTFC and TCP domains.

When a flow passes from TCP to WTFC domain, WTFC congestion is signaled to TCP sender by induced single packet loss. Proxy deliberately discards a packet when the TCP to WTFC proxy buffer occupancy exceeds double value of proxy WTFC sender congestion window. This way, the TCP sender *cwnd* is halved. Simulation results have shown that this simple mechanism operates efficiently.

In a scenario when a flow passes from WTFC to TCP domain, congestion notification from TCP domain to WTFC sender is obtained using delayed local WTFC acknowledgments. These are sent at the moment when a packet is taken from the WTFC to TCP proxy buffer. Additional proxy TCP sender *cwnd* limiting algorithm is used to prevent TCP from unnecessarily increasing *cwnd* during congestion in WTFC domain. Simulation results have shown that these two mechanisms combined provide satisfactory performance.

Simulation results presented make the WTFC-TCP flow control proxy concept promising for further research. Throughput achieved is comparable to that of a TCP-all network. Delay and jitter of a VoIP flow passing through the WTFC domain were taken in consideration as QoS metrics. They show considerable improvement over delay and jitter on a TCP-all network. Future work includes expanding algorithms with more sophisticated features as well as conducting experiments on more complex topologies and in wider condition range. Finally, the QoS for multimedia flows in integrated environment with data traffic needs to be extensively verified.

## REFERENCES


[1] A. Bakre and B. R. Badrinath, “I-tcp: Indirect tcp for mobile hosts,” in 15th International Conference on Distributed Computing Systems, pp. 136–143, 1995.

[2] H. Balakrishnan, V. N. Padmanabhan, G. Fairhurst and M. Sooriyabandara, “TCP Performance Implications of Network Path Asymmetry,” IETF RFC 3449, Dec 2002.

[3] H. Balakrishnan, S. Seshan, E. Amir and R. H. Katz, “Improving tcp/ip performance over wireless networks,” in 1st Annual International Conference on Mobile Computing and Networking, New York, NY, USA, 1995, pp. 2–11, ACM.

[4] J. Border, M. Kojo, J. Griner, G. Montenegro and Z. Shelby, “Performance enhancing proxies intended to mitigate link-related degradations,” IETF RFC 3135, June 2001.

[5] R. Chakravorty, S. Katti, I. Pratt and J. Crowcroft, “Using TCP flow-aggregation to enhance data experience of cellular wireless user,” IEEE Journal on Selected Areas in Communications, vol. 23, no. 6, pp. 1190-1204, June 2005.

[6] S. Cheng, C. Guo, J. Li and L. Zhu, “Design and Analysis of an XCP-TCP Gateway,” International Conference on Networking 2008 (ICOIN 2008), pp.1-5, Jan. 2008, doi: 10.1109/ICOIN.2008.4472746.

[7] D. Dutta and Y. Zhang, “An Active Proxy Based Architecture for TCP in Heterogeneous Variable Bandwidth Networks,” Proc. IEEE GLOBECOM 2001, pp. 2316 – 2320, November 2001.

[8] J. V. Jacobson, “Congestion Avoidance and Control,” Proc. ACM SIGCOMM ’88, vol. 18, no.4, pp. 314-329, Stanford, USA, August 1988.

[9] D. Murray, T. Koziniec and M. Dixon, “Solving Ack Inefficiencies in 802.11 Networks,” Proceedings of the 3rd IEEE International Conference on Internet Multimedia Services Architecture and Applications IMSAA'09, pp. 1-6, 2009.

[10] J. Ozegovic, “Filtering schemes for the window-time space flow control (WTFC),” Proc. ICCCN'00, pp. 575 - 580, Las Vegas 2000, USA.

[11] J. Ozegovic, “Implementation algorithms for the window-time space flow control (WTFC),” Proc. ICCCN'99, pp. 30 - 35, Boston 1999, USA.

[12] J. Ozegovic, “Window-time space flow control (WTFC),” Proc. ICCCN98, pp. 800 - 807, Lafayette 1998, USA.

[13] H. Shimonishi, T. Hama and T. Murase, “Tcp-adaptive reno for improving efficiency-friendliness tradeoffs of tcp congestion control algorithm,” PFLDnet, pp. 87–91, Feb. 2006.

[14] D. Velenis, D. Kalogeras and B. Maglaris, “SaTPEP: a TCP Performance Enhancing Proxy for Satellite Links,” Proc. 2nd International IFIP-TC6 Networking Conference on Networking Technologies, Services, and Protocols; Performance of Computer and Communication Networks; and Mobile and Wireless Communications (NETWORKING '02), pp. 1233-1238, 2002.


 ISBN: 978-1-61208-205-9 

# Extending Neutrality to Experimental Facilities

Jon Matias, Eduardo Jacob, Mariví Higuero, Nerea Toledo
University of the Basque Country (UPV/EHU)
Bilbao, Spain
{jon.matias, eduardo.jacob, marivi.higuero, nerea.toledo}@ehu.es

***Abstract*—This paper focuses on the topic of Experimental Facilities, and introduces a novel approach which extends the neutrality concept that comes from Access Networks, to the facilities. The architecture of the solution and the implementation details are also described. The OpenFlow technology is used in order to obtain network slices and virtualize the physical infrastructure. The method proposed to define the slices is the MAC address prefix. The isolation of experiments is mandatory and it is done based on these prefixes by means of a modified version of FlowVisor. A new neutral slice is introduced in the solution. No previous configuration or requirement is needed to get access to this slice. Some basic services are also available at the neutral slice (i.e., captive portal, or an authentication and authorization infrastructure). Finally, the EHU OpenFlow Enabled Facility is presented as a proof of the viability of this approach.**

***Keywords-Neutral access; Experimental Facilty; OpenFlow; netowork slice; MAC address prefix***

## I. INTRODUCTION

It is undeniable that the Internet is essential in our daily lives, at a level that was never envisaged. The problem is that the Internet was not designed for such widescale deployment. The explosion of services and the number of connected devices show some of the limitations of the Internet. Although IPv6 was designed to solve some of these limitations, IPv4 is still by far the most widely deployed Internet layer protocol.

Neverthless, the Internet is a valuable source of innovation where new services and companies find the perfect place for developing new ideas. However, these proposals should fit in network scenarios with stringent organizational rules and technical limitations (like the use of IP) to assure world wide connectivity.

Future Internet is an initiative that emerges to solve the current limitations of the Internet as we know it nowadays. There are several efforts in this direction: the GENI [1] (Global Environment for Network Innovations) project funded by the NSF (National Science Foundation) in USA, the AKARI [2] project in Japan, and the FIRE [3] (Future Internet Research and Experimentation) funded by the European Commission. Related to this, the Future Internet Assembly (FIA) is a collaboration effort between projects funded by the EU in the topic of Future Internet.

Regarding the FIRE, the European Commission envisions that promoting the innovation in the field of Future Internet is a safe bet. The idea behind this, is that any novel approach requires early experimentation and testing in large-scale environments. The FIRE initiative addresses this need, creating a multidisciplinary research environment for investigating and experimentally validating innovative ideas for new networking and service paradigms. FIRE proposes that this experimentally-driven research should take place in a large scale and sustainable European Experimental Facility.

Therefore, the Experimental Facility becomes one of the EU objectives, building one big facility available for researchers instead of funding one testbed per project. This also reduces the investment needed by new researchers and European companies to test their novel proposals in a large scale platform. The Experimental Facility provides a realistic deployment to validate revolutionary approaches, even though some of them might only be implemented in a long-term basis.

One essential requirement for the facility is to be as generic as possible in order to be able to support new clean slate approaches. Moreover, it is mandatory to accept several experiments at the same time over the same resources. In this context, the isolation between experiments is fundamental. Therefore, some kind of virtualization of the physical infrastructure is needed.

The problem is that the current technology lacks on fully supporting all these requirements. Therefore, a new proposal is needed at technological level in order to support isolation of experiments, virtualization of physical infrastructure (shared) and enabling clean slate approaches. This last requirement is the most relevant, since legacy switches are able to provide isolation and virtualization by using VLANs. However, this alternative imposes some restrictions, such as broadcast support, learning of MAC addresses, STP or Q-in-Q (if VLANs are demanded at the experiment). We are looking for a more generic approach (i.e., Layer 2 without broadcast domain or learning process).

This paper presents a novel approach for providing neutrality on the access to the Experimental Facility. Another contribution relies on the idea of using OpenFlow technology [4] to implement an facility. This means that the facility is available for everyone, and provides some basic services in order to ease and simplify the access to the platform. By adding neutrality, anyone is able to access the experimental facility and no prior step is needed (i.e., registration or authorization). A set of services and resources, such as a captive portal, are available to ease the access to the experiments. In this context, the EHU OpenFlow Enabled Facility (EHU-OEF) is presented as a proof of the viability of the proposal.

The rest of the paper is organized as follows. In Section II, several Experimental Facilities are described to analyze

 ISBN: 978-1-61208-205-9 

their evolution and how the neutrality is beneficial in those cases. Then, Section III presents the details of the proposed solution, including the system architecture and the implementation with OpenFlow. Afterwards, Section IV introduces the EHU-OEF platform deployed at the University of the Basque Country. Finally, Section V sums up some final conclusions from this paper and outlines future works.

## II. EXPERIMENTAL FACILITIES

This section focuses on some of the most relevant Experimental Facilities funded by the European Commission which are relevant for this paper providing an overview of the work carried out up to now.

### A. Evolution of Experimental Facilities in Europe

FIRE combines research into new paradigms with comprehensive test facilities where the ideas are experimented. This creates a key resource for driving European research into future networks. In fact, FIRE provides a core infrastructure and a playground for future discoveries and innovations, combining research with experimentation.

FIRE is built gradually connecting and federating existing and upcoming testbeds related to the Future Internet topic. Regarding the 7th Framework Project (FP7), there are several calls for projects specifically designed for enlarging the FIRE Experimental Facility. The FP7 ICT Call 2 (2007) represents the first wave of FIRE-specific facility projects, with projects like Federica, Wisebed, Onelab2, PII or VITAL++. The FP7 ICT Call 5 (2010) represents the next wave of FIRE facility projects, with projects like Ofelia, BonFire, Smart Santander, Tefis or Crew. Until now, the last wave of approved FIRE facility projects is the FP7 ICT Call 7, with a specific call for collaboration between Europe and Brazil resulted in a new FIRE project, FIBRE-EU. The FP7 ICT Call 8 has recently closed for evaluation.

The most relevant projects related to the topic of this paper are Federica and Ofelia. The recently started FIBRE-EU project is also relevant but there is little information available..

Federica [5] project is a Europe-wide infrastructure based on computers and network physical resources, both capable of virtualization. The facility can create sets of virtual resources according to users' specification for topology and systems. The user has full control of the resources in the assigned slice which can be used for Future Internet clean slate architectures, security and distributed protocols, routing protocols and applications.

Ofelia [6] project is creating a unique experimental facility that allows researchers to not only experiment on a test network, but also to control the network itself precisely and dynamically. To achieve this aim, the OFELIA facility is based on OpenFlow, a currently emerging networking technology that allows virtualizing and controlling the network environment through secure and standardized interfaces. In a nutshell, OpenFlow enables experimenters to change the behavior of the network as part of the experiment rather than as part of the experiment setup.

Both facilities represent important advancements in this field. However, they still suffer from several drawbacks for deploying experiments that concentrate on the protocol layer.

### B. Adding Neutrality to the Experimental Facility

This paper proposes to extend the neutrality concept which comes from Access Networks, in order to be applied in the field of Experimental Facilities.

A Neutral Access Network (NAN) [7] is a special type of Open Access Network which grants positive externality to share infrastructure, by making the access network visible to end users rather than transparent. Therefore, some services are available to users within the access network before they get access to the service edge node.

Current Experimental Facilities can benefit from applying neutrality in the access. Most of the European facilities rely on an out-of–the-band procedure to configure the slices, which is done before the slice becomes available. This limits the dynamic nature of the experiment restricting the points of access to previously configured interfaces. Moreover, it is not possible for an end user to select the target experiment, so, the user is pre-configured to access one of them. Furthermore, there is not any facility service available to support the experiments.

The main challenge of adding neutrality is the technical approach which allows the proper virtualization of resources and isolation of experiments, while providing a basic access with a set of services available for all the end users.

## III. SOLUTION DESCRIPTION

This section describes our approach for adding neutrality to the experimental facilities based on [8]. First of all, the reference architecture is presented. The Infrastructure as a Service (IaaS) paradigm is the background in which this model is defined. Resource sharing and virtualization of the network elements are the core ideas behind the IaaS concept. Once the architecture is clearly described, the next subsection presents how this is implemented. We are using the OpenFlow technology in order to build the solution. OpenFlow allows us to split up the control and data planes, and isolate and delegate the control plane of each experiment. Finally, the different types of slices that we have defined in our facility are introduced as an example.

### A. Architecture

A basic requirement for any experimental facility is to be as flexible and innocuous as possible. The aim of our Experimental Facility is to provide the required support to do research on networking, enabling the testing of new proposals in a realistic scenario.

The idea of having a common experimental facility to run multiple and diverse experiments introduces the necessity of sharing resources among different experiments. Therefore, we must deal with the idea of virtualization, since the same physical elements (i.e., nodes or links) should be available for multiple experiments.

The virtualization of the network and the delegation of the control plane to another entity (in this case the researcher behind the experiment) are common goals between our

 ISBN: 978-1-61208-205-9 

objective and the IaaS paradigm. As a result, the Generic Architecture for the Cloud IaaS Provisioning Model [9] is valid as a reference for our architecture. This model is partly a result of the EU project GEYSERS [10], which also deals with infrastructure service virtualization. In this context, it is also worth to mention the work done at 4ward project (FP7) [11]. However, this paper does not follow thoroughly their definitions and concepts, so they are properly clarified and extended when needed throughout the article.

The model consists of three layers, each playing a different role. At the bottom, the Physical Infrastructure Provider (PIP) is placed. This entity provides the physical infrastructure, i.e., it is the owner of the network nodes and links, named physical resources, PR. It is very common to find several PIPs on every experimental facility, for instance in European-wide facilities.

In the middle, the Virtual Infrastructure Provider (VIP) is located. This entity requests physical resources to one or several PIPs and generates a common view. The VIP is also in charge of virtualizing the infrastructure in order to provide these virtual resources (VR) to different experiments.

Finally, the Virtual Infrastructure Operator (VIO) is located on top of the architecture and operates the virtual infrastructure provided by one or several VIPs. The operator rules the behavior of the virtual resources and relies on the VIPs to achieve the essential isolation from other VIOs.

From the perspective of an Experimental Facility, the PIP is the owner of the hardware indispensable to build the physical facility. In the research community, it is very common that all the partners involved in the facility contribute with their own resources, while maintaining the ownership of them.

The VIP is the logical entity (i.e., it is composed of one representative of each entity) which has direct access/connectivity to the physical resources. The role of the VIP is crucial for the proper operation of the facility. On the one hand, the VIP is responsible of the virtualization of the physical resources, enabling that multiple experiments share the same network resources at the same time. On the other hand, the VIP guaranties the isolation among all the experiments, protecting each experiment from the interference of the others. A network slice is a group of virtual and interconnected resources isolated from other experiments. The VIP should assure the agreed QoS and avoid any service degradation which could have impact on their performance.

Finally, the VIO is the researcher that manages the experiment. Since we assume that our researchers do research on networking, they need the platform to impose as less requirements as possible in order to be used to prove novel approaches. In our Experimental Facility, the only requirement is the use of MAC addresses to identify the source and destination nodes. Besides, researchers need to have total control over the network slice provided by the VIP, since they want to test new networking paradigms.

### *B. OpenFlow Implementation*

This subsection describes how the previously explained architecture is implemented. First of all, the OpenFlow technology has been selected as the enabler to achieve the implementation of the three layer architecture (Figure 1).

OpenFlow is a flow-oriented technology developed at Stanford University, which splits up the control plane and the forwarding process. By doing so, an external entity, known as the controller, is able to modify (i.e., add or remove) the flow table of one or several switches through a standard interface, which implements the OpenFlow protocol.

Due to this reason, the underlying physical infrastructure of the Experimental Facility must support the OpenFlow technology. Currently, there are a great number of manufacturers that support OpenFlow, such as NEC, HP, Juniper or Brocade. The Open Networking Foundation (ONF) composed by the main actors in the networking market, aims at accelerating the delivery and use of software-defined networks (SDN) by standardizing the OpenFlow protocol. This means that the main requirement that PIPs must fulfill is the OpenFlow support by the physical resources.

As previously explained, the middle layer is the most demanding one, since it must support the virtualization of resources and the isolation of experiments. Regarding OpenFlow, there is a special deployment which enables both requirements: the FlowVisor [12]. The FlowVisor is a special type of controller which acts as a transparent proxy between OpenFlow switches (at PIP) and multiple OpenFlow controllers (VIO). The FlowVisor is the tool that allows the definition of network slices and the delegation of their control plane to the corresponding OpenFlow controller, enabling also the isolation between slices. The ability to define network slices relies on the definition of flows introduced by OpenFlow. A flow is defined as a 10-tuple (ordered list of elements) that consists of different fields, such as switch physical port, MAC address, Ethertype, IP address or TCP/UDP port.

Finally, the operator layer is responsible for ruling the actions of the virtual resources delegated to the slice which is assigned to the experiment. Therefore, the resources and the slice should follow the behavior defined by the experiment. In order to achieve this goal, each experiment has its own OpenFlow Controller managed by the researcher responsible of it. By this approach, the researcher is able to control the

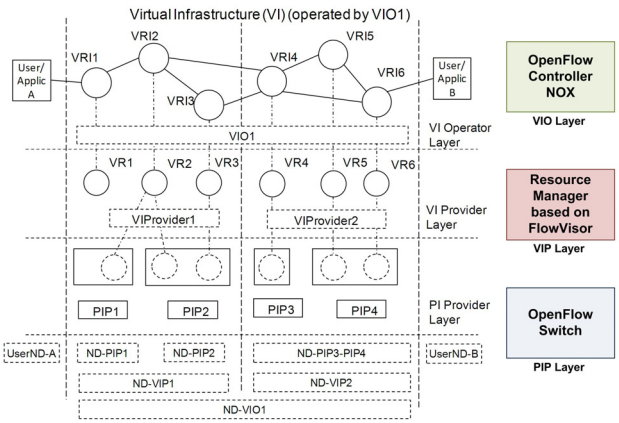


Figure 1. Experimental Facility architecture and OpenFlow implementation

entire slice, with complete isolation from other slices. As previously mentioned, the FlowVisor allows these features.

The isolation of the experiments relies on the isolation of the control plane (done by FlowVisor) of each experiment. When a new packet enters the OpenFlow enabled switch (without a previously defined/installed rule), the packet is forwarded to the FlowVisor. The FlowVisor tries to identify the target controller based on the available information/definition of slices. If there is a match, the packet is forwarded to the corresponding controller associated to the slice/experiment. In fact, all the traffic which matches the slice definition is sent to the experiment's controller. In addition, all the rules and actions allowed to be configured by this controller must be in accordance with conform the definition. Therefore, the infrastructure is shared at the data plane, but only the appropriate controller is able to install the forwarding rules associated to the experiment.

As a summary, the PIPs provide the OpenFlow switches, the VIP relies on the FlowVisor and the VIOs manage the OpenFlow Controllers.

One fundamental decision to take is how network slices are going to be defined. The FlowVisor has the ability to define the slice at different layers (physical, link, network and transport) or as a combination of them. Moreover, each slice can be defined independently of the definition of other slices. However, from the Experimental Facility point of view, it is easier to have a common definition, both for management and traceability.

In our facility, we propose a new method to recognize and distinguish the network slices: the MAC address prefix. This means that the first part of the MAC address univocally identifies the associated slice. This new method only needs one Layer 2 prefix to define and identify the slice, whereas a traditional method needs each and every MAC address to identify the associated slice. Therefore, our new method imposes less administration overhead. For instance, if there are 100 slices with 100 clients per slice, the former method manages 100 prefixes, whereas the latter method needs 10.000 entries to identify the slice associated to each client.

From the management point of view, the setup of a new experiment is very easy: the VIP only needs to find out one free MAC prefix and assign it to the slice associated to the experiment. All the decisions and control actions with regard to the traffic that use that MAC prefix (at the data plane) are redirected to the OpenFlow Controller associated to the corresponding experiment.

From the experiment perspective, all the end nodes involved in the experiment must be configured properly with a MAC address that begins with the delegated prefix. In doing so, there are different options that we have tested: manual or dynamic configuration, and rewriting.

From the user's perspective, the change of the MAC address is not relevant, since the one that they use was assigned by the manufacturer just to assure its uniqueness. From the operator's perspective, the change of their customers' MAC addresses is not a problem, since once they cross a router the MAC changes. Furthermore, the operators will pursue to change the MAC addresses if this allows them to reduce the management effort. It is worth mentioning that trying to identify or authenticate the users by its MAC address is an error. This is because on the one hand, the MACs can be easily spoofed, and on the other hand, they do not identify a user, but just the network card.

The manual configuration depends on the operating system, but there are tools to change the MAC address. For instance, in Linux it can be as easy as changing the IP address. Moreover, when using virtual machines, in some cases, the MAC address can be statically assigned.

We have also developed a service which dynamically configures the MAC address of the end user depending on the experiment that is selected which works on Linux.

The user has the ability to select the target experiment by using the facilities available at the neutral slice. This selection implies that the MAC address to be configured shares the same prefix with the rest of the users of that experiment. Therefore, the MAC is delegated by the experiment slice to the user. This process is similar to the DHCP at the IP layer (nothing in common with SLAAC in IPv6).

The third option, the rewriting, works with independence of the end device, since the MAC address is rewritten at the first OpenFlow switch. The rewriting of the MAC address is a capacity available at OpenFlow specification.

Nowadays, the 1.0 version is the most widely deployed version of OpenFlow, which we are using in our experiments. However, the definition of MAC prefixes is not supported until version 1.1, which is also available at current standard version 1.2. This means that some modifications are needed due to our network slice definition.

In order to implement our solution, the FlowVisor must be modified. The current version of FlowVisor only permits to specify a complete MAC address as a parameter to define the slice, which does not have the needed granularity. So, we decided to adapt the FlowVisor, which is open source and written in Java.

There are two main parts that we have changed: the definition of slices and the matching procedure. On the one hand, the method to describe the slice in order to associate the controller has been upgraded. A new parameter appears: the prefix of the MAC address. On the other hand, the FlowVisor analyzes all the control traffic to identify the associated slice, and corresponding controller to which the OpenFlow packet should be redirected. Therefore, the matching procedure has been also upgraded in order to enable the ability to identify MAC prefixes. With these two upgrades, the FlowVisor is able to work as expected.

### *C. Slices*

This subsection presents different types of slices identified at our Experimental Facility. Moreover, the foundations of the neutrality at experimental facilities are explained.

First of all, it is worth mentioning that we have decided to combine both production and experimental traffic over the same infrastructure. This is possible thanks to the OpenFlow technology, which allows us to isolate production traffic from experimentation, and try novel proposals using the same resources.

 ISBN: 978-1-61208-205-9 

We have identified three different types of slices: neutral slice, production slice and experiment slice.

The first slice is the neutral slice. As its name suggests, this slice enables the neutrality at the Experimental Facility. This means that anyone is able to get access to this slice. In other words, no prior requirement is needed, no registration process is demanded, and no authentication procedure has to be launched. There are some services that are available at the neutral slice, such as a captive portal with general information about the Experimental Facility, and some other web based services with free access. Therefore, the end user is conscious of the existence of the neutral slice in which several services can be accessed. The neutral slice is also the basic infrastructure to demand access to one of the other slices, either the production slice or one specific experiment slice.

The second slice is the production slice. This slice carries the corporative traffic and gives connectivity to the services provided by the University, both Intranet and Internet access. Since the corporative traffic needs a public IP, a DHCP service is running and IP spoofing is avoided (very easily configured through OpenFlow rules). The production slice relies on a NOX [13] controller with a switch module, that means that all the network elements behave as traditional switches. The access to the production slice is controlled by an authentication and authorization process, which relies on the IEEE 802.1X standard. The production slice is able to identify the EAPoL traffic and redirect all this traffic to the corresponding authenticator (an entity defined by IEEE 802.1X), and then to the RADIUS server. In order to access this production slice, the users must be part of our research group and hence, be subscribed to our LDAP service. Once the AuthN/AuthZ process is successfully completed, the user gets access to the production slice. The first step then is the DHCP service, which is needed to request a valid public IP to get access to Internet.

The last type of slices are the experiment slices. Each experimental slice is requested by a researcher who wants to try a novel proposal, and a new MAC prefix is allocated and assigned to the experiment. As mentioned before, this operation reduces the management overhead, since it is not required to track the MAC addresses of each client. From that moment and on, all the traffic which enters to the Experimental Facility with such prefix is ruled by the Controller owned by the same researcher who asked for the slice. Each experiment has a different behavior and relies on different layers, which can be the commonly known link or network layers or innovative and new layers. This means that each experiment has a unique manner of doing forwarding, and nothing should be assumed. As an example, in one slice a node can be working as a switch, in another one as a router, or in another as something completely new. However, there are some common procedures among all the experiment slices: (1) the user must configure the MAC address (manually, dynamically, or rewriting); (2) an authentication and authorization procedure must be completed before getting access to the experiment slice; (3) from this point and on everything depends on the experiment. The AuthN/AuthZ procedure is similar to the one that takes place at the production slice because both are based on IEEE 802.1X standard. In this case, the authenticator and the RADIUS server can be part of the experiment resources or the experiment can rely on a general authentication service which is provided at the neutral slice. In both options the researcher manages the users who are able to access his experiment slice. In order to manage the users and their credentials, the researcher can rely on the LDAP service (managed by our group) or any other service configured by the researcher.

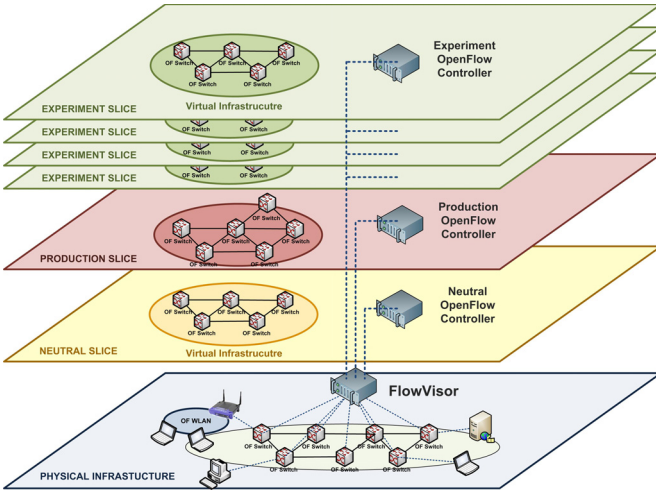


Figure 2. Slices at the Experimental Facility

In conclusion, at this moment, we have one neutral slice, one production slice and as much experiment slices as new good proposals to be tested.

## IV. EHU-OEF AS A RESULT

This section introduces the EHU OpenFlow Enabled Facility (EHU-OEF). This facility represents a campus wide infrastructure that supports an early implementation of the previously explained approach. The EHU-OEF validates and demonstrates the feasibility of the proposed solution. This facility also applies the neutrality concept to the Experimental Facilities. This is done by adding a new neutral slice with a set of resources and services (available for anyone), which are helpful for the entire facility.

To the best of our knowledge, the EHU-OEF is one of the biggest OpenFlow infrastructure deployed in Europe for daily operation. Moreover, it is one of the few OpenFlow infrastructures in production, which means that both production and experimental traffic share the same resources.

The EHU-OEF can be categorized also as a Campus Network case, and serve as an example of what can be achieved in both a Campus and an Experimental Facility. Obviously the objectives of both networks are different, but the EHU-OEF presents a wide variety of use cases which can cover both types.

### A. *Platform description*

This subsection describes the EHU-OEF infrastructure and provides a low level detail about the platform.

 ISBN: 978-1-61208-205-9 

From the architectural point of view, the three entities have been implemented: PIP, VIP and VIO. Starting from the bottom, there are several PIPs providing infrastructure to the facility. The I2T research group (our group [14]) provides all the OpenFlow enabled switches and some of the fiber and copper links between them. The University of the Basque Country mainly provides the interconnection fiber links at campus level. Euskaltel, a local Telco operator, provides the intercampus fiber links (20 km link at 10 Gbps). The Basque NREN, i2Basque [15], provides a redundant 1 Gbps link for the intercampus connectivity. Finally, the Spanish NREN, RedIRIS [16], provides the 10 Gbps connectivity to the RedIRIS Nova PoP.

On top of the physical infrastructure, the VIP layer is provided by the I2T research group. In particular, a modified version of FlowVisor is managed (and also developed) by the I2T. This enables the virtualization of resources and isolation. In addition, it is based on the approach presented in this paper to define the network slices, the MAC prefixes.

The last layer defines multiple VIOs running on top of the FlowVisor. Last but not least, there is a NOX controller for the neutral slice, another NOX controller with a legacy switch module for the production slice, and several different controllers (most of them are NOX controllers with different specific modules developed by network researchers at I2T) one per each experiment slice.

From the organizational point of view, since the EHU-OEF is located at the University, there are several types of spaces covered by the Experimental Facility. The I2T research laboratory constitutes the core of the facility and the first area deployed. There are also some professor's offices also connected to the platform. Moreover, some of the laboratories used at the telecommunication degree for teaching purposes are also involved in the facility. Finally, there are also Data Centers connected to the EHU-OEF. One of this is owned and maintained by the I2T research group, while another one is run by the UPV/EHU.

From the physical and OpenFlow resources point of view, the EHU-OEF consists of a variety of equipment. There are seven NEC switches (IP8800/S3640 OpenFlow enabled), two NetFPGAS and four WiFi APs (Pantou). The OpenFlow Enabled Facility has a 10 Gbps core, with at least 1 Gbps links to connect the end nodes and redundant paths. Figure 3 shows the current deployment of the facility.

The OpenFlow control traffic is configured as in-band traffic at the NEC switches, which means that the same physical links are used to carry both data and control planes. The VLAN 100 has been defined for this purpose. The in-band configuration has the advantage of not using an extra link to each node (maintaining a parallel network), but the main drawback is that the control plane is affected by the data plane traffic, so congestion, or link failures can happen.

### *B. Use cases at I2T*

Several use cases have been identified at the EHU-OEF, which demonstrate the benefits of using this approach. First of all, different profiles appear at the platform: professor, researcher and student. Each type of user has its own permissions and different scope and necessities.

Currently, the profiles are managed by using VLANs, which are statically assigned to physical ports. Nevertheless, it is possible to dynamically configure the VLANs depending on the result of an AuthN/AuhtZ process, but this is not the case at the University. However, by using dynamic configuration, the facility will be restricted by the legacy behavior of the switches, and new proposals will need to deal with procedures like broadcasting, learning or STP. Therefore, it is not possible to fully support the aforementioned use cases.

One of the main advantages of having a procedure to select the target slice and an identity based access control, is that the location is no more a limitation for accessing specific resources. On the other hand, the specific location does not grant indiscriminate access to a set of resources.

If we consider the professor use case, there are multiple alternatives. Professors can demand corporative access not only at their office, but also at the research lab or even in class for some explanation. That is, they demend privileged access to specific resources. They also do research, so they need to get access to the experiment slices not only from the lab, but also from their offices. Finally, the students use a specific slice for setting up a experiment at the lab, after that the professor may need access to that slice to evaluate the work done by the students. The professor has the ability to evaluate the students from its office anytime. Moreover, there can be other students at the lab at the same time.

The second possibility is the researcher use case. The main focus of researchers is doing research. For this use case, we assume that the research lab is their main point of connection. They need corporate connectivity and access to experiment slices. The researchers are the main developers of new modules for the OpenFlow Controllers which rule the different slices. However, due to the distributed nature of the networking experiments, it is expected that they have both types of access at any location throughout the facility. Moreover, the researchers can give lessons as an assistant lecturer or even attend classes as PhD student.

The third option is the student use case. The main point of connection for students is the practice lab. They need both corporative connection to get access to the Internet, and

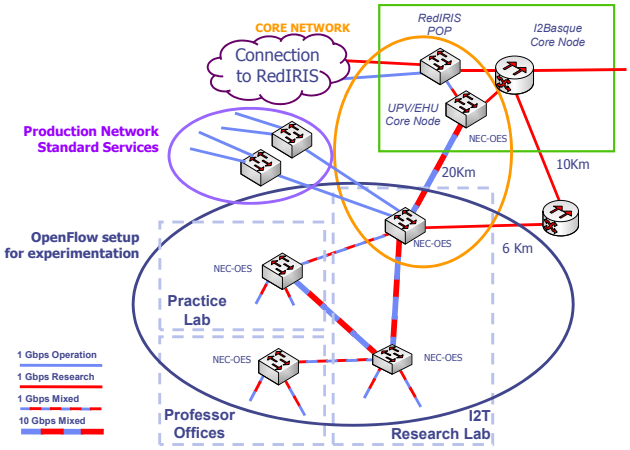


Figure 3. EHU OpenFlow Enabled Facility

 ISBN: 978-1-61208-205-9

access to experiment slices defined by the professors. However, the students can be also be part of research groups, in which they develop and test their own projects (i.e., MSc thesis). Therefore, they also need to get access to some specific experimental slices. Students can develop their own modules for the Controller.

We expect to have performance results that will show the proper operation of the solution and the saving at the operational and administration level.

## V. CONCLUSIONS

In this paper, the applicability of the neutrality concept, which comes from access network, in the context of Experimental Facilities is analyzed and tested. In addition, we also provide an overview of the efforts conducted hitherto in the field of FIREs and Experimental Facilities.

The main benefit of adding a neutral access to the facility is that the experimental setup and the location of end users can be more flexible and easily evolved over time. Otherwise, the initial setup should be done previously, with some out-of-band tools, as it is done in most of the current facilities. Another important benefit is that the neutral slice provides the platform with a group of basic services that are available for the rest of the slices. Moreover, this neutral slice lowers the barrier of entry to the facility.

The core contribution presented in this paper is the specification of a novel network slice definition. In our approach, the network slices are defined by a unique MAC prefix, which enables a full VLAN space per slice. Each slice defines its own behavior relying on its Controller, can be IP-based, Ethernet-based, MAC prefix-based, with or without support of certain features such as broadcast and so on. Each Controller has total control over the resources assigned to the slice, enabling the path computation and traffic engineering abilities. Regarding the slice isolation, the control plane is isolated by the FlowVisor, and the data plane relies on the flow entry definition and its associated action.

Due to the fact that the facility relies on the MAC prefix to identify the target slice, MAC spoofing could be a problem. However, this problem has a known scope, because the facility only allows traffic with that MAC address on one physical port, as long as it was previously authenticated. It should be noted that this attack only succeeds if it is done at the same physical port and using a MAC address previously authorized. Therefore, the attacker must be at the same port, which it is only possible if the port is shared between multiple end users. Otherwise, the access control is done and the new MAC address should be authorized at the slice. The establishment of the IEEE 802.1AE standard (MACsec) completely solves the problem, since integrity and ciphering support in the access removes the possibility of any spoofing. On the other hand, IP spoofing should be controlled by each slice's controller, whereas the MAC spoofing is controlled by the facility.

The scalability of this approach has two sides. On the one hand, the management is reduced by administering the Layer 2 by using MAC prefixes, instead of the complete list of the client's MAC addresses. On the other hand, the scalability of OpenFlow is a known topic on which people are doing research. The main issue is that the control plane is centralized, with the benefits and also the drawbacks that this implies. A resilience architecture and well dimensioned system could reduce the impact on their scalability.

Currently we are working on adding QoS support to the EHU-OEF. By doing this, we will be able to assure the required network performance for each slice. The main challenge is the lack of QoS support (quite rudimentary) in current versions of OpenFlow. The good news is that it is a known drawback and people are working to solve this issue.

The main proof of the feasibility of this approach is the EHU-OEF infrastructure, which is up and running in a real deployment with production traffic. In the same platform, there are multiple and different experiments which coexist over the same physical resources. We are currently conducting massive tests which are showing the proper behavior and operation of the facility.

## ACKNOWLEDGMENT

This work has been partially funded by the Spanish MICINN project A3RAM-NG (TIN2010-21719-C02-01), and the Basque Government Strategic Research Project Future Internet II (IE11-316). It is also supported by the University of the Basque Country's Training and Research Unit for Telecommunications and Electronics (UFI11/16).

## REFERENCES

[1] GENI [http://www.geni.net: April, 2012]

[2] AKARI [http://akari-project.nict.go.jp/eng/index2.htm: April, 2012]

[3] FIRE [http://cordis.europa.eu/fp7/ict/fire: April, 2012]

[4] N. McKeown et al., "Openflow: Enabling innovation in campus networks". ACM SIGCOMM Computer Communication Review, vol. 38, no. 2, pp. 69-74, 2008

[5] FEDERICA [http://www.fp7-federica.eu: April, 2012]

[6] OFELIA [http://www.fp7-ofelia.eu: April, 2012]

[7] A. Bogliolio, "Introducing Neutral Access Networks", Next Generation Internet Networks (NGI 09), Aveiro (Portugal), pp. 1-6, 2009

[8] J. Matias, E. Jacob, N. Toledo, and J. Astorga, "Towards Neutrality in Access Networks: A NANDO Deployment with OpenFlow", 2nd International Conference on Access Networks (ACCESS 2011), Luxembourg, pp. 7-12, 2011

[9] Y. Demchenko et al., "On-demand provisioning of cloud and grid based infrastructure services for collaborative projects and groups". Collaboration Technologies and Systems (CTS 2011), Philadelphia (USA), pp. 134-142, 2011

[10] GEYSERS [http://www.geysers.eu: April, 2012]

[11] Z, Liang et al., "Virtualization Approach: Evolution and Integration". Public Deliverable D_3.2.1. 4ward – Architecture and Design for the Future Internet. June 2010.

[12] R. Sherwood et al., "Flowvisor: A network virtualization layer", Technical Report Openflow-tr-2009-1, Stanford University, October 2009

[13] N. Gude et al., "NOX: Towards an Operating System for Networks", ACM SIGCOMM Computer Communication Review, vol. 38, no. 3, pp. 105-110, July 2008

[14] I2T research group [http://www.i2t.ehu.es: April, 2012]

[15] i2Basque [http://www.i2basque.es: April, 2012]

[16] RedIRIS [http://www.rediris.es: April, 2012]

 ISBN: 978-1-61208-205-9 

# NAN Tools: An Open-Source Tool Suite for Interoperable Neutral Access Networks

Roberto Del Bianco Andrea Seraghiti Alessandro Bogliolo
*Information Science and Technology Division of DiSBeF*
*University of Urbino*
*Urbino, Italy 61029*
*Email: alessandro.bogliolo@uniurb.it*

***Abstract*—Although IP traffic has been growing exponentially for years and it is expected to keep following the same rate in the near future, current business models do not allow operators to benefit from traffic growth and they fail in motivating investments in next generation networks. In the absence of sufficient investments, operators are induced to avoid congestion by means of traffic management strategies which raise neutrality issues. In spite of the heated debate on net neutrality, all the players involved in the Internet value chain agree in saying that new models are required to overcome broadband stagnation and support innovation. Neutral access networks (NANs) have been recently proposed as means for enabling the development of the Internet without threatening network neutrality. Although the NAN model has been implemented and tested for several years in the *Urbino Wireless Campus* test-bed, its actual applicability requires the availability of a tool suite flexible enough to adapt to different situations and to enable inter-operation among networks managed by different entities. This paper presents the *NAN tools*, an open-source tool suite which enables the employment of scalable and inter-operable NANs on top of Linux. The NAN tools have been successfully ported on embedded systems based on OpenWrt and tested on low-cost MikroTik RouterBOARD.**

***Keywords*-Neutral access network; Tunneling; Policy routing; Scalability; Interoperability**

## I. INTRODUCTION

It is a fact that the vertically integrated business models adopted by network operators, combined with flat-fee access rates, have become inadequate to sustain the development of network infrastructures. Although such a model has played a fundamental role in the diffusion of the Internet, it has created a short-circuit between end-users and *over-the-top* (OTT) service providers which has determined an exponential growth of IP traffic with limited benefits for network operators [1]. The misalignment between costs and revenues, together with the imbalance of capitalization in the Internet market [2], is bringing access networks to congestion, inducing operators to adopt counter-measures which threaten neutrality either by applying traffic management policies, or by signing discriminatory agreements with OTT operators. The public consultations on network neutrality launched worldwide by the regulation authorities provide evidence of the awareness of the urgency of a transformation [3]. It has been recently shown that a service-oriented network model, as opposed to an access-based model, could help overcome the stagnation without threatening network neutrality [4]. *Neutral access networks* (NANs), originally proposed as a mean for bridging digital divide in market-failure regions [5], provide a viable support to the implementation of the changes required to sustain the development of the Internet.

This paper presents the *NAN tools*, an open-source tool suite which enables the implementation of a NAN on top of a Linux-based OS, according to the model described by Seraghiti et al. in 2009 [6]. In particular, the paper is focused on scalability and interoperability issues and solutions. Section II provides an overview of the NAN model and architecture, pointing out scalability and interoperability issues, Section III outlines the solutions provided by the 1.1 release of the NAN tools, Section IV describes the embedded version of the NAN tools and reports the results of preliminary experiments conducted on a low-cost MikroTik RB133 running OpenWrt, Section V concludes the work.

## II. NAN MODEL AND ARCHITECTURE

A NAN is an open access network which provides a shared access infrastructure with three main features: *i)* it allows end-users to associate with the network even if they are not registered with an operator; *ii)* it allows service providers to expose their service to unauthenticated users directly within the access infrastructure; *iii)* it allows end-users to dynamically select the gateway (i.e., the Internet service provider) to be used to connect to the Internet. Although the NAN model is access-technology agnostic, its most natural embodiment is provided by open Wi-Fi networks exposing a common SSID, because of the ease of association of any kind of mobile and portable devices.

Figure 1 shows the reference architecture of a NAN, as proposed by Seraghiti et al. [6]. The network is open to any unauthenticated user, who associates with an it access island and is assigned (either statically or dynamically) with a unique IP address. In general, IP addresses can be taken either from public or from private pools. For the sake of explanation, private IPs are used in Figure 1 to annotate network nodes.

 ISBN: 978-1-61208-205-9 

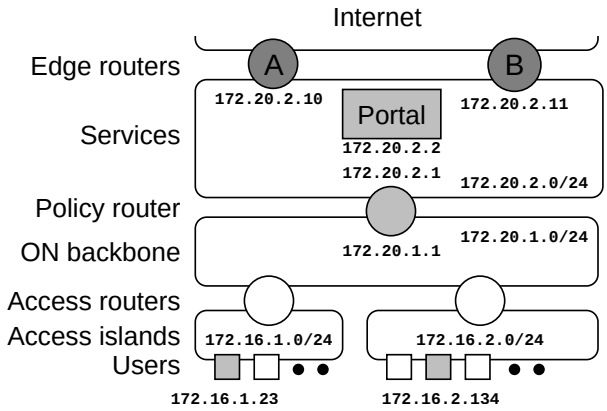


Figure 1. Reference architecture of a NAN.

Technological diversity and evolution are guaranteed by the coexistence of multiple access islands possibly managed by different operators. All of them are connected to the *operator-neutral* (ON) backbone by means of access routers. In the simplest scenario, access routers are network termination points, which can be Wi-Fi hot spots, Hiperlan/WiMax base stations, or digital subscriber line access multiplexers (DSLAMs). The ON backbone is the networked infrastructure which provides connectivity between access routers and services.

The main architectural element is the router placed between the backbone and the service network, called *policy router*. The name denotes its ability to implement advanced routing policies possibly based not only on destination IP addresses, but also on other parameters, such as the source IP address used for the so-called *source-based policy routing*. For the sake of simplicity here we assume that the ON backbone is organized as a unique sub network and that there is only one policy router, which is the default gateway of the ON backbone. Generalization and scalability will be discussed in Section II-A.

Online services available within the access network are published in a service subnet, which includes a captive portal (denoted by Portal in Figure 1) used to redirect end-users to a predefined landing page as they attempt to access an external URL which is not included in any white-list. The landing page belongs to the internal web portal which grants direct access to all internal services and allows end-users to make a choice among many different edge routers (managed by different SPs/ISPs) to gain access to the external services and to the Internet.

As the user makes his/her choice, a source-based policy rule is dynamically created on the policy router in order to forward across the selected edge router all the external packets originated from the IP address of the user.

### A. Scalability and interoperability

There are three main issues which limit the scalability of the NAN architecture depicted in Figure 1: *i*) the ON backbone is implemented as a single broadcast domain, *ii*) all the services are published within the same subnetwork, and *iii*) the policy router is a bottleneck for the traffic generated by the end users. Figure 2 shows a generalized architecture which has been proposed to address such issues by allowing network segmentation, load balancing, and interoperation [6].

*Network segmentation* can be used both to split the backbone into several broadcasting domains and to organize services and edge routers in several subnetworks. Subnetworks containing edge routers need to be connected to the backbone by means of policy routers, while standard routers can be used to grant access to those subnetworks which publish only internal services (this is the case of service Sy in Figure 2).

*Load balancing* and path optimization strategies can be implemented in the ON backbone by using more than one policy router. Each policy router can be either statically defined as default gateway for specific access islands, or dynamically chosen by the routing protocol, such as *boarder gateway protocol* (BGP) and *open shortest path first* (OSPF). In Figure 2, two policy routers (namely, 1 and 2) can be used to gain access to service Sx and to edge routers $A$ and $B_L$ in the left-hand side NAN.

*Interoperability* among different NANs can be achieved by creating a tunnel between their backbones and by allowing end-users to traverse the tunnel as any other edge router. Figure 2 shows two inter-operating NANs, denoted by **L** (i.e., left) and **R** (i.e., right), the ON backbones of which are connected by means of a tunnel.

## III. NAN Tools

The NAN tools exploit the support for advanced routing provided by the Linux kernel [7] in order to implement the key elements of the NAN architecture of Figure 2, namely, the policy router and the portal.

In the simple example of Figure 2 we have two NANs (**L** and **R**), three policy routers (1, 2, and 3), two portals (Portal$_L$ and Portal$_R$), 4 edge routers (A, B$_L$, B$_R$, and C), and a tunnel. Each policy router contains specific routing tables for all the edge routers which can be selected by the end-users. All the tables are statically created and listed in the `rt_tables` file with the corresponding priorities. Whenever an end-user makes his/her choice, his/her source IP is dynamically added to the corresponding table in the policy router in order to set the preferred edge router as default gateway for that user by means of *source-based policy routing* [7]. It is worth noticing that tunnels leading to other NANs are treated as edge routers at this level. For instance, policy routers 1 and 2 in NAN **L** contain three

 ISBN: 978-1-61208-205-9 

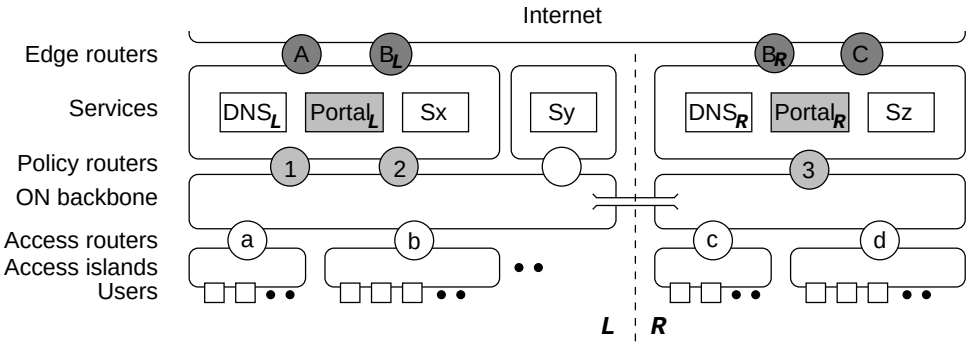


Figure 2. Generalized architecture of two inter-operating NANs.

routing tables for A, for $B_L$, and for the tunnel leading to NAN **R**.

The NAN tools prevent the IP address of a given user to appear in two or more tables simultaneously. Synchronization between the web-based front-end, which allows the end-user to make his/her choice, and the back-end, which implements the corresponding rule, is based on a data base: the front-end adds a pending rule in the DB upon user's request, while the back-end periodically checks the DB, applies all pending rules, and changes their status to active.

When the edge router of choice is a tunnel towards a different NAN (say, NAN **R** in our example), the end-user is redirected to the captive portal of the target NAN (i.e., $Portal_R$) where he/she can eventually make a further choice among the edge routers available in that network (i.e., $B_R$ and C).

This simple mechanism, which has been implemented in the release 1.0 of the NAN tools and applied on the *Urbino Wireless Campus* test-bed since 2009 [8], [6], assumes that each policy router has its own DB and works independently of all other policy routers. These assumptions, however, limit the flexibility of the architecture depicted in Figure 2 and make it difficult to maintain consistency in case of multiple inter-operating NANs. The solutions adopted in release 1.1 of the NAN tools are outlined in the rest of this section.

### A. Dynamic load balancing and redundancy

If more than one policy router is made available on a NAN, the trivial solution for load balancing consists on statically assigning different access islands to each of them. In this case, each access island has one of the policy routers specified as default gateway and it works exactly as if it was the only policy router in the NAN. In particular, each policy router contains only the rules of the end-users assigned with it. For instance, in our example routers 1 and 2 could be used by access islands a and b, respectively.

This situation, however, is incompatible with the optimizations possibly performed at run time by dynamic routing protocols which route packets towards the least loaded nodes. In fact, the traffic generated from access island b cannot be routed across policy router 1 if this latter doesn't contain the rules set by end-users originally assigned to policy router 2.

To provide support to dynamic load balancing, policy routers 1 and 2 should be allowed to share the same DB of policy routes. This can be done by connecting the back-end of both policy routers to the same DB, and by replacing the status flag associated with each rule with a status table which specifies the status associated with each `(rule, router)` pair. In this way, the back-end daemons of the policy routers are allowed to independently access the DB and change the status flags of their rules without interfering with each other.

The same mechanisms can be exploited to enhance reliability by allowing each user to specify a secondary router to be used in case of failure of the default gateway without losing the settings.

### B. Loop avoidance

According to the basic inter-operation mechanism described so far, any user of a NAN can reach one of the edge routers available on another NAN provided that a path exists between his/her own default gateway and the policy router leading to the target edge router. Consider, for instance, a user associated with access island `a` who wants to reach edge router C. First, he/she has to set a rule on policy routers 1 and 2 in order to forward his/her traffic towards the tunnel leading to router 3. Then he/she has to set a new rule on 3 in order to be forwarded to edge router C. The captive portal of NAN **R**, however, allows end-users not only to choose between edge routers $B_R$ and C, but also to be forwarded to NAN **L** across the tunnel (which is always treated as an additional edge router). If, by any chance, the end-user coming from **L** decides to make this last choice, a loop occurs which causes the packets originated by that end-user to keep bouncing between the policy routers of the two NANs until the *time to live* expires and the packets are dropped.

In order to avoid this situation, each policy router should prevent end-users from choosing the network they come

 ISBN: 978-1-61208-205-9 

from. This can be done by making policy routers aware of the pools of source IP addresses belonging to each NAN. In the NAN tools, this mapping is stored in a specific table of the DB the records of which associate the identifier of each NAN with one or more IP ranges. It is worth noticing that *network address translation* (NAT) can be performed at the termination points of the tunnel established between two NANs, by changing the addresses of the IP packets traveling across the tunnel, in order to relax the constraints on the address ranges used in each NAN.

### C. Go back mechanism

The loop avoidance solution described in the previous subsection has an annoying side effect: it doesn't provide to end-users any intuitive mechanism to go back to their original networks. To this purpose, in fact, they should explicitly go to the landing page of their original captive portal (the reachability of which could be guaranteed by top-priority routing tables local to the original policy routers) and select a different edge router to avoid their traffic to be redirected towards the tunnel.

Instead of pretending end-users to remind the addresses of the captive portals of their own networks, the landing page of the captive portal of the host NAN (**R** in our example) should contain a `GO BACK` button directly linking to their original NAN (**L**). Since the actual link associated with the `GO BACK` button depends on the NAN from which the user comes, such a link is stored in the same table introduced in previous subsection for loop avoidance reasons, which contains the IP ranges associated with each neighboring NAN.

When the user presses the `GO BACK` button, he/she is redirected to the landing page of the captive portal of his/her NAN, the rule is removed from the DB, and a new edge router can be chosen.

It is worth mentioning that multiple hops can be made by the same user across inter-operating NANs before reaching the target edge router leading to a specific service or to the Internet. In case of multiple source-based policy rules, the `GO BACK` mechanism allows the end-user to backtrack step by step.

### D. Persistence

As explained so far, source-based policy rules are dynamically applied upon user's request. Each rule, however, can be specified either as volatile or as persistent by setting a flag in the DB. Persistent rules are restored upon reboot of the policy router, while volatile rules are reset. In the NAN tools this choice is made by the network administrator, since it has to be consistent with network configurations. In particular, since policy rules are based on source IP addresses, it would be inconvenient to have persistent rules in a network which dynamically assigns IP addresses to users' terminals. For the same reason, a maximum idle time can be specified which allows the policy router to remove the rules of idle users.

## IV. EMBEDDED VERSION

The tool suite described so far makes use of three main components: the support for advanced networking provided by Linux, a data base management system (dbms), and a http server with PHP support. In general, the policy router provides only networking functionalities, while it relies on external servers for dbms and httpd functionalities. Nevertheless, in a simple scenario of a NAN with a few access islands serving a limited number of users (say, less than 100 simultaneous users) it would be more practical and less expensive (both in terms of investments and in terms of operating costs) to have the entire tool suite running on an all-in-one appliance. Examples of such a scenario include common situations like small companies, hotels, and coffee shops.

The embedded version of the NAN tools has been developed to provide a low-cost all-in-one solution to these needs, targeting *MIPS* architectures running *OpenWrt* (a Linux distribution for embedded systems providing packet management and a writable file system [9]).

OpenWrt provides all the packets required to solve the dependences of NAN tools 1.1 without any porting effort: namely, Apache web server, MySQL dbms, PHP, openvpn, and the advanced networking functionalities of the Linux kernel (i.e., *iptables* and *iproute2*). In order to minimize hardware requirements, however, the embedded distribution of the NAN tools makes use of *SQLite* [10] in place of MySQL and *uHTTPd* [11] in place of Apache.

While the PHP code written for Apache is fully compatible with uHTTPd, switching from MySQL to SQLite required a partial redesign of some of the classes due both to the serverless nature of SQLite and to the different syntax it understands. The object-oriented paradigm adopted in the development of the NAN tools enabled a suitable encapsulation of the changes required. As for the firmware, an image of OpenWrt was created containing all the packages required to run the NAN tools. Once the image file is installed on the target device, the *unified configuration interface* (UCI) can be used for configuring the policy router before installing the NAN tools. An example of system configuration is provided in Figure 3.

### A. Performance

Conservative performance tests of the embedded version of the NAN tools were run on a MikroTik RouterBoard RB133, featuring a 175MHz MIPS CPU with 32MB of DRAM, 3 ethernet interfaces, 3 MiniPCI slots, 2 802.11g wireless interfaces, and 128MB of NAND flash. The computational power of the RB133 is lower than that of all state-of-the-art low-cost RouterBoards featuring at least 3 network interfaces [12].

 ISBN: 978-1-61208-205-9 

```
# uci set system.@system[0].hostname=NANTools
# uci set system.@system[0].zonename=Europe/Rome
# uci set system.@system[0].timezone=CET-1CEST,M3.5.0,M10.5.0/3
# uci commit system
# echo "$(uci get system.@system[0].hostname)" > /proc/sys/kernel/hostname
# uci set network.lan.ipaddr=192.168.1.222
# uci set network.lan.netmask=255.255.255.0
# uci set network.lan.gateway=192.168.1.1
# uci set network.lan.dns=8.8.8.8
# uci commit network
```

Figure 3. Example of configuration of a policy router based on OpenWrt.

Tests where performed using *ab*, the Apache http server benchmarking tool, and *curl-loader*, an open-source tool simulating application load coming from multiple clients with their own IP addresses.

Since the typical usage pattern of a NAN entails a set-up phase, in which a new client choses its preferred edge router and the corresponding rules are set in the policy router, and a navigation phase, in which the rules are used to forward client's packets to the edge router of choice, two sets of experiments were needed to test the performance. The first set was aimed at measuring the time taken by the policy router to serve incoming requests, while the second set was aimed at measuring the overhead introduced by source-based routing during normal transactions.

The average time per request was of: 16.23ms to provide a static html page containing a single line of text, 518.35ms to provide a dynamic PHP page with the same content, 615.48ms to access a PHP page reading a record in the DB, 922.05ms to access a PHP page inserting a record in the DB, 666.75ms to insert a rule in iptables, and 761.00ms to insert a rule in iproute2. The most time consuming tasks were PHP executions (around 500ms) and DB insert operations (about 400ms). All the tests were iteratively performed for increasing levels of concurrency (up to 250) to test both robustness and performance scalability. All incoming requests were properly served, while, as expected, the delay scaled linearly with the number of concurrent requests. No significant overhead was introduced by source-based policy routing in terms of round-trip time and throughput.

To summarize the performance of the low-cost embedded platform used as policy router, we can say that it can take up to 1 second to set up a rule, while it introduces a negligible overhead on any other network operation.

## V. Conclusions

The *NAN tools* are an open-source tool suite for implementing *neutral access networks* (NANs) [5]. This paper has presented the solutions provided by the NAN tools to the main scalability and interoperability issues which have to be faced in order to enable the actual applicability of the NAN model. The proposed solutions rely on source-based policy routing, as made available by the Linux support for advanced networking.

All the solutions outlined in this paper have been implemented in release 1.1 of the NAN tools, which is now under test within the *Urbino wireless campus* testbed [8], which counts more than 20,000 registered users and serves up to 500 simultaneous users.

An all-in-one embedded version of the NAN tools has been also implemented and tested on a MikroTik RouterBoard RB133 running OpenWrt, the performance of which can be regarded as a lower bound of state-of-the-art low-cost network processors. Experimental results demonstrate the practical applicability of the proposed solution.

The source code of the NAN tools is available online at http://www.wireless-campus.it:8000/nan-tools/.

## Acknowledgment

The research leading to these results has received funding from the EU IST Seventh Framework Programme ([FP7/2007-2013]) under grant agreement n 25741, project ULOOP (User-centric Wireless Local Loop), and from the Italian ICT4University Programme, project U4U (University for University).

The authors would like to thank Andrea Mazza and Tommaso Battazzi for their valuable contribution to the implementation of the NAN tools.

## References

[1] A. T. Kearney, "A Viable Future Model for the Internet," *A.T. Kearney report*, 2010.

[2] ——, "Internet Value Chain Economics," *The Economics of the Internet, Vodafone Policy Paper Series*, 2010.

[3] European Commission, "Report on the public consultation on The open internet and net neutrality in Europe," *Electronic Communications Policy*, 2010.

[4] E. Pigliapoco and A. Bogliolo, "A Service-Based Model for the Internet Value Chain," in *Proceedings of Int. Conf. on Access Networks*, 2011.

[5] A. Bogliolo, "Introducing neutral access networks," in *Proceedings of Int.l Conference on Next Generation Internet Networks (NGI 2009)*, 2009.

 ISBN: 978-1-61208-205-9 

[6] A. Seraghiti and A. Bogliolo, “Neutral access network implementation based on linux policy routing,” in *Proceedings of the 2009 First International Conference on Evolving Internet*. IEEE Computer Society, 2009, pp. 158–162.

[7] M. Marsh, *Policy Routing Using Linux*. SAMS, 2006.

[8] A. Bogliolo, “Urbino wireless campus: A wide-area university wireless network to bridge digital divide,” in *Proceedings of AccessNets-07*, 2007, pp. 1–6.

[9] F. Fainelli, “The OpenWrt embedded development framework,” in *Free and Open Source Software Developers’ European Meeting*, 2008.

[10] C. Newman, *SQLite (Developer’s Library)*. Sams, 2004.

[11] OpenWrt Wiki, *Web Server Configuration (uHTTPd)*, 2012. [Online]. Available: http://wiki.openwrt.org/doc/uci/uhttpd

[12] MikroTik, *RouterBoard Products*, 2012. [Online]. Available: http://routerboard.com/

 ISBN: 978-1-61208-205-9 

# Active Queue Management in Blind Access Networks

Ronit Nossenson and Hagit Maryuma
Faculty of Computer Science
Jerusalem College of Technology
Jerusalem, Israel
nossenso@jct.ac.il, hagit.maryuma@gmail.com

*Abstract*— **Per-flow AQM schemes are designed to provide fair resource management between flows and limit the negative effects of non-adaptive UDP-based flows. To overcome the flow bandwidth limitation, P2P and file sharing applications usually open multiple simultaneous TCP based flows. Although each TCP-based flow is adaptive and responds to network congestion, the aggregated demand of such application consumes network resources and dominates the queue space. In this article we suggest a new per user AQM policy designed to remedy this problem. Since user traffic in access networks is usually carried in user tunnels such as PPP or GTP, an access network device cannot identify the underlying applications and TCP/UDP flows. The new per-user AQM policy presented here operates in the dark and only uses tunnel aggregated statistics. Simulation results show that it significantly reduces the bias effects of heavy, demanding applications.**

***Keywords-Active Queue Management; Resource Management; Access Networks.***

## I. INTRODUCTION

Peer-to-Peer (P2P), file sharing and streaming applications attract millions of users every day [8]. This has led to a deterioration in the quality of service perceived by Internet users as well as frequent network collapse [10]. Active Queue Management (AQM) is a well known network device-based form of congestion control where the network device notifies end-systems of incipient congestion. This notification consists either of dropping a packet from the queue or "marking" a packet [15]. All AQM are designed to detect an impending queue buildup and to notify the sources before the queue overflows. AQM designs fall into three categories: per packet AQM policies (e.g., RED [7], BLUE [6], REM [3]), per class of service AQM policies (e.g., Cisco's WRED [5], [9]) and per flow AQM policies (e.g., FRED [11], [2]). A well known drawback of per packet AQM and per class of service AQM policies is lock-out and bias effects from the few flows that dominate the queue space [11]. The latter per flow AQM category is designed to avoid this problem. However, a common method used by P2P applications to overcome per flow bandwidth limitations is to open multiple simultaneous flows between the peer and the content sources. Hence, a new category of AQM is now needed to provide fair resource management between users – a *per user* AQM policy.

The user traffic in access networks is usually carried in user tunnels such as the Point-to-Point Protocol (PPP) [16], the GPRS Tunneling Protocol (GTP) [17] or Radio Link Control (RLC) encryption [17]. In tunneled traffic, the access network device cannot identify the underlying applications or the underlying TCP/UDP connections and cannot analyze any application header, TCP/UDP header or IP header. A network device located inside the access network operates in complete darkness: it can only identify the tunnel (from the packet header) and can only use tunnel aggregated statistics.

In this study, we propose and evaluate a new *per user* AQM policy designed for *blind* network optimization. The new scheme, dubbed the User Random Early Drop (URED), enforces fair resource allocation among users (tunnels). It complements the admission control mechanisms of the core network such as the Policy and Charging Rules Function (PCRF) server. The proposed algorithm is a modification of the Flow Random Early Drop (FRED) algorithm [11] together with the drop function suggested in [1], adjusted for the requirements of blind access networks and per tunnel consideration.

The algorithm's performance is compared to Drop Tail, RED and FRED. The simulation shows that the new algorithm handles P2P traffic better than the other algorithms and the negative effect of heavy demanding applications is significantly curtailed. Hence, the bandwidth over a bottlenecked link is fairly divided between the P2P and the regular users. URED reduces the average throughput of the P2P user from more than 6.8 times that of a regular user with the DT algorithm to less than 1.5, which is considerably better than the RED (4.51) and FRED (3.76) algorithms.

This paper is organized as follows. In the next section, related works are outlined. We describe our new URED algorithm in section III. In section IV, we present the simulation setup and results. Finally, further research directions are discussed in section V.

## II. RELATED WORK

One of the major drawbacks of per packet AQM policies and per class of service AQM policies is the lock-out and bias effects generated by non-adaptive flows that dominate the queue space [11].

To reduce the cost of maintaining flow state information, Stoica et al. [14] proposed a scheduling algorithm called Core Stateless Fair Queueing (CSFQ). A similar method, called Rainbow Fair Queueing, was proposed in [4]. In these methods, routers are divided into two categories: edge routers and core routers. An edge router maintains per flow state information and estimates each flow's arrival rate. These estimates are inserted into the packet headers and

 ISBN: 978-1-61208-205-9 

passed on to the core routers. A core router simply maintains a stateless FIFO queue and during periods of congestion, drops a packet randomly based on the rate estimates. These schemes reduce the core router's design complexity. The edge router's design nevertheless remains complicated. Furthermore, because of the rate information in the header, core routers have to extract packet information differently from traditional routers. This solution is not satisfactory for access networks since this device categorization is not feasible.

The CHOKe (CHOose and Keep for responsive flows, CHOose and Kill for unresponsive flows) [13] algorithm aims to approximate max-min fairness for the flows that pass through a congested router. The basic idea behind the CHOKe is that the contents of the FIFO buffer form a "sufficient statistic" about the incoming traffic and can be used in a simple fashion to penalize misbehaving flows. When a packet arrives at a congested router, CHOKe draws a packet at random from the FIFO buffer and compares it with the arriving packet. If they both belong to the same flow, they are both dropped, or the randomly chosen packet is left intact and the arriving packet is admitted into the buffer with a probability that depends on the level of congestion. Similar, a new promising method called FavourQueue aims to improve delay transfer of short lived TCP flows over a best-effort network [2]. When a packet arrives, a check is done on the whole queue to find another packet from the same flow. If no other packet is found, it becomes a favored packet and a drop protection is provided when the queue is full via a push-out scheme that drops a standard packet from the queue in order to insert a favored packet into it. These solutions are not applicable to our problem since they are basically theoretical – commercial traffic managers can drop packets only upon packet arrival and cannot drop packets from the queue.

The FRED [11] is a modified version of RED [7]. FRED uses per-active-flow accounting to impose a loss rate on each flow that depends on the flow's shared buffer use. It provides better protection for adaptive (fragile and robust) flows. In addition, FRED is able to isolate and manage non-adaptive greedy traffic. A FRED gateway maintains state only for flows for which it has packets buffered, not for all flows that traverse the gateway.

These algorithms are not completely suitable for this specific problem, although FRED comes the closest. A modification of the FRED algorithm to operate in a per user tunnel mode instead of per flow mode initially appeared promising. However, we identified several problems in the FRED algorithm that need to be addressed in blind access networks:

- In FRED, there is a requirement for a minimum guarantee of two-four packets space per active flow. It is not clear how to support this requirement in a blind access network with an unknown number of active flows. Furthermore, providing a minimum guaranteed two-four packet space per *active user* (that is, "translating" this requirement into a "per user" format) is unrealistic in a switch located high in the network hierarchy, since such a device has to handle thousands of simultaneously active user tunnels.
- The condition for identifying the non-adaptive flows should be change to a proper condition for identifying non-adaptive users. A user with multiple TCP connections can be considered non-adaptive although each of its TCP flow is adaptive.
- The actions on traffic of non-adaptive users should be less drastic if the device is not congested.
- The drop probability should increase more "smoothly" as suggested in [1]. Dropping with probability 1 results in low utilization and should be implemented only when the device is highly congested.

Below, we suggest a new algorithm inspired by FRED with modifications to handle these problems.

## III. THE URED ALGORITHM FOR PER USER AQM

In this section, we present our URED algorithm for per user AQM. The URED algorithm holds a state for every active user that has packets in the queue. The state includes the following local variables (i) the user tunnel ID, as it appears in every packet header $t_i$; (ii) the number of packets from this tunnel in the queue $q_i$; and (iii) the average number of packets from this tunnel $avg_i$. In addition the algorithm uses the following global variables: (i) the number of active users, *Nactive*; (ii) the number of packets in the queue, *q*; and (iii) the average number of packets in the queue, *avg*.

Similar to many other AQM algorithms, queue buildup detection is based on the relationship between the average queue and two global static parameters $Gmin_{th}$ and $Gmax_{th}$. However, the URED algorithm is unique in that it considers two layers in its drop probability calculation: a *universal* layer and an *individual* layer. In each layer, a drop probability is calculated according to the Hazard function suggested in [1], denoted by $P_u$ (universal) and $P_i$ (individual). Obviously, as the average queue increases and a specific user tunnel is increasingly responsible for this queue buildup, the drop probability of packets from this tunnel increases. To evaluate the responsibility of a specific user tunnel in the queue buildup, the URED algorithm uses two dynamic parameters $Lmin_{th}$ and $Lmax_{th}$. These dynamic parameters are calculated on the fly and estimate the virtual individual queue size with respect to the number of active users. That is, they mark the recommended limits of space that an individual tunnel can consume at a specific moment, given the number of active tunnels at this moment. Specifically, $Lmin_{th}$ and $Lmax_{th}$ are calculated as follows: $Lmin_{th}$ = min{BufferSize/Nactive, BufferSize/3} and $Lmax_{th}$ = min{2·BufferSize/Nactive, BufferSize/2}. A user is considered non-adaptive if the global average queue size is large and its share (represented by its individual average queue size) is large compared to the current per user available space. The description of the URED algorithm is given below.

 ISBN: 978-1-61208-205-9 

```
For each arriving packet P of tunnel t_i:
   Calc the average universal queue avg;
   Calc the average individual queue avg_i;
   If (avg < Gmin_th) no-drop;
   Else If (Gmin_th < avg < Gmax_th){
      If (avg_i < Lmin_th) no-drop;
      Else If (Lmin_th < avg_i < Lmax_th)
         Drop with probability P_u·P_i;
      Else If (avg_i > Lmax_th)
         Drop with probability P_u;
   }
   Else If (avg > Gmax_th){
      If (avg_i < Lmin_th)
         Drop with probability P_u·P_i;
      Else If (Lmin_th < avg_i < Lmax_th)
         Drop with probability P_u;
      Else If (avg_i > Lmax_th)
         Drop;
   }
```

Regarding the four problematic issues discussed in section II:

- The URED algorithm does not guarantee space for active users.
- The condition for identifying a non-adaptive user is proper for any user with multiple flows either TCP or UDP-based.
- The actions on a non-adaptive user are adjusted to the level of the queue buildup and consider both the global state of the universal queue and the local state of the individual queue.
- The URED algorithm uses the smooth hazard drop functions of [1].

## IV. PERFORMANCE EVALUATION

The performance of our new per user AQM algorithm was evaluated by simulation in the ns2 network simulator [12]. The simulation network topology is presented in Fig. 1. It consists of one source of Constant Bit Rate (CBR) with a rate of 5 mbps, nine sources of FTP over TCP (*regular users*) and one source of P2P with five simultaneous TCP connections (*P2P user*). Two sets of experiments are presented below, with bottlenecked link of 20 mbps and 10 mbps. The simulation parameters are listed in Table I.

Regarding the user throughput, Fig. 2 plots the statistics for the average throughput per time unit for the Drop Tail (DT), RED, FRED and URED algorithms under the 20 mbps bottlenecked link. The figure shows that applying the DT algorithm results in the highest un-balanced traffic between the users. The average throughput of the P2P user ($User_{11}$) was more than 6.8 times higher than the average throughput of a regular user ($User_2$-$User_{10}$). Our new URED algorithm leads to much better results. Its average throughput for the P2P user was less than 1.5 times the average throughput of a regular user. Fig. 3 plots the statistics for the average packet delay. The figure shows that the DT algorithm results in the highest delays, and all other algorithms have similar results.

Table II depicts the average throughput gap between the P2P user and a regular user for every algorithm under bottlenecked links of 20 mbps and 10 mbps. As expected, with a 10 mpbs bottlenecked link, the traffic become more un-balanced than with a 20 mpbs bottlenecked link. An interesting observation is that RED outperforms FRED under a heavy bottlenecked link.

Regarding the user packet loss, Table III plots the statistics for the average packet loss per time unit for the Drop Tail (DT), RED, FRED and URED algorithms under a 20 mbps bottlenecked link for regular and P2P users. RED drops the fewest packets compared to the other algorithms. FRED drops more packets than the other algorithms.

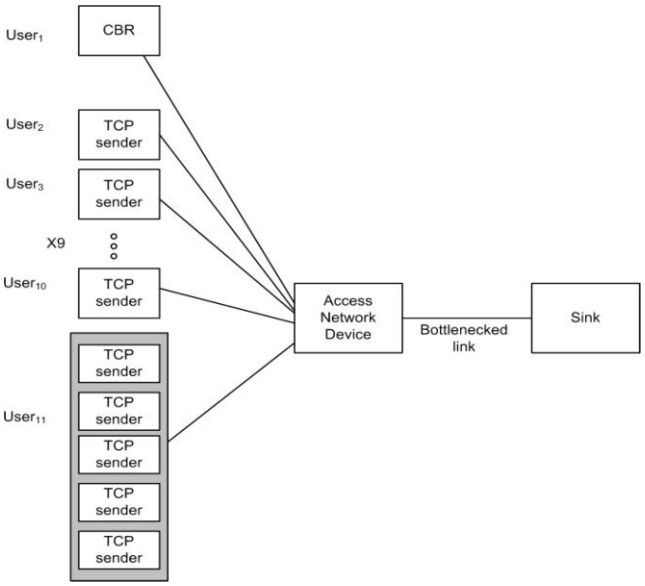


Figure 1: Simulation setup

TABLE I. THE SIMULATION PARAMETERS

| **Parameter** | ***Value*** |
|---|---|
| Bottlenecked link BW | 10, 20 mbps |
| Number of Regular Users | 9 |
| Number of CBR Users | 1 |
| Number of P2P Users | 1 |
| CBR Rate | 5 mbps |
| FTP Burst time | 2000 ms |
| FTP Idle Time | 200 ms |
| FTP File Shape | 1.7 |
| Packet size | 1600 B |

TABLE II. THE AVERAGE THROUGHPUT GAP

| **Algorithm** | **P2P user throughput/Regular user throughput** | |
|---|---|---|
| | ***20 mbps bottlenecked link*** | ***10 mbps bottlenecked link*** |
| DT | 6.81 | 7.81 |
| RED | 4.51 | 4.48 |
| FRED | 3.76 | 4.56 |
| URED | 1.46 | 1.66 |

 ISBN: 978-1-61208-205-9

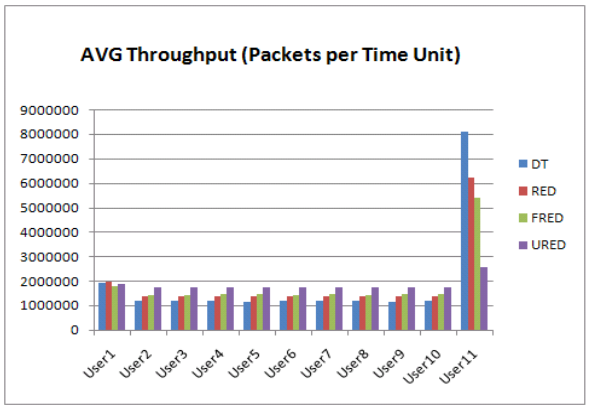


Figure 2: Average user throughput (20 mbps bottlenecked link)

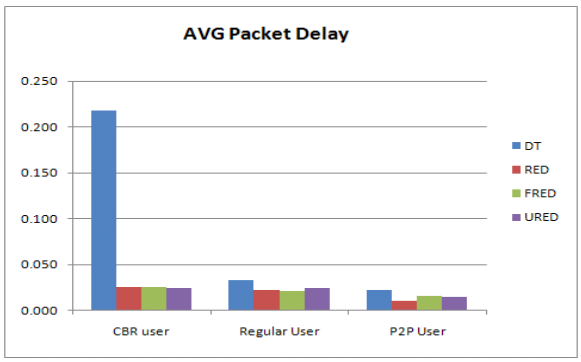


Figure 3: Average packet delay (20 mbps bottlenecked link)

TABLE III. AVERAGE PACKET LOSS

| **Algorithm** | ***Regular User*** | ***P2P User*** |
|---|---|---|
| DT | 72064 | 158847 |
| RED | 62270 | 275521 |
| FRED | 150064 | 489503 |
| URED | 106303 | 288112 |

## V. CONCLUSION AND FUTURE WORK

This paper described on-going research on a new URED algorithm for AQM that is designed to handle congestion in a blind access network device. The proposed method uses available tunnel statistics and does not use information from TCP and IP headers. This method ensures fair resource allocation among network users on a congested link and can help operators limit the resource consumption of P2P applications.

Future work includes additional simulations to improve the evaluation of the algorithm's potential and identify its limitations. In addition, we are working on a self configuration method for the algorithm parameters.

## ACKNOWLEDGMENT

The authors thank the anonymous referees for helpful comments on an earlier version of this paper.

## REFERENCES

[1] B. Abbasov and S. Korukoğlu, "An Active Queue Management Algorithm for Reducing Packet Loss Rate", Mathematical and Computational Applications, Vol. 14, No. 1, pp. 65-72, 2009.

[2] P. Anelli, E. Lochin, and R. Diana, "FavourQueue: a Stateless Active Queue Management to Speed Up Short TCP Flows (and others too!)", ArXiv e-prints, 1103.2303, March, 2011.

[3] S. Athuraliya, S. H. Low, V. H. Li, and Y. Qinghe, "REM: active queue management", IEEE Network, Vol. 15(3)., pp. 48-53, May 2001.

[4] Z. Cao, Z. Wang, and E. Zegura, "Rainbow fair queueing: Fair bandwidth sharing without per-flow state", In Proceedings of INFOCOM'00, pp. 922–931, Tel-Aviv, Israel, March 2000.

[5] Cisco's web site http://www.cisco.com/en/US/docs/ios/12_2t/12_2t8/feature/guide/ftwrdecn.html, retrieved: May, 2012.

[6] W. C. Feng, K. G. Shin, D. D. Kandlur, and D. Saha, "The BLUE Active Queue Management Algorithms" IEEE ACM Transactions on Networking, Vol. 10(4)., pp. 513-528, August 2002.

[7] S. Floyd and V. Jacobson,"Random Early Detection Gateways for congestion Avoidance" ,IEEE/ACM Transaction on Networking, Vol. 3., pp. 397-413, August 1993.

[8] X. Hei, C. Liang, J. Liang, Y. Liu, and K.W. Ross "A Measurement Study of a Large-Scale P2P IPTV System", IEEE Transactions on Multimedia, Dec. 2007

[9] B. J. Hwang, I.S. Hwang, and P.M.Chang, "QoS-Aware Active Queue Management for Multimedia Services over the Internet", EURASIP Journal onWireless Communications and Networking, Article ID 589863, 2011.

[10] E. Leonardi, M. Mellia, A. Horvath, L. Muscariello, S. Niccolini, and D. Rossi, "Building a cooperative P2P-TV application over a Wise Network: the approach of the European FP-7 STREP NAPA-WINE",IEEE Communication Magazine,Vol. 64, No. 4, pp. 20-22, April 2008.

[11] D. Lin and R. Morris, "Dynamics of random early detection", Proceedings of the ACM SIGCOMM '97 conference on Applications, technologies, architectures, and protocols for computer communication, pp. 127-137, September 14-18, 1997, Cannes, France.

[12] NS: The Network Simulator (NS 2), http://isi.edu/nsnam/ns/ retrieved: May, 2012.

[13] R. Pan, B. Prabhakar, and K. Psounis., "Choke, a stateless active queue management scheme for approximating fair bandwidth allocation", In Proceedings of IEEE INFOCOM'00, pp. 942-951, Tel Aviv, Israel, March 2000.

[14] I. Stoica, S. Shenker, and H. Zhang, "Core-stateless fair queueing: achieving approximately fair bandwidth allocations in high speed networks", ACM SIGCOMM Computer Communication Review, Vol. 28 (4), pp.118-130, Oct. 1998.

[15] G. Thiruchelvi and J. Raja, "A Survey On Active Queue Management Mechanisms", IJCSNS International Journal of Computer Science and Network Security, VOL.8 No.12, pp. 130-146, Dec. 2008.

[16] RFC 1661, http://tools.ietf.org/html/rfc1661, retrieved: May, 2012.

[17] 3GPP the mobile broadband standard web site, http://www.3gpp.org/ftp/Specs/, retrieved: May, 2012.

 ISBN: 978-1-61208-205-9 

# Towards a Dynamic and Adaptative Prioritization of Wireless Broadband Vehicle-to-Ground Communications

## Communication Management based on Network Utility Maximization and QoS Requirements

Itziar Salaberria, Asier Perallos, Roberto Carballedo
Deusto Institute of Technology (DeustoTech)
University of Deusto
Bilbao, Spain
{itziar.salaberria, perallos, roberto.carballedo}@deusto.es

***Abstract*—The growth of the use of wireless and internet technologies in transport systems, enables the provision of new information services based on vehicle-to-ground communications. There are many broadband management systems, but most of them come from non-mobile environments. This results in a poor performance when deployed to environments where senders and receivers are moving. Such problems appear because transportation systems environments present specific requirements related to coverage, bandwidth and also a mix of communications networks. In order to tackle these challenges, this paper presents the work in progress of a vehicle-to-ground communication middleware that aims to manage communication requests using a dynamic schema. The core of this new communications manager is an adaptive algorithm that selects the most favorable network link taking into account several actual and past aspects of the communications requests.**

***Keywords-Communications Management; Limited Bandwidth; Quality of Service; Vehicle-to-Ground Communications.***

## I. INTRODUCTION

Transportation industry is demanding more bandwidth, more immediate response time and more reliability for their communication networks in order to perform intra-vehicle, vehicle-to-ground or trackside communications. In this way, research is being promoted to provide more convenient and efficient vehicular systems by using broadband networks to link onboard systems with ground systems.

Nowadays, the use of wireless and Internet technologies is increasing in the transportation enabling bidirectional vehicle-to-ground communications [1]. However, these kinds of communications applied to this environment have to respond to several challenges related to aspects like coverage, bandwidth, communication disruptions, multiple network interfaces for communications and different priorities in the information transmission, responding at the same time to applications Quality of Service (QoS) [2] requirements.

On the other hand, the existing broadband management systems, which are used in other (non-mobile) environments, do not satisfy the needs of vehicular applications [3] [4]. In addition, there are several applications trying to transmit information to/from the vehicles at the same time. This implies the existence of a bandwidth monopolization problem.

To tackle these challenges, it is necessary a smart intermediate element which manages when the applications (both terrestrial and vehicular-side) can communicate with each other and makes the most favorable available network link selection for communications. This is the aim of the work presented here.

In contrast to existing initiatives, the proposed solution enables a continuous broadband communication channel between applications in vehicles and ground control centers based on an application layer middleware which do not require specific considerations in the rest of the protocol layers. Existing standards for Intelligent Transportation Systems (ITS) communication architectures, such as [5] [6] [7], are principally focused on network level issues in order to fulfill Vehicle-to-Vehicle (V2V) and Vehicle-to-Infrastructure (V2I) communication requirements. Unlike the proposed ones, these architectures are usually oriented to traffic security applications that need immediacy and a low volume of data transmission.

This paper is organized into the following sections: the second section includes a brief state of the art. The third section details the proposed communication middleware requirements and architecture. To close, the fourth section of the paper describes the future work indicating the following steps in the work in progress.

## II. STATE OF THE ART

The presented research work is focused on vehicle-to-ground broadband communications prioritization management focusing on high level protocols. Thus, in the following subsections the state of the art related to the two main issues of the work will be discussed: (1) vehicle-to-ground wireless communications, and (2) broadband communications prioritization and QoS.

### *A. Vehicle-to-Ground Wireless Communications*

Wireless communication technologies are growing in vehicular systems due to transportation companies are demanding greater efficiency for their systems while they are

 ISBN: 978-1-61208-205-9 

also seeking to provide new information services [8]. Consequently, vehicular systems are enabling not only vehicle-to-ground continuous communications, they also tend to install wireless equipment in stations and other wayside locations for broadband communications where large quantities of maintenance [9] [10] and multimedia [11] data can be transmitted between vehicle and ground system while vehicle is in coverage area.

It is important to point out that the emphasis in developing wireless network is on network bandwidth and coverage. Therefore, the applicability of the communication system will largely depends on their ability to provide sufficient data rates (QoS requirements), considering introduced protocol overhead, packet fragmentation and possible retransmissions. A major problem with using unlicensed frequency bands like 802.11x is obviously the interference on and shared access of the wireless medium. These aspects can cause blocking of information services communication. In order to solve this kind of questions, one option is to enable multiple wireless interfaces making possible switching from one interface to other. It is for this reason that the vehicular wireless communication systems tends to be designed using multiple radio and mobile interfaces (GPRS, UMTS, WLAN, etc.) in "always best connected" [12] way to enhance communications availability and obtain the possible major bandwidth capabilities [13], selecting the most favorable link for the communications at every moment. This kind of solutions increases system cost, but can help to improve system availability greatly.

Therefore, the use of multiple network interfaces simultaneously allows building a better combined wireless communication channel. The objective is to achieve the highest data rates being able to meet different mobile scenarios as well as mobile applications requirements. To that end, there are solutions that advocate exploiting network diversity from different wireless networks and operators in order to be able to aggregate bandwidths that can then be offered as a single large, more stable pipe to end users [14].

Furthermore, it is important to point out the emergent application of Internet protocols, languages and technologies (TCP/IP, HTTP, XML, etc.) [15].

### *B. Broadband Communications Prioritization and QoS*

Wireless communications applied to mobile environment present several limitations related to coverage and bandwidth that can cause service disruptions. Moreover wireless stations that need to transmit relevant information must deal with wireless stations wishing to transmit less priority traffic.

With the purpose of achieve QoS requirements demanded by services, several communication management and prioritization heuristics [16] [17] and mechanisms exist [18] [19] [20]. Although existing solutions are mainly focused on network aspects and not in final applications and services, other approaches are focused in optimizing the use of the network technologies according to the type of traffic generated by applications (QoS control). Therefore, there is an open research field that can be tackled from two complementary points of view: (1) QoS requirements management which involves technology concepts related to the information to transmit, and (2) aspects about network conditions that make possible the transmission of that information (bandwidth, coverage, latency, etc.).

In addition, many of these solutions are focused on mobile environments and are able to monitor network parameters (like bandwidth). The main idea in these solutions is to prioritize communications services allowing or denying communications, or readjusting its data rates, in accordance with QoS requirements demanded by the communication requests and available networks bandwidth limitations.

These mentioned solutions applied to transportation would allow prioritizing vehicle-to-ground wireless communications taking into account its QoS restrictions. However, they are mostly oriented to regulate wireless stations communications and not final individual applications communication requests. Moreover, they do not monitor previous performance aspects (variable) not allowing to the system to dynamically adjust its performance for more efficiency.

These questions open an interesting line of work to develop adaptive algorithms and interactive control methods that perform this adjustment dynamically. The basic idea is to monitor network conditions in real-time, receive feedback measures of the variables of interest, and based on these measures and QoS requirements, make a wireless communication prioritization assigning them the considered bandwidth data rate.

## III. PROPOSED COMMUNICATION MIDDLEWARE

The proposed solution consists on a communication middleware that aims to enable several physical network communication links between vehicle and ground system (3G, WiFi, etc.), choosing the network link considered as the best at every moment according to the bandwidth availability (not having final applications to get involved in the network management).

Focusing on an application layer middleware it is a more flexible approach allowing the introduction of new parameters or factors that can be managed to improve communications performance. So, the objective is to develop a dynamic and adaptive communications requests mechanism based not only on network conditions and applications request priorities. This mechanism will be based also on system historical performance parameters (previous bandwidth values, time in network coverage areas during the transportation routes, previous applications communications performance, etc.).

### *A. Requirements*

The final system should respond to several requirements:

*1) Dynamic and efficient communication request management:* this system will prioritize vehicle-to-ground communcations requests taking into account communication urgency creteria, as well as previous performance logs.

*2) The best bandwidth:* the system will always select the physical link considered as the best taking into account the

bandwidh in order to respond to final applications communication requirements.

3) *Quality of Service:* it is necessary to know the bandwidth availability offered by the network link which is active at every moment, as well as the bandwidth offered by the rest of communications links (although they are not being used). At this point, it is essential to establish a set of connection procedures which permit to reserve a certain bandwidth for a particular communication.

### *B. Architecture*

The architecture of the presented solution (Figure 1) is composed by two software elements; one in the terrestrial side (Terrestrial Communication Manager, TCM), and the other boarded in vehicles (Vehicular Communication Manager, VCM). The former manages terrestrial aspects of the architecture and the latter vehicular-side issues, and they interact to each other in order to control and manage vehicle-to-ground communications. In addition, this system develops a Bandwidth Measurement Service (BMS) that notifies available links bandwidth values to the VCM at every moment. It is necessary to emphasize that bandwidth measurement would be an independent research field that is not explored in this work.

Therefore, the final objective is to demonstrate that this communication management system improves vehicle-to-ground broadband communications efficiency especially in these situations where applications communications needs are higher than the bandwidth offered by the available network links ensuring at the same time applications QoS requirements.

Thus, the proposed solution is composed by several functional modules:

1) *Active Link Selection:* the communication platform is based on different physical communication link existence so that the combination of these independent links offers a continuous vehicle-to-ground connectivity in order to respond to the final applications communications demand. So, taking into account the availability of enabled different physical links, the system always selects as active link this network interface that offers the best bandwidth (based on the features and coverage of the physical link).

Therefore, to establish vehicle-to-ground communications, VCM and TCM can communicate through different communications network physical links. The VCM is who selects the active link considered most favorable for communications based on available links bandwidth measurements notified by BMS, and then establish active link connection with TCM. So, BMS is continuously monitoring all enabled network links status, and VCM switch from one to other in two cases: (1) when active link connectivity is lost and (2) when BMS measurements indicate that another link is better than this established as the active. In these two cases, the active communication link change is transparent for final applications that do not detect connection interruptions if these link changes occur while they are transmitting.

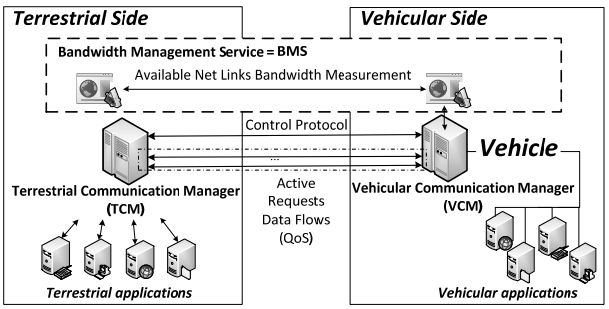


Figure 1. Dynamic Communication Prioritization Architecture for Vehicle-to-Ground Communications based on QoS Requirements and Network Conditions

At this point it should be emphasized that the basis is that the system always defines a single vehicle-to-earth network link as active for communications (the most favorable). So, all communications will always be generated by the channel set as active (WiFi, GSM/GPRS, Tetra, etc.) regardless of the availability of other physical channels simultaneously.

2) *Requests Prioritization Management:* the objective is to prioritize vehicle-to-ground communications based on several criteria so that the transmission of critical information has more priority over other information that need less "immediacy" when being transmitted. Therefore, this platform proposes a set of communication requests prioritization criteria divided into two categories: (1) static criteria and (2) dynamic criteria. Static criteria are related to applications QoS requirements like information priority level, required minimun data rates, or requests cronological order. Dynamic criteria are variable factors that are related directly with the communications that have been carried out previously (the average duration of vehicles stopping in a known wireless network coverage area, the average duration that takes the communications of a particular application at certain data rates, bandwidth values obtained previously, wireless networks coverage values, etc.). Thus, combining these two kinds of criterias, the system calculates a numeric value that represents the fitness of serving a request. Once calculated this value, it is used to discern which communication request is served. Hence, in order to perform requests prioritization, this system develops several queues where requests are sorted by vehicle and this calculated value (priority).

Therefore, the idea is that the system reconfigures how it prioritizes the communication requests depending of its behavior over time, always seeking the most optimal configuration based on system feedback.

*3) Vehicle-to-Ground Control Protocol:* TCM and VCM on each vehicle communicate each other and exchange commands in order to establish active links and manage vehicular and terrestrial final applications communications requests prioritization. The control protocol is defined using XML messages where information is exchanged via TCP/IP sockets.

 ISBN: 978-1-61208-205-9 

*4) Final Application Communication Control and Management:* the described platform aims to enable vehicle and terrestrial vehicular applications to communicate each other in a more efficient way. So when an application attempts to start a new communication makes a request to the platform. Then the system makes a decision about what priority requests can be served concurrently taking into account active link bandwidth limitations, priority parameters and requests QoS requirements. Thus, once the system give way to a communication request, adjust this communications data rate taking into account its QoS requirements, active link bandwidth availability and active priority requests communicating concurrently. In addition, system should assign more bandwidth than minimaly required to a request depending on bandwidth availability and priority active requests requirements.

### C. Developing State

The proposed middleware is already developed and is being debugged in order to improve its performance and fix detected errors. Besides, with the purpose of test the platform there have been developed applications simulators that permit making communication requests to the system under different QoS requirements.

## IV. FUTURE WORK

Once the system is developed, it will be tested configuring several testbed scenarios. The idea is to have a preconfigured scenarios including a set of known communication requests (generated both on terrestrial side and on vehicles) and network conditions.

Therefore, the testing scenarios will include different kind of final applications that generate different kind of data traffic (multimedia, text, files, binary, etc.) that are usual in transportation systems, as well as predefined network conditions (using an external tool that allows to regulate network interfaces bandwidth values). The objective is to evaluate the systems performance, launching several communication requests and causing network active link changes (because of more favorable link or link lost detections), that allows checking whether obtained results are as expected.

On the other hand, these tests will be useful to evaluate communications prioritization algorithm in order to improve its efficiency.

## REFERENCES


[1] M. Aguado, E. Jacob, P. Saiz, J. Unzilla, M. Higuero and J. Matias, "Railway signaling systems and new trends in wireless data communications", Veh. Tech. Conference, pp. 1333-1336, Sep. 2005

[2] W.C. Hardy, "QoS measurement and evaluation of telecommunications Quality of Service", Review R.Chodoreck, IEEE Communications Magazine, 40(2), pp. 30–32, 2002

[3] D. Marrero, E.M. Macías, and A. Suárez, "An admission control and traffic regulation mechanism for infrastructure WiFi networks", IAENG International Journal of Computer Science, Vol. 35, Issue 1, pp. 154-160, ISSN: 1819-656X, 2008

[4] T. Okabe, T. Shizuno and T. Kitamura, "Wireless LAN Access Network System for Moving Vehicles", 10th IEEE Symposium on Computers and Communications (ISCC), pp. 211-216, 2005

[5] Car to Car Communication Consortium, "Car to Car Communication Consortium Manifesto: Overview of the C2C-CC System", C2C-CC, version 1.1, 2007

[6] ETSI TR 102 638, "Intelligent Transport System (ITS); Vehicular Communications; Basic Set of Applications; Definition, ETSI specification TR 102 638, v.1.1.1, June 2009

[7] G. Karagiannis, O. Altintas, E. Ekici, G.J., Heijenk, B. Jarupan, K. Lin, T. Weil, (2011) "Vehicular networking: A survey and tutorial on requirements, architectures, challenges, standards and solutions", IEEE Communications Surveys & Tutorials, 13 (4). pp. 584-616

[8] L. Qi, "Research on Intelligent Transportation System Technologies and Applications", Workshop on Power Electronics and Intelligent Transportation System, pp. 529-531, 2008

[9] A. Bondavalle, Andrea Ceccarelli, et al., "Design and Evaluation of a Safe Driver Machine Interface", International Journal of Performability Engineering, Vol. 5, No. 2, pp. 153-166. January 2009

[10] Min-Song Li, Duan Zhuo-hua, "Wireless Monitoring System in The Application of Train", International Conference on Internet Computing and Information Services, pp. 589-590, 2011

[11] Y.K. Choong, C. Lin and L. Xiaoyu, "BlueBus: A Scalable Solution for Localized Mobile Service in a Public Bus", Mobility Conference, pp- 712-715, 2007

[12] E. Gustafsson and A. Jonsson, "Always bes connected", Wireless Communications IEEE, 10 (1), pp. 49-55, Feb. 2003

[13] G.M. Shafiullah, A. Gyasi-Agyei and P. Wolfs, "Survey of Wireless Communications Applications in the Railway Industry", The 2nd International Conference on Wireless Broadband and Ultra Wideband Communications (AusWireless), pp. 65, 2007

[14] P. Rodriguez, et al., "MAR: A Commuter Router Infrastructure for the Mobile Internet", 2nd International Conference on Mobile Systems, Applications and Services (MobiSys), 2004

[15] A.Gatti, "Trains as Mobile devices: the TrainCom project", Wireless Design Conference, London, 2002

[16] P. Dharwadkar, H.J. Siegel, and E.K.P. Chiong, "A Heuristic for Dynamic Bandwidth Allocation with Preemption and Degradation for Prioritized Requests", 21st International Conference on Distributed Computing Systems (ICDCS), 2001

[17] P. Jayachandran and T. Abdelzaher, "Bandwidth Allocation for Elastic Real-Time Flows in Multihop Wireless Networks Based on Network Utility Maximization", 28th International Conference on Distributed Computing Systems, 2008

[18] D.Marrero, E.M. Macias and A. Suarez, "Dynamic Traffic Regulation for WiFi Networks", Proceedings of the World Congress on Engineering (WCE), 2007

[19] M.F. Horng, Y.H. Kuo, L.C. Huang and Y.T. Chien, "An Effective Approach to Adaptive Bandwidth Allocation with QoS Enhanced on Ip Networks", International Conference on Ubiquitous Information Management and Communication (ICUIMC), 2009

[20] P. Noh-sam and L. Gil-Haeng, "A framework for policy-based sla management over wireless LAN", Proceedings of the Second International Conference on e-Business and Telecommunication Networks (ICETE), INSTICC Press, ISBN 972-8865-32-5, pp. 173-176, UK, October 2005


 ISBN: 978-1-61208-205-9 

# Process-Stacking Multiplexing Access for 60 GHz Millimeter-Wave WPANs

Claudio Estevez[†], David Fuentealba[†], Aravind Kailas[‡]
[†] Department of Electrical Engineering, Universidad de Chile, Santiago, Chile | {cestevez, dfuentea}@ing.uchile.cl
[‡] Electrical and Computer Engineering Department, UNC Charlotte, Charlotte, NC, USA | aravind.kailas@uncc.edu

***Abstract*—Millimeter-waves technology shows high potential for future wireless personal area networks, reaching over 1 Gb/s transmissions using simple modulation techniques. This technology is on the innovation stages; therefore current specifications consider dividing the spectrum into effortlessly separable spectrum ranges. In this work, a process-stacking multiplexing access algorithm is designed for single channel operation. The concept is intuitive and simple, but its implementation is not trivial. The key to stacking single channel events is to operate while simultaneously obtaining and handling a-posteriori time-frame information of scheduled events. This information is used to shift a global time pointer that the wireless access point manages and uses to synchronize all serviced nodes. The performance of the proposed multiplexing access technique is lower bounded by the performance of legacy TDMA and can improve the effective throughput significantly. Detailed implementation is presented and hypothesis is validated by simulation results.**

***Keywords-60 GHz; access; MAC; millimeter; mm-wave; multiplexing; process-stacking; WPAN.***

## I. INTRODUCTION

Throughout history, technologies have demonstrated a logistic function growth pattern, commonly referred as the technology s-curve. The s-curve is composed of an innovation, improvement, maturity, and aging stage. In the wireless local area network (WLAN) field, the current dominating technology is WiFi, which has a 2.4/5 GHz modulating frequency with typical channel widths of 20/40 MHz, and can reach throughputs of 600 Mb/s [1]. To achieve these speeds WiFi requires multiple-input multiple-output (MIMO) antenna arrays, orthogonal frequency division multiplexing (OFDM), and relatively dense quadrature amplitude modulation (QAM) constellations, which indicate that this technology is reaching the maturity stages of the technology s-curve and in the future it will become increasingly difficult to make significant throughput improvements. For this reason, millimeter-wave technology is rapidly becoming the new alternative for wireless personal area network (WPAN).

mm-Wave systems have already proven to transmit at over 2.5 Gb/s [2], using single-input single-out (SISO) antenna setup and on/off keying (OOK) modulation. Considering the simple methods employed to achieve this throughput, this can be categorized to be in the innovation stages of the technology s-curve. This is a good indication that when this technology reaches maturity it could potentially transmit at over 40 Gb/s by using spectrally-efficient modulation methods, dense frequency multiplexing, wide bandwidths due to frequency reuse, efficient use of time allocation, MIMO, beamforming algorithms for spatial filtering, and other potential techniques.

The 60 GHz frequency range is attractive to very-high-throughput applications found in research fields such as: WPANs [3][4], e-Health [5], and home entertainment. Some examples are: cloud computing services, web-based file hosting, health related traffic (a single high-quality multi-focal microscope picture format can occupy 1 GB), distribution link to a body area network, low-latency high-capacity gaming capabilities, and high-definition video-on-demand. Because this technology is still callow many of these applications are still not implemented but are feasible.

Initial attempts to standardize the 60 GHz frequency range already exists. Among these standards the ECMA-387 [6] is one the best known. The ECMA-387 discusses issues related to the physical and data-link layers. One particular interest to our work is the band allocation. This initial attempt by ECMA-387 to standardize the 60 GHz region divides the operating frequency range (57 – 66 GHz) in four bands: 57.240 ↔ 59.400 ↔ 61.560 ↔ 63.720 ↔ 65.880, as seen in Figure 1. One motive for having a low number of bands is that filter design becomes less trivial and more expensive as the Q-factor increases and since the design is for WPAN it is not expected to have large number of users per wireless access point (WAP). For this reason, the focus of this work is to design a time-domain multiplexing technique with efficient allocating capabilities.

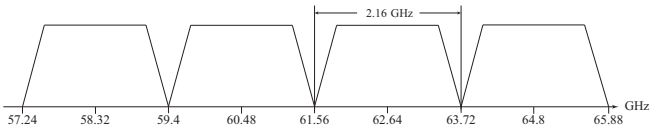


Figure 1. ECMA-387 operating frequency range and band allocation.

To multiplex various transmitting nodes into a single channel, a process-stacking multiplexing access (PSMA) algorithm is proposed. If frequency reuse is incorporated by taking advantage of the topology, as in [7], a two-dimensional space/time domain algorithm can be achieved, but this work focuses on improving the time dimension efficiency. The reason for naming this access technique process-stacking is because its versatility expands the packet-transmission-time reservation to a diverse-process-time reservation ideology. This allows for easy incorporation of any process that wishes to reserve access to the antenna, even if it does not require to transmit data.

Various useful processes could be implemented without modifying the algorithm, a few examples are: idle time, QoS

 ISBN: 978-1-61208-205-9 

and beacon signal. In many environments, particularly in those associated with e-Health, energetically self-sustainable nodes are desirable. If the node were equipped with an energy-harvesting device and it drained most of its energy, an idle-time process can be inserted into the packet transmission cycle to allow the device to recharge, by trading-off throughput, as suggested in [8][9]. The advantage of PSMA over TDMA (used in [8][9]) is that the idle-time process can be inserted at any time that the system determines is necessary while TDMA divides the cycle in slots and if it needs to enter the energy-savings mode it needs to undo the slot assignments. Another advantage of process-stacking is that QoS can be implemented in several ways. For example, if the information is labeled as time sensitive, the algorithm can switch to smaller and more frequent process reservations such that the effective throughput remains the same but the stream is more continuous rather than bursty. Also, different priority level traffic can have different reservation frequency privileges and different reservation time frames. The final example is the use of a broadcast synchronization signal, which some literature refer to beacon signal. If a collision is detected by the WAP, usually due to a new node attempting link, the WAP can insert a beacon signal and idle time (to wait for a response) process allowing the unlinked node to connect. A graphical comparison between TDMA and PSMA is portrayed in Figure 2.

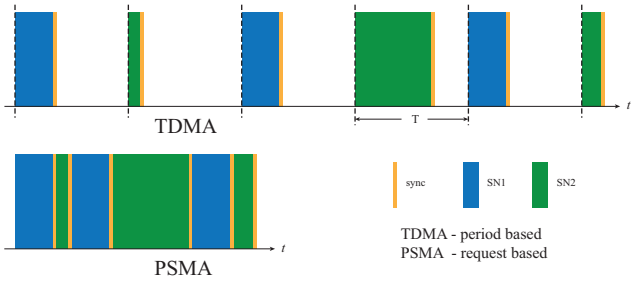


Figure 2. Comparison between time allocation schemes PSMA vs TDMA

There are many advantages to having a process-stacking multiplexing access (PSMA) algorithm: 1) Time is used more efficiently: In a TDMA regime each node has a fixed time-slot and the width of the slot is independent of the amount of data that is queued, in worse-case scenario there is no data queued and the time slot goes unused. In PSMA each node occupies the channel for the amount of time required, hence does not occupy time if it does not need to transmit. 2) No limit for amount of nodes per channel: In TDMA, the period is divided into N time slots and each node has a dedicated slot, if an $(N+1)^{th}$ node requests transmission there will be no slots available. In PSMA, there is no limit, but having an excessive amount of nodes will result in a low throughput per node. 3) It is versatile; In TDMA, if a process or control signal needs to be inserted into the channel, the recurrent period needs to be interrupted and reconfigured. In PSMA, if distinct processes (other than scheduling nodes) need to reserve the antenna in a PSMA scheme, the WAP is designed to perform this task without disrupting the transmission of the already linked nodes. 4) Quality of service (QoS) integration: In TDMA, QoS is limited to assigning more time-slots to higher priority nodes, but the configurable granularity is limited to units of time-slots. In PSMA, as discussed previously, it can be implemented using various techniques.

This paper is organized in the following order: Section II describes the proposed PSMA algorithm and explains how it was implemented. In Section III, the simulation scenario is described and results are presented. Finally, in Section IV the conclusions are summarized.

## II. PROCESS-STACKING MULTIPLEXING ACCESS (PSMA)

PSMA functions using a different technique than TDMA; the only similarity is that both perform multiplexing access in the time domain. PSMA schedules processes, which means that time is reserved only when it is requested and for the amount of time requested. To organize transmissions a global time pointer is used. In the event that a process or node requests the use of the antenna, this process is scheduled at the time stored in the global pointer and the pointer is shifted by the amount of time requested, in practice a buffer time is also inserted. If the current time reaches the global pointer time, then the node switches to listen mode. This is the basic operation, but the details are found in the WAP section below. The serviced node also plays an important role, as it must report to the WAP the reserved time window.

The detailed operation of the nodes follows. For simplicity only the upstream process is described. The half-duplex mode can be obtained by extending the process reservation procedure to the downstream direction. If both stream directions are using the same modulation frequency, this implies that the throughput in both directions will decrease due to the sharing of the channel.

The network topology consists of a wireless access point (WAP) and four serviced nodes (SNs) as shown in 0 All nodes operate at the same frequency in both upstream and downstream directions, for reasons mentioned in the introduction. As the technology matures the spectrum can be divided into narrower bands (than ECMA-387) and models can have control packets in a different (smaller bandwidth) channel, or separate upstream and downstream channels for full-duplex transmission.


Figure 3. Modeled network topology

### A. *Serviced node (SN) operation*

Packets flow through the following elements: incoming port, queue, packet encapsulator, main processor, and antenna, as shown in Figure 4. It should be pointed out that this model uses the same modulating frequency for upstream and downstream traffic, therefore when a frame is sent through the transmitter its own receiver captures this frame returning it to the main processor. These frames are referred to as echo frames and they are discarded.

 ISBN: 978-1-61208-205-9 

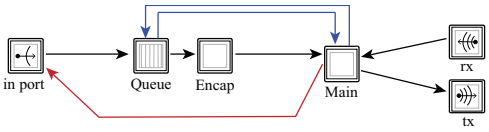


Figure 4. Internal arquitecture of the serviced node

*1) Queue*

If a packet enters the queue, the queue processor informs the main processor it has at least one packet that needs to be serviced. The main processor connects the SN to the WAP; once connected the main processor sends a request to the queue. The queue forwards all stored packets (up to defined limit) to the packet encapsulator followed by a completed-signal.

*2) Packet Encapsulator*

The packet encapsulator has a crucial role in the PSMA scheme. It gathers the network layer packets (typically IP) coming from the queue and encapsulates these into a frame. Once the frame is built, its size is translated into a synchronization time using the transmission bit rate. The time, which is used to synchronize this frame, is inserted in a previously stored frame. The previous frame is sent to the main processor for transmission, while the recently encapsulated frame is temporarily stored. Since the recently built frame triggers the transmission of the previously stored frame, this process is referred to as a push (i.e. the arriving frame pushes the stored one). This continues until the queue is empty. The frame format is composed of a header, data, and ECC field, as shown in Figure 5. The header is composed by the source, destination, flags, and sync fields. The flags are: hello and close. Additional flags can be reserved for QoS and/or other implementations. The methodology, including the use of the frame field, is explained in detail ahead.

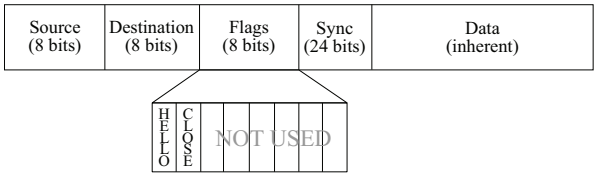


Figure 5. Frame format for PSMA

*3) Main Processor*

The process-stacking multiplexing access algorithm is located in this processor. The main processor is composed of various states, as shown in Figure 6. Overall, the processor collects the frame and sends it at the synchronization time specified by the WAP. The details of each state follow:

**init**: Initializes state variables, assigns a unique MAC address to the node, and schedules a starting time based on a uniformly distributed random variable (within a specified range).

**hello timer**: Awaits for an interrupt. If the interrupt is a self-timer, a signal is sent to queue to release the stored packets to the encapsulation process where (besides encapsulating) the packets are counted and temporarily stored (as described in Section II-A-2) and pushes an empty packet that contains the synchronization information of the next packet. If the interrupt is a packet arrival from the encapsulation processor, it extracts the sync information and discards the packet. Afterwards, it moves to the hello state.

**hello**: Creates first packet with frame format, also called the hello frame in this work. It inserts its own MAC address in the source field, 0 in the destination field (since it does not know the WAP's MAC address at this stage), the hello flag is set to 1, and the first sync information is appended. The hello frame is sent to the antenna port. It moves to the id state after completing these steps.

**id**: Waits for frame [hello response]. If a frame arrives, the header information is extracted: If the hello flag is set to 1 and destination field is its own MAC address then sender field is stored as the WAP MAC address, the first synchronization information is extracted, and the node is synchronized accordingly. If sender field has stored its own MAC address this is an echo frame, therefore discarded. If LOST condition is met it moves to the hello state. It moves to idle state if SYNC condition is met.

**idle**: Waits for an interrupt. If the interrupt is due to a frame arrival then the header information is extracted before moving to the SYNC state. If the interrupt is a self-timer then it moves to the tx state.

**sync**: Upon the frame arrival, the destination field is examined to check if it is equal to its own MAC address. If this is the case, the sync field is extracted and the next transmission time is scheduled. If the destination field does not match the node's MAC address, the frame is ignored. Afterwards it returns to idle state.

**req_pkt**: Upon entering this state the main processor signals the queue processor to release the packets and it waits for the frame. Once a packet arrives, it checks if it is the frame from the encapsulation processor, if so it extracts the close flag field and moves to the tx state, otherwise it returns to the state (to wait for the frame).

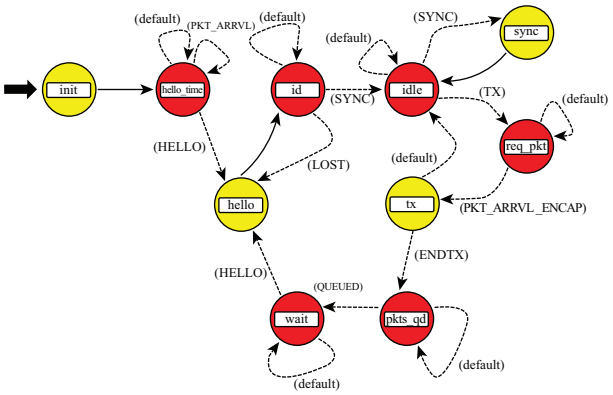


Figure 6. State diagram for the serviced node main processor.

**tx**: The header information is appended to the frame, which already contains the synchronization and data information. Subsequently, it is sent to the antenna port. If ENDTX condition is set it moves to the pkts_qd state, otherwise it moves to the idle state.

**pkts_qd**: Once it enters this state it monitors the queue, if a packet enters the QUEUE condition is met and it assigns a

 ISBN: 978-1-61208-205-9

random (but small) time to reestablish the link with the WAP. It then moves to the wait state.

**wait**: Waits for hello timer before moving to hello state [and reestablish another session].

### B. Wireless Access Point (WAP) operation

The WAP contains a main processor (WAP label) and a decapsulation processor, as shown in Figure 7.

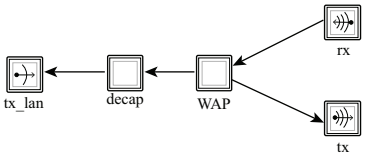


Figure 7. Internal arquitecture of the wireless access point.

#### 1) Main Processor

The WAP's main processor links all nodes requesting service to the distribution network and organizes the transmission order. It uses a global time pointer that shifts each time a new event is scheduled. If current time is greater than the pointer time it means that no events are scheduled and the WAP goes into the wait state. It is designed to recover from collisions and, since all nodes are being multiplexed into the same channel, collisions are expected.

The main processor is composed of several states, which are shown in Figure 8. The operations performed at each state are described below:

**init**: Initializes state variables and assigns a unique MAC address to the WAP.

**wait**: Awaits for first serviced node to connect. Upon a packet arrival the header is extracted and the time pointer is set to the current time.

**sync**: This state is entered only if a frame is received. Upon reception, it checks if the frame is an echo frame, in this case it is discarded, otherwise it performs these operations: extracts the hello flag to determine if the node is new, in which case it stores in the order log and adds one to the number of currently connected nodes. Then it extracts the close flag to determine if node is closing the session, if its closing it checks if there are any remaining nodes connected, if no other nodes are connected it moves to the wait state, otherwise it moves to the idle state. Also, if it is closing it fixes the order log to remove this node and updates the number of currently connected nodes. If the close flag indicates it is not closing, then the lost expiration time is scheduled (self-timer), a synchronization frame is created, the fields are written including the sync field using the global time pointer, the frame is sent to the antenna port, and the global time pointer is shifted.

**idle**: Awaits for interrupt. If a frame arrives, the header information is extracted. The synchronization order is checked and if the expected packet arrived the log is updated and it moves to the sync state. If no frames arrive before a predetermined deadline, a self-timer triggers and the PKT_LOST condition turns true, forcing it to move to the lost state. If the interrupt is a broadcast timer (set after entering the lost state), it will move to the bcast state.

**lost**: It enters this state only if a frame was lost. Once entered it stores the expected MAC address in the destination field of a newly created frame, it sends the frame to the antenna port, and updates the synchronization order. Since the sync field of the lost packet could not be retrieved the time pointer is shifted to the maximum allowable time window (known by the serviced nodes) and a self-timer is set with the new deadline. Also, a beacon message is scheduled. The reason for this is that if the packet was lost due to collision a new node is trying to enter the cycle and the beacon process will allow it to sync. The global time pointer is shifted to include this beacon message and its response.

**bcast**: Creates and sends a beacon frame to the antenna port.

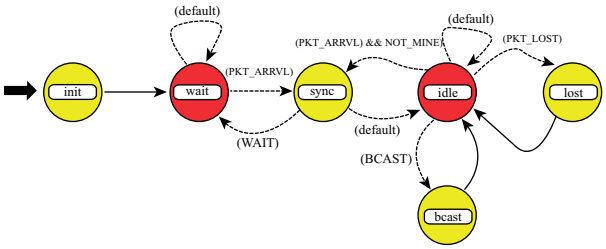


Figure 8. State diagram for the serviced node main processor.

### C. Communication Dynamics of PSMA

This section explains the inter-process communication of the SN processors and a broad view of the frame exchange between SN and WAP. These two mechanisms are essential in the operation of PSMA.

#### 1) Inter-process Communication in the SN

To support PSMA, the SN must include the synchronization information of the subsequent frame into each frame. To accomplish this task a well synchronized and systematic routine is implemented, described ahead and portrayed in Figure 9. After resetting the system the queue is empty, the encapsulation processor has an empty frame and the main processor has nothing to transmit. Upon a packet arrival at the queue, the queue signals the main processor. The main processor initiates the linking process between the SN and WAP by creating an empty hello frame and signals back to the queue that it is ready to receive frames. Once the queue receives the signal, it releases all queued packet (up to certain limit) and follows it with an empty packet with a close instruction. Once the packets start arriving at the encap, it creates a new empty frame where it encapsulates these packets. When the close instruction arrives, the frame size is multiplied by the bit rate to compute the time it will take to transmit the frame. This time is stored in the sync field of the empty frame that was initially in the encapsulation process (at reset). The empty frame is sent to the main processor where the sync time is extracted and included in the hello frame. The hello frame is sent to the WAP. The WAP assigns the next available time to transmit indicated by the global time pointer. It sends this information through the sync frame. The SN, upon receiving the sync frame, schedules the next transmission time. Once this time is reached the main processor signals the queue to release the

 ISBN: 978-1-61208-205-9 

queued packets and the cycle is repeated, with the only difference that in the encapsulation processor there is a queued frame ready to receive the frame size of the subsequent frame. This routine iterates until the queue is emptied. When this happens the queue only sends the close instruction. This informs the encap that there are no more packets to transmit and the encap sets the close flag of the last frame. The close flag is eventually read by the WAP, which does not schedule further occurrences for this SN until a new request arrives.

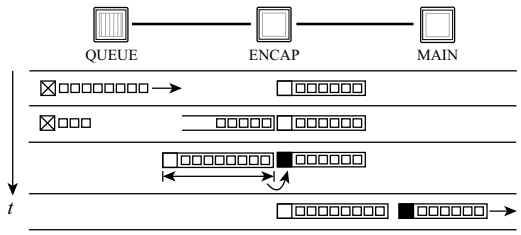


Figure 9. Inter-process Communication in the SN

*2) Frame Exchange between the SN and the WAP*

To stack the frames the following rules are applied, see Figure 10. The task of inserting the first SN is trivial, since there are no active transmissions. If various nodes are sharing the channel and an inactive node turns active, such that is must enter the sharing cycle, it will send a hello frame. The processes are stacked such that there is insufficient time to transmit in between frames; this will cause collisions†. A collision-free MAC protocol can be designed by incorporating cyclic beacon signals, but since this is an infrequent event and this measure consumes time its usefulness depends on the specific application. When collisions occurs, the WAP sends a new schedule time to the expected SN with the maximum allocation time (assuming the sync field could not be recovered). Since this is the last event a beacon signal is scheduled after this allowing enough time for a hello frame to be retransmitted.

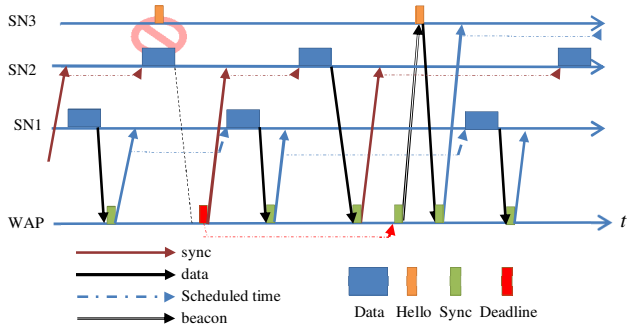


Figure 10. Frame Exchange between multiple SNs and the WAP.

Because there is a scheduled SN the unlinked SN has to wait until the beacon signal to establish a link. Once the WAP has serviced and rescheduled the linked SNs, it sends the beacon signal. The unlinked SN detects that this is a broadcast message (not a hello frame response) and retransmits the hello frame and holds on to the data until the next cycle. The WAP links the SN and from there on frame exchange returns to its routine, but with an additional SN.

## III. RESULTS

The simulation scenario is portrayed in Figure 3. It consists of one WAP servicing 4 SNs. All nodes have a bit rate of 1 Gb/s. The scenario is built in OPNET modeler 16.0. The first test is to demonstrate that the WAP is capable of synchronizing the SNs in the WPAN network.

### *A. Scenario 1 - Systematic Synchronization Capability*

The starting times are pseudorandom with a uniform distribution within a 0.2 second interval. The starting times of the four SN nodes are: 0.0108, 0.0705, 0.1129, and 0.1493 seconds, but do not transmit data until 0.0108, 0.0901, 0.1488, and 0.2075 seconds, respectively, as observed in Figure 11. This simulation run has several interesting aspects: SN1 enters at the same time it requests to enter since it is the only active node at that instant. At 0.0705 s SN2 requests the use of the channel and causes a collision. When the deadline for SN1 expires it is rescheduled; since it is the only node this occurs immediately. It is assumed that upon collisions the sync field is unrecoverable, so the maximum allocation time is granted (in this case 8.3 ms) for the next transmission. It can be seen that SN1 does not require the full allocated time and a gap is produced. Near the end of the gap a beacon frame is sent and the SN2 is linked, but does not transmit data until the following iteration (shown in red). SN3 is requests to use the channel at time 0.1129 s. It can be seen that it collides with SN2. SN2 is rescheduled and following this the beacon frame (near 0.13 s), at which time SN3 is linked. In the next cycle SN3 transmits data. SN4 achieves a link in the same way SN2 and SN3 accomplish it. This shows the implementation is success at establishing links, handling collisions and organizing transmissions in a systematic manner.

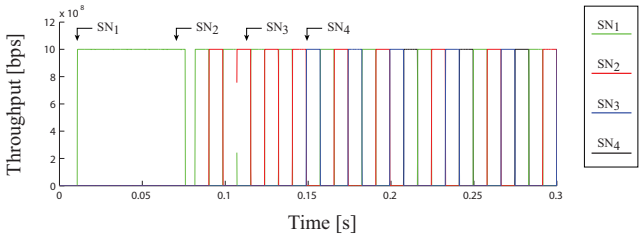


Figure 11. Interlacing of serviced nodes data multiplexed with PSMA.

### *B. Scenario 2 – Diverse SN Load Transmission*

To demonstrate the performance capabilities of PSMA it is compared with the legacy TDMA. In this scenario SN1 transmits 34950 packets, SN2 69900 packets (SN1x2), SN3 139800 packets (SN1x4), and SN4 279600 packets (SN1x8), and the results are shown in Figure 12. The implementation of TDMA used reserves a time slot for each node and does not have knowledge about the amount of packets that need to be serviced. In this scenario, TDMA takes approximately 13.3 seconds to complete all transmissions. Because PSMA stacks all pending events, it achieves to transmit the same load in approximately 6.25 seconds, nearly half the time consumed by TDMA.

 ISBN: 978-1-61208-205-9

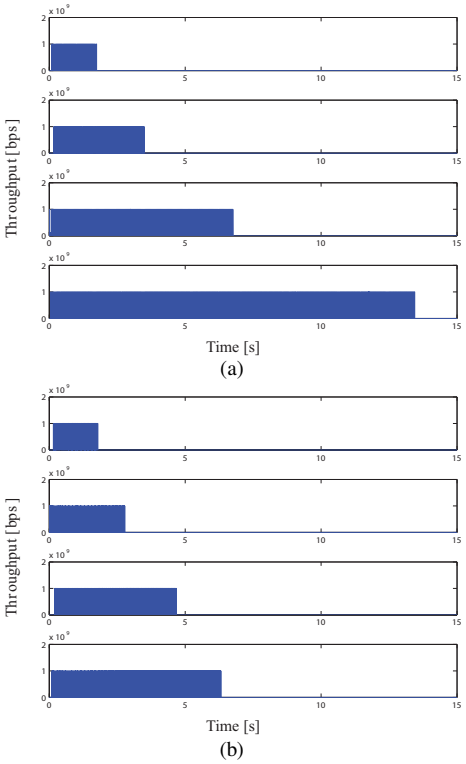


Figure 12. Diverse load transmission using (a) TDMA and (b) PSMA

### C. *Scenario 3 – Relative Percentage Loads*

In this scenario, SN4 transmits a fixed number of packets (699000), while all remaining nodes transmit a percentage of this load. Results are shown in Figure 13.

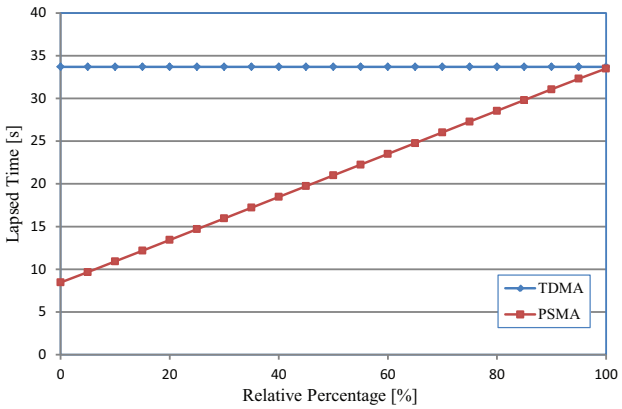


Figure 13. Transmission duration time for varied load percentages.

Since TDMA reserves the slot times independently of there usage, SN4 is unable to take advantage of the unused portions. Regardless of the amount of traffic delivered by the other nodes (as long as it is less than SN4), SN4 will occupy the same amount of time, in this case 33.48 seconds. For the case of PSMA, the processes are stacked, so there is no unused time. If no packets are transmitting, SN4 will use the full channel bandwidth. Compared with TDMA, it will improve the effective throughput by a factor proportional to the number of nodes present in the network.

## IV. CONCLUSIONS

PSMA is an efficient time-domain multiplexing access technique. It has many advantages over legacy TDMA: PSMA has a very efficient use of time as it not only stacks processes that actively require the use of the channel but it allocates only the necessary amount of time for this process to complete. The proposed access algorithm does not have a theoretical node limit as there is no predefined number of time slots, but individual throughput is sacrificed. PSMA is versatile in the sense that in can easily schedule processes not related to data exchange without affecting significantly the transmission of the linked SNs. PSMA supports QoS, as different priority levels can have different benefits, e.g., time duration of allocations and scheduling frequency.

## ACKNOWLEGMENTS

Partially funded by U-INICIA VID 2011 program, grant U-INICIA 11/14; Vicerrectoría de Investigación y Desarrollo, Universidad de Chile.

## REFERENCES

[1] H. Kano, S. Yoshizawa, T. Gunji, T. Saito, and Y. Miyanaga, “Development of 600 Mbps 2×2 MIMO-OFDM baseband and RF transceiver at 5 GHz band,” International Symposium on Communications and Information Technologies (ISCIT), Tokyo, Japan, Oct 2010, Page(s): 891-894.

[2] H.-C. Chien, Y.-T. Hsueh, A. Chowdhury, J. Yu, and G.-K. Chang, “Optical Millimeter-Wave Generation and Transmission Without Carrier Suppression for Single- and Multi-Band Wireless Over Fiber Applications,” Journal of Lightwave Technology, vol. 28, no. 16, pp. 2230-2237, 2010.

[3] S. Singh, F. Ziliotto, U. Madhow, E. M. Belding, and M. J. W. Rodwell, “Millimeter Wave WPAN: Cross-Layer Modeling and Multihop Architecture,” IEEE International Conference on Communications, Dresden, Germany, June 2009.

[4] C.-S. Sum, R. Funada, J. Wang, T. Baykas, M. A. Rahman, and H. Harada, “Error Performance and Throughput Evaluation of a Multi-Gbps Millimeter-Wave WPAN System in the Presence of Adjacent and Co-Channel Interference,” Vol. 27, No. 8, pp. 1433-1442, 2009.

[5] C. Estevez, W. Jian, A. Kailas, D. Fuentealba, G.-K. Chang. “Very-High-Throughput Millimeter-Wave System Oriented for Health Monitoring Applications,” IEEE Healthcom, Columbia, MO, June 2011.

[6] ECMA International, “Standard ECMA-387: High Rate 60 GHz PHY, MAC and HDMI PALs,” 2nd Ed., Dec. 2010.

[7] C.-S. Sum, Z. Lan, R. Funada, J. Wang, T. Baykas, M. A. Rahman, H. Harada, and S. Kato, “Virtual Time-Slot Allocation Scheme for Throughput Enhancement in a Millimeter-wave Gbps WPAN Cross Layer Design,” IEEE International Conference on Communications, Dresden, Germany, June 2009.

[8] W. Jian, A. Chowdhury, Z. Jia, C. Estevez, G.-K. Chang, “Energy-Efficient Multi-Access Technologies for Very-High-Throughput Avionic Millimeter Wave, Wireless Sensor Communication Networks,” Journal of Lightwave Technology, Vol. 28, No. 16, pp. 2398-2405, Aug. 15, 2010.

[9] W. Jian, C. Estevez, A. Chowdhury, Z. Jia, G.-K. Chang, “A Hybrid MAC Protocol Design for Energy-Efficient Very-High-Throughput Millimeter Wave Wireless Sensor Communication Networks,” Asia Communications and Photonics Conference and Exhibition, Shanghai, China, December 2010.

 ISBN: 978-1-61208-205-9 

# Deployment of Femtocells in Pakistan: A Consumer's Perspective

Javed Iqbal
Transmission Division
National Telecom Corporation
Pakistan
javed.iqbal@ntc.org.pk

Sahibzada Ali Mahmud, Gul M Khan, Fahad Ullah
Electrical Engineering Department
University of Engineering and Technology
Peshawar, Pakistan
sahibzada.mahmud@nwfpuet.edu.pk,
gk502@nwfpuet.edu.pk, fahadullah@nwfpuet.edu.pk

***Abstract*—Femtocell base stations operate in the licensed cellular band, and are small and low power devices providing a feasible and low cost alternative to microcell deployment in order to improve indoor signal coverage at homes and small buildings. Despite many benefits that can be offered by wide scale femtocell deployment by network operators, there are some mandatory factors related to the end user perception in adopting and paying for the technology. In this paper, a thorough survey has been conducted to get an idea about the end user perspectives in regard to the deployment of femtocells. The survey contains a number of questions asked from over 150 participants from different backgrounds in order to determine the user opinion on installing femtocells and opting for data services offered by cellular network operators. Different categories have been made from the survey questions and results obtained are presented and discussed. Although the survey has been conducted in urban and rural areas of Pakistan, the survey can prove to be valuable in assisting network operators to adopt better marketing strategies outside Pakistan as well. Based on the general user response, it is evident that the users showed their interest in utilizing femtocells if better and low cost packages for using data services are provided. Furthermore, in those areas where DSL connectivity options are not available, users are willing to pay for femtocell base stations that can connect them to the cellular network via the microcell base station.**

***Keywords—Femtocell; Fixed Mobile Convergence; Cellular Networks***

## I. INTRODUCTION

Cellular networks have been providing new and innovative services to its users while on the other hand they are also facing expansion problems. In cellular networks frequency re-use, better signal strength in indoor environments, and capacity enhancements in populated areas keeping in mind the cost constraints are nontrivial issues. The radio signal carrying information degrades as it enters a closed structure for instance, a building. Femtocells are small base stations that operate in the licensed cellular bands. They are small and inexpensive devices similar in size to a Wireless LAN (WLAN) Access Point, and transmit at a low power and are to be placed in individual homes and backhauled onto the operator's network via conventional Digital Subscriber Lines (DSL).

Both the concept and the economics of femtocells constitute a radical arrival from traditional macro radio access networks, where each macro base station typically covers a fairly large geographical area and serves a relatively large number of users. Their strategic positioning inside the home and ability to be customized to the needs of individual consumers promise to rapidly make them major future components of the operators' business. Femtocells have gained a lot of attention from the research community due to the benefits offered in terms of infrastructure cost saving, load balancing, and improved user experience indoors [1]. The idea of femtocells was presented in 1999; however, it started attracting wide spread market attention in 2007 [2]. Cellular operators have shown interest in the commercial deployment of femtocells in order to increase network capacity and improve coverage.

Since it is unlikely that the network operators are going to deploy additional microcell base stations in order to improve signal strength in indoor environments because of the substantial cost that is associated, femtocells provide a very low cost and feasible alternative. However, the wide scale presence of DSL being the prevalent means of access connectivity for consumers and providing data services at much better data rates than the cellular alternatives, mostly at a flat monthly rate, raises the question whether the end consumers are ready and willing to pay extra for provision and deployment of femtocells. Even though femtocells can offer better indoor reception for the consumer, still extra cost is associated if data services of the cellular network operator are used. Therefore, another important question is whether the consumers while having the option of utilizing data services using the existing DSL connection at a flat rate (which they are already paying) are going to utilize the data services of the cellular network operator (for which they have to pay extra) if the femtocell base station is deployed. Most of the new mobile phones in the market have a Wireless LAN interface and the users can use their mobile phone to connect with a wireless router to get access to data services and even make free voice calls using applications like Skype. Therefore, the end user perception about femtocell deployment can assist in answering these questions and help the network operators to shape their policies accordingly regarding wide scale femtocell deployment with better packages to entice the consumer in using their data services.

In this paper, a survey has been carried out using the most pertinent questions regarding femtocell deployment in order to gather the relevant statistics that portray the consumer perception in a way that can be helpful to the network operators to shape their marketing strategy regarding femtocell deployment in Pakistan. Section II of the paper gives a brief introduction about the generic network architecture that can be used for femtocell deployment. Section III gives specifics about femtocell deployment in Pakistan. Section IV describes the main advantages which femtocell deployment can offer. Section V contains the main contribution of the paper and gives the details of the survey and its results. Section VI has some recommendations based on the result of the survey. Section VII concludes the paper.

 ISBN: 978-1-61208-205-9 

## II. GENERAL ARCHITECTURE

For femtocell deployment, initially, a flat network architecture was proposed with IP used as a backhaul transport protocol to the operator's network. In the flat architecture a Security Gateway (SG) is placed between the cellular operator network and the femtocell that acts as the residential Node-B. In other proposed architectures, a Radio Access Network (RAN) Gateway is placed between the IP Network and the operator's core network [3][4]. When a RAN gateway is deployed some of the functions of the Radio Network Controller (RNC) are moved to the femtocell base station. These RAN gateways can incorporate substantial traffic from large number of femtocells on Iu over IP (the interface introduced for femtocell access to a UMTS network) [5]. The RAN gateway than forwards that traffic to the UMTS network on the Iu-PS (Iu- Packet Switched Interface defined for RAN gateway and Serving GPRS Support Node (SGSN) of a UMTS network) and Iu-CS (Iu circuit switched, interface between RAN gateway and MSC of the network) interfaces. Other interfaces include Iub (between the RNC and the Node B) and Iur (between RNCs in the same network). Iu interfaces carry user traffic (such as voice or data) as well as control information. The Iu interface is specified at the boundary between the Core Network (CN) and the RAN. The Iu-CS and Iu-PS interfaces are specified in the 25.41x series of UMTS technical specifications. The RAN gateway provides a simplified means to assist in wide scale femtocell deployment for cellular network operators with lower infrastructure expenditure. An example architecture can be seen in Fig. 1.

## III. FEMTOCELL DEPLOYMENT IN PAKISTAN

In Pakistan, the Telecom sector is in the process of evolution and new standardized technologies are being adopted. End users can opt for different broadband packages that utilize ADSL with cheaper and more attractive offers and bandwidths of up to 50 Mbps. Above 60% of the population has access to voice and data services using either the cellular network or DSL. However, the issue of poor indoor reception usually thwarts the end user to go for data connectivity using the cellular network mainly because of lower data rates and the associated cost.

Since many popular internet applications especially streaming voice and video applications have high throughput requirements, the cellular network operators in Pakistan are gradually expanding their coverage and improving their capacity to accommodate more users and offer them higher data rates. However to fully satiate the requirements of the end users and encourage them to utilize the cellular networks for data services, the operators have to provide better packages and improve the link budget for indoor environments. Currently the data services are provided by the network operators using GPRS and EDGE in Pakistan.

In order to provide better throughputs, the planning has already started to upgrade their networks to UMTS and make use of newer 3GPP [6] specifications like High Speed Data Packet Access (HSDPA), High Speed Packet Access (HSPA+), Long Term Evolution (LTE) and LTE Advanced. In order to improve the indoor coverage and signal quality, implementation of femtocell base stations shall prove to be a viable and low cost solution from the network operator's perspective. However, to find out the feasibility of mass deployment in the urban and rural areas surveys have been conducted in 9 major cities of Pakistan as well as the rural areas. In the survey, the opinion was inquired from more than 150 participants. The questions asked in the survey were prepared in such a way that the results can be utilized and prove to be useful to network operators outside Pakistan. In near future Pakistan Telecommunication Authority (PTA) is going to auction the IMT2000 frequency band for UMTS (WCDMA) services.

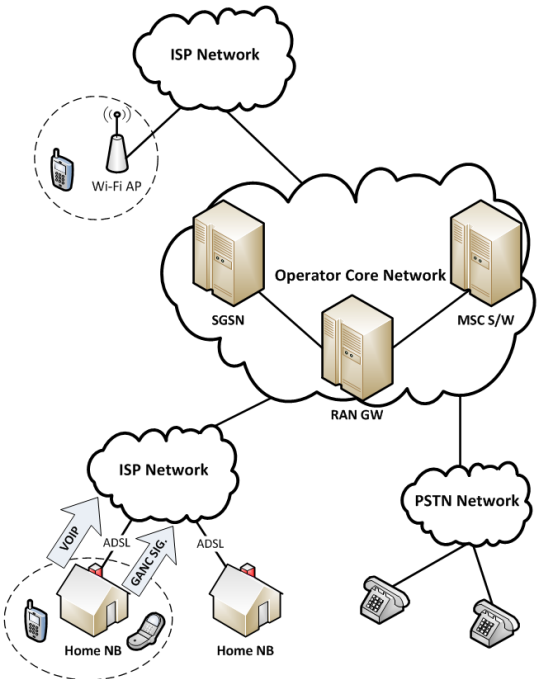


Figure 1 GAN-based Home NodeB architecture

## IV. ADVANTAGE OF INSTALLING FEMTOCELLS

According to the statistics, above 70% calls are originated from homes and inside the buildings [7]. To mitigate the issue of poor indoor reception microcell installation is a solution with substantial cost associated with it. The femtocell base station installation in a home or a building does not only ensure lower infrastructure expenditure but can also relieve the traffic from the microcell base stations [8]. The reason is that the femtocell base station is connected to the available DSL connection and all the user traffic is backhauled to the cellular network directly using that connection. Even users can share the cost of femtocell implementation if the femtocell base station is provided at a lower cost by the operator or provided freely as a part of an attractive package.

By installing Femtocells, in addition to better voice quality, multimedia and other data traffic can be accessed at higher

 ISBN: 978-1-61208-205-9 

data rates because of improved Signal to Noise Ratio (SNR). Femtocells will deliver converged services (voice, video and data services) at home and will enable users to have a seamless experience across both outdoor and indoor environments [9]. Because of a lesser distance between users' mobile device and the femtocell, the user device can connect to the femtocell base station using lower transmission power hence reduced battery consumption and lower probability of health concerns.

## V. CONSUMER PERSPECTIVE SURVEY

The survey was conducted in cities of Karachi, Lahore, Islamabad, Rawalpindi, Quata, Bannu, Peshawar, Mardan and Nowshera. In this section, questions from the survey are categorized in different sections. Each section has the relevant questions tabulated, the tables representing the questions and the percentage response, and finally the graph giving an insight of the received response.

### *A. Connection and Reception*

Five questions asked in this category of survey are listed n Table I. Most of the questions asked were about the connectivity options that a user has and about the cellular service signal reception. In Table II, the results of the survey are tabulated and based on the results (answers), percentage plots are made as shown in Fig. 2.

Question 4 is particularly worth mentioning because it is obvious from the results that people are interested in paying more in order to get a better signal strength at their homes i.e. for indoor usage of cellular service.

TABLE I CONNECTION AND RECEPTION RELATED QUESTIONS

| Q.No | Question | Answer Choices | Remarks |
|---|---|---|---|
| 1 | Do you have a DSL connection at home? | i. Yes<br>ii. No | |
| 2 | Do you use your cell phone to access data services i.e. access the internet? | i. Yes<br>ii. No | |
| 3 | Do you have a good signal reception at your home (indoors)? | i. Yes<br>ii. No | |
| 4 | Would you prefer to have good/better signal reception at your home for a one off payment? | i. Yes<br>ii. No | |
| 5 | Do you intend to receive good signal reception at home only to receive phone calls or also to make phone calls using your cell phone? | i. Yes<br>ii. No | Answer if "Yes" to 4 |

TABLE II RESULTS OF THE CONNECTION & RECEPTION RELATED QUESTIONS

| Question No. | Answer Percentage | |
|---|---|---|
| | *Choice (i)* | *Choice (ii)* |
| 1 | 93% | 7% |
| 2 | 40% | 60% |
| 3 | 58% | 42% |
| 4 | 79% | 21% |
| 5 | 86% | 14% |

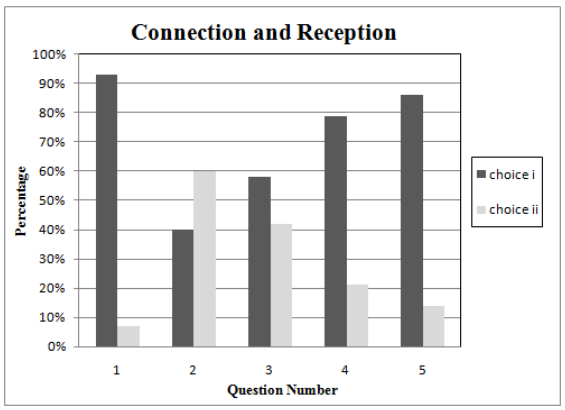


Figure 2 Answer Choices Plot for Table II

### *B. Making Phone Calls*

This section categorizes the questions asked about using which service for making phone calls. Table III tabulates the questions asked from the users. Based on the questions asked, the results are obtained as shown in table IV. Fig. 3 depicts the corresponding bar graphs for each question asked.

TABLE III MAKING PHONE CALLS RELATED QUESTIONS

| Q.No. | Question | Answer Choices |
|---|---|---|
| 6 | When at home, do you primarily use your landline phone to make calls more often or do you use your mobile phone to make calls? | i. Landline<br>ii. Mobile Phone |
| 7 | Does cost of making the phone call affect your priority in any way? | i. Yes<br>ii. No |
| 8 | Does the reception quality of your mobile phone affect your priority in any way? | i. Yes<br>ii. No |

TABLE IV RESULTS OF THE MAKING PHONE CALLS RELATED QUESTIONS

| Question No. | Answer Percentage | |
|---|---|---|
| | *Choice (i)* | *Choice (ii)* |
| 6 | 60% | 40% |
| 7 | 73% | 27% |
| 8 | 76% | 24% |

Question 8 in this category is important because users are interested in changing their means of making a call based on the reception quality. Poor reception quality usually leads to calling from another source, landline for instance, rather using the mobile phone.

### *C. Accessing Internet*

Data services and internet related questions are listed in this category as Table V shows. Based on the feedback, the results of the questionnaire are tabulated in Table VI. Finally, the results are plotted in Fig. 4.

 ISBN: 978-1-61208-205-9 

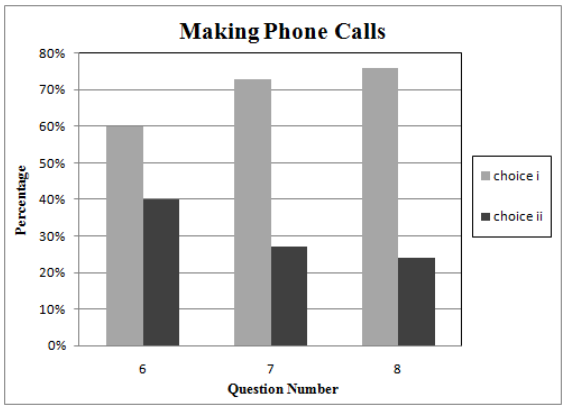


Figure 3 Answer Choices Plot for Table IV

As the results show, most of the users are interested in using mobile phone for internet access. The principle reason behind choosing a mobile phone for internet access is the associated mobility and convenience. Also, users most of the time use both cellular data service and a WLAN for mobile internet in phones though there isn't a particular higher priority for either one. Both are used by most of the users, most of the time. For better indoor reception and hence accessing data services, almost half of the users who were part of the survey are willing to pay more. The results obtained and discussed show that the deployment of femtocells in an indoor environment is very likely in near future.

TABLE V ACCESSING INTERNET RELATED QUESTIONS

| Q.No. | Question | Answer Choices |
|---|---|---|
| 9 | When at home, which device do you use to access the internet more often i.e. your mobile phone or the DSL connection? | i. Mobile Phone<br>ii. DSL Connection |
| 10 | In case it's the mobile phone, do you connect your cell phone to the WLAN router and access the internet or do you use the services of your cellular operator or both? | i. WLAN Router<br>ii. Cellular Operator<br>iii. Both |
| 11 | In case you don't use your mobile phone to connect to the internet, is any one of the following any reason for you to do so? | i. Poor indoor reception<br>ii. Comparatively higher cost of using data services from cellular operator |
| 12 | Would you prefer the convenience of using mobile phones to access the internet even at a comparatively higher cost when compared to the DSL connection? (if the option of femtocell is available and as a result good reception is available) | i. Yes<br>ii. No |
| 13 | What percentage of time do you utilize accessing data services each day using your cellular operator while at home compared with the total time utilized throughout the day doing the same? | i. 10-20 %<br>ii. 20-40 %<br>iii. 40-60 %<br>iv. 60-80%<br>v. 80-100% |

TABLE VI RESULTS OF ACCESSING INTERNET RELATED QUESTIONS

| Q.No. | Answer Percentage | | | | |
|---|---|---|---|---|---|
| | *Ch. (i)* | *Ch. (ii)* | *Ch. (iii)* | *Ch. (iv)* | *Ch. (v)* |
| 9 | 79% | 21% | - | - | - |
| 10 | 29% | 27% | 44% | - | - |
| 11 | 48.3% | 51.7% | - | - | - |
| 12 | 48.4% | 51.6% | - | - | - |
| 13 | 41.8% | 20.6% | 22% | 12.1% | 3.6% |

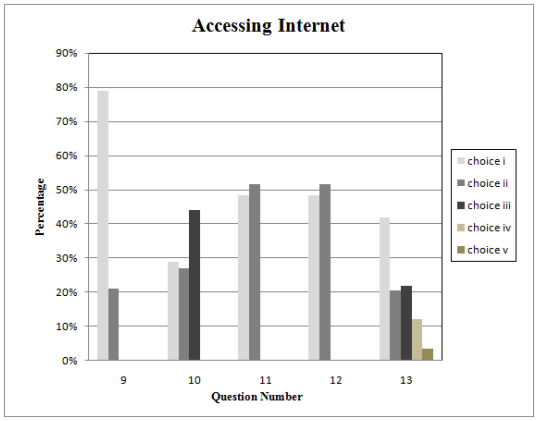


Figure 4 Answer Choices Plot for Table VI

### *D. Femtocell Installation*

Table VII lists the questions asked about the deployment of Femtocells. The results of the survey are tabulated in Table VIII and the corresponding plots are shown in Fig. 5. Different inferences can be made from the results in this category of the survey. Users are interested in installing femtocells to get good reception for the signal itself as well as to use the data services. Half of the users in this case chose for both options. Question 15 is important because it reflects user opinion on installing femtocells at their homes—or any indoor enclosure for that matter—in case DSL services are not reachable especially in rural areas.

One major reason not to opt for a Femtocell deployment at home is the price of the device itself although the results are comparable with another reason for not using a Femtocell device at home i.e. the data service charges set by the operators. Users will be interested in deploying a Femtocell at their homes if the operators can lower the data services charges or introduce reasonable data packages. Finally, most of the users are ready to share their Femtocell service with other external users even though the limited user capacity is explicitly mentioned in the question.

 ISBN: 978-1-61208-205-9 

TABLE VII FEMTOCELL INSTALLATION RELATED QUESTIONS

| Q. No. | Question | Answer Choices |
|---|---|---|
| 14 | If you would opt to install a femtocell base station, would it be because you prefer to have good signal reception for making/receiving voice calls using your cell phone or because you prefer to access the data services or both? | i. Good Signal Reception<br>ii. Access Data Services<br>iii. Both |
| 15 | If you don't have DSL connectivity because it is not available in your area, would you consider buying a Femtocell Base station to get better reception and high speed data services? | i. Yes<br>ii. No |
| 16 | What is the main reason for not opting for a femtocell solution? | i. Cost of Femtocell base station<br>ii. Cost of data services provided by the cellular operator |
| 17 | Would any of the following make you reconsider about getting a femtocell solution? | i. Femtocell base station provided free of cost by the cellular operator<br>ii. Lower charges for data services or better packages at lower cost<br>iii. Data services provided free of cost by the cellular operator |
| 18 | In case your decision to install a femtocell is to improve the signal reception for making/receiving phone calls, would you still sometimes use the facility to access data services from your cellular operator? | i. Never<br>ii. Maybe<br>iii. If a good offer is available<br>iv. don't know |
| 19 | In case DSL connectivity is not available in your area for some reason and your femtocell has a direct wireless connection to the nearby macrocell base station, would you be willing to share your femtocell coverage with external users who might need to connect to the nearby macrocell base station by using your femtocell as one of the relay devices to send their signal across (Considering the fact that a femtocell base station might not support more than 4 users at a single instant)? | i. Yes<br>ii. No |

TABLE VIII RESULTS OF FEMTOCELL INSTALLATION RELATED QUESTIONS

| Q. No | Answer Percentage | | | |
|---|---|---|---|---|
| | *Ch. (i)* | *Ch. (ii)* | *Ch. (iii)* | *Ch. (iv)* |
| 14 | 24.8% | 24.8% | 50.4% | |
| 15 | 84.4% | 15.6% | | |
| 16 | 52.8% | 47.2% | | |
| 17 | 35.1% | 40.3% | 24.3% | |
| 18 | 17.9% | 28.5% | 47.0% | 6.6% |
| 19 | 64.2% | 35.8% | | |

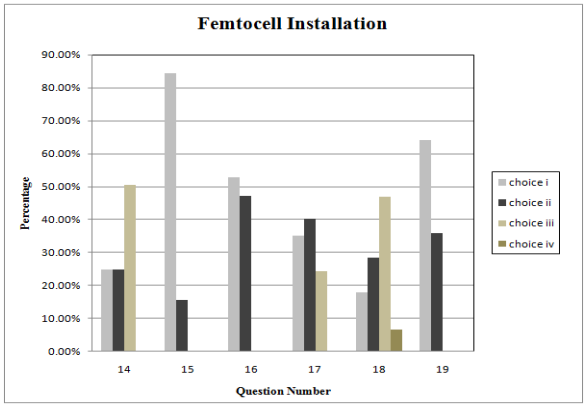


Figure 5 Answer Choices Plot for Table VIII

### *E. Skype Users*

In this category of the survey, questions are asked from around 100 users who used Skype in their smartphones and are different from the pool of users who were asked Questions 1-19. Table IX lists the questions that were asked. The results obtained are tabulated in Table X and based on those results; the corresponding plots are drawn as shown in Fig. 6.

More than half of the users didn't use Skype application in their phones. Half of the users with Skype installed in their smartphones were interested in using the application for making free local and international phone calls and most of them were interested in paying for deploying a femtocell base station at their homes in order to get better reception for faster data services.

TABLE IX SKYPE USER RELATED QUESTIONS

| Q.No. | Question | Answer Choices | Remarks |
|---|---|---|---|
| 20 | Do you own a smart phone that has Skype installed? | i. Yes<br>ii. No | |
| 21 | Do you use your Skype service to make free calls nationwide and internationally? | i. Yes<br>ii. No | Answer if "Yes" to 20 |
| 22 | Would you opt to pay for a femtocell base station to get better indoor coverage as well as faster data services? | i. Yes<br>ii. No | Answer if "Yes" to 21 |

 ISBN: 978-1-61208-205-9

TABLE X RESULTS OF SKYPE USERS RELATED QUESTIONS

| Question No. | Answer Percentage | |
|---|---|---|
| | *Choice (i)* | *Choice (ii)* |
| 20 | 44.30% | 55.70% |
| 21 | 50.60% | 49.40% |
| 22 | 65.50% | 34.50% |

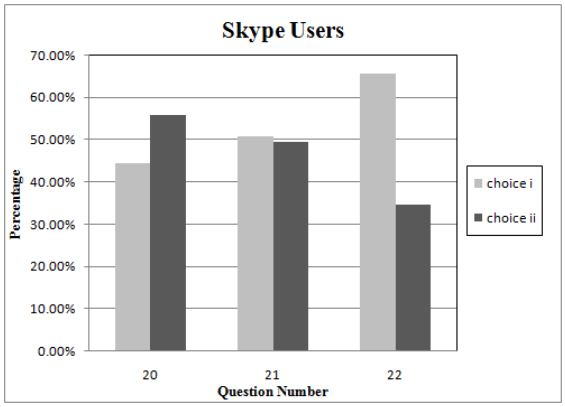


Figure 6 Answer Choices Plot for Table X

## VI. RECOMMENDATIONS BASED ON SURVEY RESULTS

Based on the results of conducted survey, it is evident that the potential consumers of femtocell based services are interested in getting data services from the cellular operators at a lower cost. The response to Question 19 suggests the willingness of most of the end consumers to share their femtocell coverage in case there is no DSL connectivity available especially in rural areas, in order to indirectly access the macrocell base station or Node b. This option if exercised shall have an impact on the overall deployment architecture since multihop communication can be considered in order to give access to users to indirectly access the macrocell base stations or Node b's via connected femtocells. Furthermore, Hybrid Access Points (HAPs) can be considered in the future that can give access to WLAN users as well as femtocell users and backhaul their traffic to the respective networks via a single, high bandwidth DSL connection and has the ability of traffic differentiation.

## VII. CONCLUSION

Femtocell deployment in urban and rural areas in Pakistan is expected in the near future. It is clear that a wide scale implementation shall benefit the operators in terms of substantial infrastructure cost savings. However, the end user can also benefit in terms of improved indoor signal reception for voice and data access. The results of the survey carried out show that the users are willing to acquire femtocell based solutions if cost effective and better packages are offered by the network operators. The results of the survey can prove to be a good yardstick for network operators in and out of Pakistan to shape their marketing strategies in an effective manner in order to increase the utilization of their networks in terms of substantial data services and as a result more revenue generation.

## REFERENCES

[1] Kim, R.Y., Jin Sam Kwak, and Etemad, K.,"WiMAX Femtocell: Requirements, Challenges, and Solutions," *IEEE Communications Magazine,* Vol. 47, Issue: 9, pp. 84-91, Sep. 2009.

[2] Douglas, N. K., Takahito Y., and Favichia F.,"Standardization of Femtocells in 3GPP," *IEEE Communications Magazine*, Vol. 47, Issue: 9, pp. 68-75 Sep. 2009.

[3] 3GPP TS 43.318, Generic Access Network (GAN) Stage 2, Rel-5.

[4] 3GPP TS 44.318, Generic Access Network (GAN); Mobile GAN Interface Layer 3 Specification, Rel-5.

[5] Zhang J., and de la Roche, G., *Femtocells: Technologies and Deployment.* Sussex, UK: John Wiley and Sons Ltd, 2010

[6] www.3gpp.org

[7] G. Mansfield, "Femto cells in the US market - business drivers and femtocells in the US market - business drivers and consumer propositions," in *FemtoCells Europe 2008*, AT&T, Oct. 2008.

[8] Claussen, H., and Calin, D.,"Macrocell Offloading Benefits in Joint Macro and Femtocell Deployments," *Personal, Indoor and Mobile Radio Communications, 2009, IEEE 20th International Symposium on*, pp. 350 – 354, Sep 2009.

[9] Chandrasekhar, V., Andrews, J., and Gatherer, A.,"Femtocell Networks: A Survey," *IEEE Communications Magazine*, Vol. 46, Issue: 9, pp. 59–67, Sep 2008.

 ISBN: 978-1-61208-205-9 

# Efficient OEO-based Remote Terminal Providing a Higher Power Budget of an Asymmetric 10/1G-EPON

Kwang-Ok Kim[1,2]/Jie-Hyun Lee[1]/Sang-Soo Lee[1]
[1]Department of Optical Internet Research
Electronics and Telecommunications Research Institute
218 Gajeong-ro, Yuseong-gu, Daejeon, 305-700, Korea
E-mail: {kwangok, jhlee, soolee}@etri.re.kr

Youn-Seon Jang[2]
[2]Department of Electronics Engineering
Chungnam National University
99 Daehak-ro, Yuseong-gu, Daejeon, 305-764, Korea
E-mail: jangys@cnu.ac.kr

***Abstract*—This paper proposes the design of an efficient Optical-Electrical-Optical (OEO)-based Remote Terminal (RT) that can provide the higher power budget required for a long-reach transmission in an asymmetric 10 Gbit/s Ethernet Passive Optical Network (10/1G-EPON). The current 10/1G-EPON specification supports a maximum physical distance of only 20km in a 32-way split due to a power budget limitation. However, many service providers prefer a transmission reach of over 40km in a 64-way split for an efficient access network design. In this paper, the proposed OEO-based RT provides quad-port architecture for a cost-effective design, supports a high power budget of 58 dB through 3R signal regeneration, and offers over a 50 km reach and 128-way split per port with no modification of a legacy 10/1G-EPON system. In addition, it can satisfy a Packet Loss Rate (PLR) of 10^-10 in the downstream and upstream paths.**

***Keywords-10Gbit/s EPON, Remote Terminal, Long Distance EPON, Reach Extender***

## I. INTRODUCTION

A 10 Gbit/s Ethernet Passive Optical Network (10G-EPON) is one of the fastest access technologies for providing next-generation ultra-broadband services to subscribers. In the current Fiber-to-the-Home (FTTH) optical access system, 1 Gbit/s EPON (1G-EPON) is being extensively utilized, particularly in Asian countries such as Japan, Korea, and China. However, with the recent growth of user traffic, a 10G-EPON is expected to provide end users with a more comfortable online environment in the near future [1].

The 10G-EPON specification was ratified as the IEEE 802.3av standard in 2009, and supports two configuration modes: symmetric mode, operating at a 10 Gbit/s data rate in both directions; and asymmetric mode, operating at a 10 Gbit/s in the downstream direction and 1 Gbit/s in the upstream direction [2]. Additionally, to reduce the costs for laying fibers and equipment, 1G-EPON and 10G-EPON use the same outside plant. In particular, an asymmetric 10G-EPON (i.e., 10/1G-EPON) can be easily applied to the Single Family Unit (SFU) market as a cost-effective next-generation solution, as its upstream transmission is identical to that of 1G-EPON, and its downstream transmission relies on the maturity of 10Gbit/s Ethernet devices.

The current 10/1G-EPON is defined into three classes of power budget: PRX10, PRX20, and PRX30. For compatibility with the PX10 and PX20 power budgets defined for a 1G-EPON, a 10/1G-EPON should mainly use the PRX10 and PRX20 power budgets [2][3][4]. These power budgets support channel insertion losses of 20 and 24 dB, respectively. Therefore, a legacy 10/1G-EPON can support a physical distance of only 20 km for Single Mode Fiber (SMF) in a 1:32 split ratio [5].

However, many network operators worldwide have placed an increased emphasis on combining an optical access network with a metro network by consolidating their central offices (COs) through a long-distance EPON solution. This combination results in a considerable reduction in Capital Expenditure (CAPEX) and Operating Expenditure (OPEX) budgets. In particular, EPON service providers require the high power budget to support long distances and a high split ratio such as 1:64@40 km. In addition, they hope to discover a solution satisfying the following key questions [5]: how to leverage the EPON architecture in rural areas, how to further increase subscriber density in their COs, how to decrease the connection cost per subscriber, and how to serve more people at a larger distance from the COs using IEEE802.3 EPON equipment.

To satisfy these requirements, we suggest the cost-effective 3R-type Optical-Electrical-Optical (OEO)-based Remote Terminal (RT) that can provide a higher power budget of 58 dB in a legacy 10/1G-EPON without modification. We also demonstrate the performance of the OEO-based RT using a commercialized 1G-EPON system.

The remainder of this paper is organized as follows. In Section II, we briefly review related work, while in section III we describe the detailed structure and design scheme of the proposed OEO-based RT. In Section IV, we show experimental results proving the effectiveness of our method and provide an analysis of its performance. Finally, we present a brief summary of our work in Section V.

## II. RELATED WORK

A long-distance 10/1G-EPON helps with network evolution, and reduces network levels and nodes from an increased high power budget. It can also provide significant cost savings by reducing the amount of electronic equipment and real estate required at a local exchange. Moreover, it can support service to small towns, suburbs, and rural areas [6].

To achieve these purposes, the IEEE802.3 extended EPON study group is standardizing a new definition of the

 ISBN: 978-1-61208-205-9 

power budgets or reach extender solutions that can support a higher power budget [5]. Recently, several methods were suggested by the extended EPON study group. The first method is to define new power budget classes (i.e., PRX40 and PRX50) through an increase in the receiver sensitivity and launch power of the transmitter. The second method is to use an extender box providing optical amplification (OA) or OEO for passing data streams. The final method is to decrease Optical Distribution Network (ODN) loss through an improved splitter design [7][8].

As a first option, the current extended EPON study group is focusing mainly on the Physical Media Dependent (PMD) development of new power budget classes for application in the Multiple Dwelling Unit (MDU) market, as many operators would prefer a completely passive solution. However, much of the market demand for high split ratios of over 1:64 also requires a 40 km reach through a high power budget of over 35 dB. Among the methods described above, only the use of an extender box can easily satisfy this requirement. In an extended EPON study group, the line cost and power consumption per subscriber are also primary considerations when designing a high power budget solution for a 10G-EPON [9].

Figure 1 shows the 10G-EPON link structure ratified by the IEEE802.3av, and suggested by the extended EPON study group. This 10G-EPON can support a maximum transmission reach of 20 km in a 1:64 split ratio when using a PR(X)30 with a high power budget of 29 dB, as shown in Figure 1-(a). An extended PMD solution is provided through the insertion of an optical amplifier within the transceiver, and can support a power budget of 35 dB using the newly defined PR(X)50 PMD, as shown in Figure 1-(b). A 10G-EPON using a PR(X)50 PMD can support a long distance of

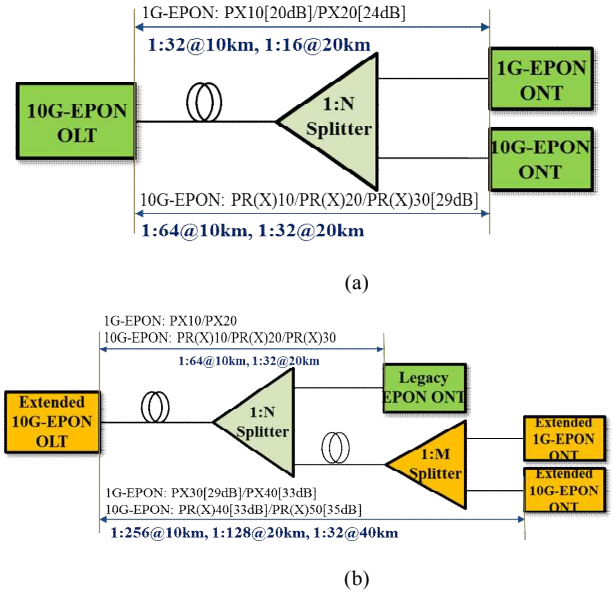


Figure 1. EPON link structure: (a) Standardized 10G-EPON line structure ratified by the IEEE802.3av Working Group, and (b) the 10G-EPON link structure suggested by the ExPMDs Study Group.

up to 40 km in a 1:32 split ratio without an extender box in the remote node, and can also support a high split ratio of 1:128@20 km and a very high split ratio of 1:256 within a very short distance of 2 km [10].

However, an efficient 10/1G-EPON extender box solution supporting a cost-effective design, low power consumption, and a power budget of about 58 dB using the already developed PRX30 PMD has yet to be reported. Therefore, to support a physical distance of over 40 km and a greater than 1:64 split ratio under the worst-case ODN design scenarios without any problems, a 10/1G-EPON must apply a remote terminal as an extender box utilizing an active device. Active in-field components are also acceptable to many operators.

In this paper, our proposed OEO-based 10/1G-EPON RT can efficiently provide a high power budget of 58 dB using the following functions: 3R signal retiming, remote management through a Simple Network Management Protocol (SNMP) agent and an embedded Optical Network Unit (ONT), and upstream burst-to-continuous signal conversion.

## III. PROPOSED OEO-BASED REMOTE TERMINAL FOR LONG-DISTANCE ASYMMETRIC 10G-EPON

Figure 2 illustrates the 10/1G-EPON link structure applied to the proposed OEO-based 10/1G-EPON RT in the remote node to support a long distance and high split ratio. A 10/1G-EPON system utilizing the 10/1G-EPON RT can provide a physical reach of over 60 km using an existing PX20 or PRX30 PMD in the trunk fiber, and can support a 1:256 or 1:64 high split ratio for a 5 or 10 km reach, respectively, using standardized 10/1G-EPON PMDs under the worst-case ODN design scenarios without any problems. That is, when considering an optical fiber loss of 0.4 dB/km, the 10/1G-EPON applied to our 10/1G-EPON RT can easily support a high split ratio of 1:256@ over 60 km from a central office to end users. This makes a flexible access network configuration possible.

The 10/1G-EPON RT mainly provides wavelength conversion and a signal retiming function based on 3R signal regeneration between a 10/1G-EPON OLT and 10/1G-EPON ONTs or 1G-EPON ONTs. In addition, it provides an optional upstream burst-to-continuous signal conversion to support WDM multiplexing in the trunk fiber. In particular, because the 10/1G-EPON RT is necessary for electrical power, it requires a remote management function and low-cost, low-power design.

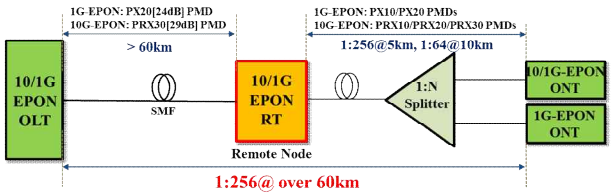


Figure 2. 10/1G-EPON link structure applied to the proposed OEO-based RT.

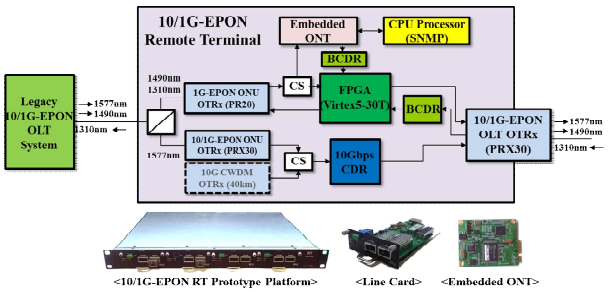


Figure 3. The design architecture and prototype of the 10/1G-EPON RT.

Figure 3 shows the design architecture and prototype of the developed 10/1G-EPON RT. The 10/1G-EPON RT is composed of a 3-port edge WDM filter for interconnection with the 10/1G-EPON OLT, a single FPGA for retiming of a 1 Gbit/s downstream signal, an embedded ONT for SNMP packet transmission to the 10/1G-EPON OLT, a CPU processor providing SNMP for remote management, a Burst-mode Clock & Data Recovery (BCDR) device for retiming of the burst-mode upstream signal, a Crosspoint Switch (CS) device for electrical signal division, a 1G-EPON ONU transceiver for receiving and transmitting a 1 Gbit/s optical signal, a 10/1G-EPON ONU transceiver for receiving a 10 Gbit/s downstream optical signal, and a 10/1G-EPON OLT optical transceiver for inter-connection with the ODN.

The 10/1G-EPON RT divides a 10 Gbit/s wavelength signal into 1 Gbit/s wavelength signals using a 3-port edge WDM filter. These wavelength signals are then inserted into each EPON ONU transceiver, and an optical signal is then converted into an electrical signal. These electrical signals are retimed by an FPGA and 10Gbit/s CDR in the electrical domain. The retimed signals then are retransmitted to the optical domain using a 10/1G-EPON OLT transceiver. In contrast, the signal retiming for a 1 Gbit/s signal in the upstream is performed using a BCDR device, which then converts the retimed upstream burst-mode signal into a continuous-mode signal through the FPGA.

The 10/1G-EPON RT is designed using a quad-port architecture, and provides a signal retiming function through a Virtex-5 FPGA (XC5VLX-30T) for lower design costs and power consumption. However, the signal retiming function for a 10 Gbit/s downstream signal is performed using a commercialized low-cost 10 Gbit/s CDR device. Each port of the 10/1G-EPON RT was also designed as a plug-and-play type.

To provide remote management of the 10/1G-EPON RT, an embedded ONT is activated using a 10/1G-EPON OLT system with a CS device, BCDR device, and FPGA. An embedded ONT is provided using a compact-type of commercialized 1G-EPON ONU MAC as shown in Figure 3. That is, the 10/1G-EPON RT is connected with a 1 Gbit/s data channel of the 10/1G-EPON OLT, and only port 0 of the 10/1G-EPON RT is supported.

An embedded ONT receives a downstream signal through a CS device, and transmits an upstream signal to the 10/1G-EPON OLT using a BCDR device and FPGA, as

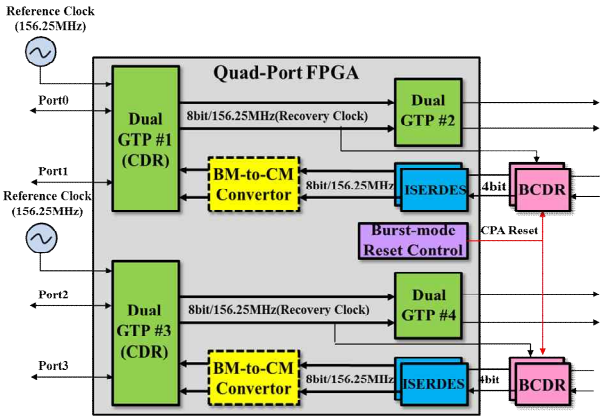


Figure 4. A Internal structure of the FPGA for the signal retiming of 1 G-EPON.

shown in Figure 3. This upstream signal is merged with the upstream signal of port 0. The CPU processor gathers and manages the status of the installed optical transceivers based on the SFF-8472 and FPGA through a local CPU interface. The CPU processor is also connected directly with a User Network Interface (UNI) port of an embedded ONT at the electronic domain using a CS device without an external optical tap (e.g., an optical splitter), which is unlikely to have been used in previous methods. The 10/1G-EPON RT can use as a hybrid-type remote terminal by replacing the 10/1G-EPON and 1G-EPON ONU optical modules with 10 Gbit/s and 1 Gbit/s Coarse Wavelength Division Multiplexing (CWDM) optical modules.

Figure 4 illustrates the internal architecture of the signal retiming logic in the FPGA used to recover the 1G-EPON signals. Because the 10/1G-EPON OLT transceiver does not require a burst-mode reset signal, the 10/1G-EPON RT can easily provide a signal retiming function using the CDR within the FPGA for a downstream signal and the BCDR device for an upstream signal.

In the downstream direction, the FPGA provides a 3R signal retiming using a recovery clock extracted from the CDR, which is included in the dual Gigabit Transfer Protocol (GTP). The dual GTP extracts a 156.25 MHz recovery clock and 8-bit data from a 1.25 Gbit/s continuous-mode downstream signal using an external 156.25 MHz reference clock. This recovery clock is then used as a reference clock source necessary for an external BCDR device. On the other hand, in the upstream direction, the 10/1G-EPON RT performs a signal recovery using the BCDR device and transmits this recovered signal to an Input Serializer/Deserializer (ISERDES) as shown in Figure 4.

Also, a burst-mode reset signal for a BCDR device is generated by a Loss of Signal (LOS) output from the 10/1G-EPON OLT transceiver. The BCDR device aligns with the input data within the 12-bit start of the preamble, and changes a 1-bit serial signal into a 4-bit parallel signal to provide the lower clock speed at the data transmission to the FPGA. The burst-to-continuous convertor in the FPGA optionally changes a burst-mode signal into a continuous-

 ISBN: 978-1-61208-205-9 

mode signal through the insertion of a particular pattern (e.g., h'55) during the guard time.

In this paper, our proposed OEO-type 10/1G-EPON RT can provide low-power consumption and a cost-efficient design through a quad-port structure using a single FPGA and generalized low-cost EPON optical transceivers.

## IV. EXPERIMENTAL SETUP AND PERFORMANCE RESULTS

The experimental setup for a performance measurement of the proposed OEO-based 10/1G-EPON RT is shown in Figure 5. As there is no commercialized 10/1G-EPON systems at present, we used the existing 1G-EPON system and a 10 Gbit/s jig board for the performance test of the 10/1G-EPON RT. The legacy 1G-EPON system generates downstream and upstream signals with a line rate of 1.25 Gbit/s, while the 10 Gbit/s jig board transmits a downstream signal with a line rate of 10.3125 Gbit/s using a Pulse Pattern Generator (PPG).

For the 1 Gbit/s path link configuration, we used a single legacy 1G-EPON OLT and two 1G-EPON ONTs, and connected the trunk fiber using a 50 km SMF between the 1G-EPON OLT and 10/1G-EPON RT. In addition, we configured a fixed 5 dB attenuator and 128-way split as the drop fiber between the 10/1G-EPON RT and 1G-EPON ONUs. For the 10 Gbit/s path link configuration, we also connected the trunk fiber using a 20 km SMF between the 10 Gbit/s jig board and 10/1G-EPON RT, as the 10/1G-EPON PMDs used in this experimental setup are unable to provide a transmission reach of 40 km owing to a dispersion problem.

The 1G-EPON used optical modules supporting both the IEEE 802.3ahTM-2004-PX20 and PX10 [3][4], while the 10/1G-EPON RT used a 1G-EPON ONU optical module supporting an IEEE 802.3ahTM-2008-PX20, a 10/1G-EPON OLT, and an ONU optical module compliant with an IEEE802.3avTM-10/1GBASE-PRX30 [2]. The 1.25 Gbit/s and 10.3125 Gbit/s optical signals generated were merged using a 3-port edge WDM filter, and then separated again into 1.25 Gbit/s and 10.3125 Gbit/s optical signals using a 3-port edge WDM filter in the 10/1G-EPON RT. The 10/1G-EPON RT transmits the retimed 1.25 Gbit/s and 10.3125 Gbit/s optical signals to the optical splitter via the 10/1G-EPON OLT optical module. The optical power budget in the trunk fiber is adjusted using a Variable Attenuator (VA) value. In this experimental setup, the insertion losses in the trunk and drop fibers are about -12.8 dB and -26.8 dB, respectively.

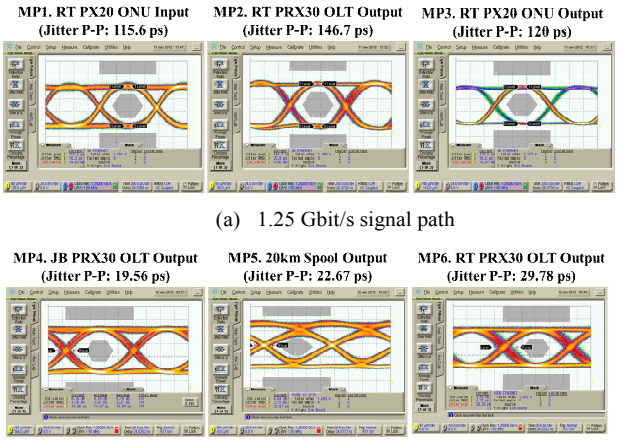


(a) 1.25 Gbit/s signal path

(b) 10.3125 Gbit/s signal path

Figure 6. An optical eye diagram measured at MPs.

Figure 6 shows the optical eye diagrams of each Measure Point (MP) in the experimental setup for the proposed 10/1G-EPON RT. Our 10/1G-EPON RT performs signal retiming using a recovery clock extracted through a 1 Gbit/s CDR within the FPGA and 10 Gbit/s CDR device, and this re-timed signal is recovered by the 1G-EPON ONUs. In a 1.25 Gbit/s path, the downstream optical signal measured at MP1 is received by the 1G-EPON ONU optical module installed in the 10/1G-EPON RT through a 50 km SMF and two 3-port edge WDM filters. In an optical eye diagram measured at MP2 and MP3, shown in Figure 6-(a), we can see a clear eye-pattern satisfying the optical eye mask

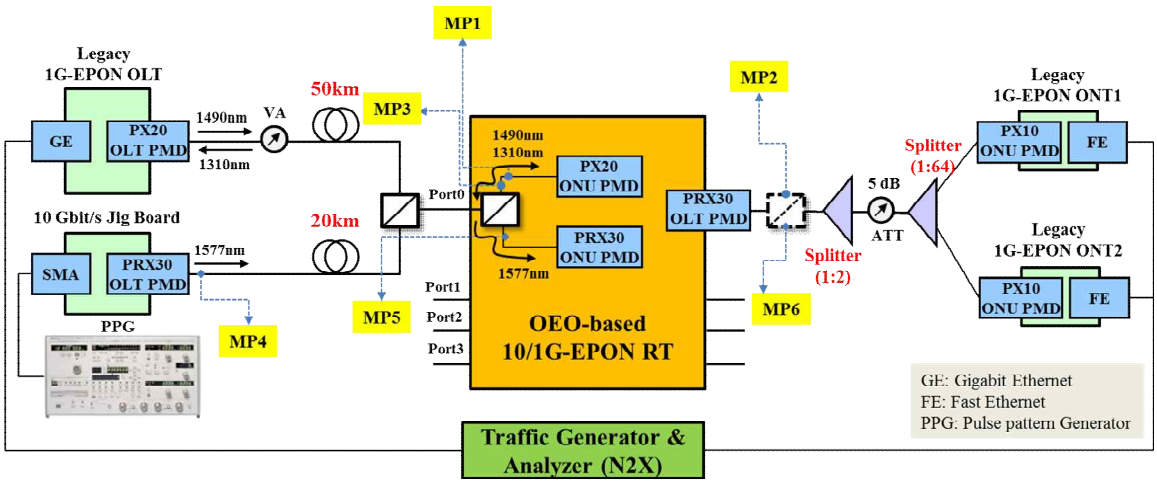


Figure 5. Experimental setup for the performance measurement of the proposed OEO-based 10/1G-EPON RT.

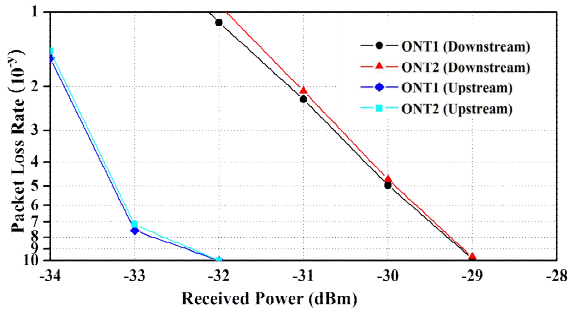


Figure 7. The PLR results measured at 1.25 Gbit/s EPON link.

adapted from the IEEE Gigabit Ethernet standard through 3R signal regeneration. We can confirm that a jitter of about 31 ps is added by the signal recovery. In a 10.3125 Gbit/s path, MP5 shows the results of a transmission dispersion caused by the 20 km SMF. We can also confirm that the output optical signal measured at MP6 satisfies the optical eye mask adapted from the IEEE 10.3125 Gbit/s Ethernet standard by the 3R signal retiming, as shown in Figure 6-(b), although a slight amount of jitter is added. This means that is possible to support a transmission reach of over 20 km through our proposed 10/1G-EPON RT, including a legacy 10G-EPON PMD in a 10 Gbit/s channel.

Using a commercially available router tester (Agilent N2X), the performance of the proposed 10/1G-EPON RT was evaluated in terms of packet loss rate (PLR) through Ethernet frames with random lengths ranging from 64 to 1518 bytes. We transmitted 10^10 frames for the PLR test.

Figure 7 shows the PLR results measured at the 1.25 Gbit/s path of the proposed 10/1G-EPON RT using a legacy 1G-EPON system according to the VA value. Because a 1G-EPON OLT uses a continuous-mode transmitter with a Distributed Feedback Laser Diode (DFB-LD) and a burst-mode receiver with an Avalanche Photodiode (APD), we can be certain that the upstream optical link budget increases by about 3 dB more than that of the downstream. Our experimental results confirm that the 1G-EPON system supports a physical distance of 50 km in a 1:128 split ratio using the proposed OEO-based 10/1G-EPON RT, and satisfies a PLR of 10^-10 for up to -29 dBm in a downstream path, and -32 dBm in an upstream path. This means that the

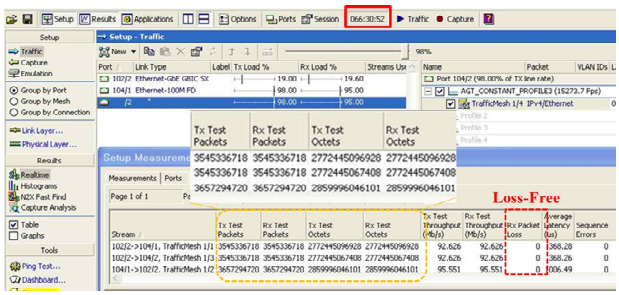


Figure 8. The results of a long-term test for the 10/1G-EPON RT.

TABLE I. TECHNOLOGY COMPARISON

| Items | *Standard 10/1G-EPON* | *Extended 10/1G-EPON* | *RT-based 10/1G-EPON* |
|---|---|---|---|
| Power Budget | Max. 29 dB | Max. 35 dB | Max. 58 dB |
| Reach & Split Ratio | 1:32@ 20km | 1:32@ 40km | 1:128@ 80km[Note.1] |
| BW per User | 300Mbps | 300Mbps | 100Mbps |
| Upstream Mode | Burst | Burst | Burst & Continuous |
| WDM application | No | No | Yes |
| Remote Node | Passive | Passive | Active |
| Cost per User | Middle (100% / 32) | High (130% / 32) | Low (180% / 128) |
| Cost of trunk fiber | 1 | 1 | 1/8[Note.2] |

Note.1. Using a PRX30 PMD type at the EPON ONU.

Note.2. When a CWDM solution is applied to the trunk fiber.

10/1G-EPON RT is able to provide transmission service at a distance of about 70 km with a 128-way split, when we take into account a budget loss of a 0.4 dB/km in an optical fiber.

Figure 8 shows the results of a packet transmission test of a legacy 1G-EPON system using our proposed 10/1G-EPON RT during a 66-hour period. During this test, we transmitted a 100 Mbit/s packet from a 1G-EPON OLT to each 1G-EPON ONU, while assigning a 98 Mbit/s packet at each 1G-EPON ONU for measurement of the upstream PLRs. From Figure 8, we can confirm the possibility of loss-free service in the downstream and upstream paths.

Table 1 shows the results of a technology comparison of 10/1G-EPON using the proposed OEO-based 10/1G-EPON RT, a 10G-EPON standardized by IEEE802.3av-2009, and an Extended 10/1G-EPON suggested by IEEE802.3 extended EPON study group [2][5]. As the table shows, with the exception of an active component used in a remote node, our proposed 10/1G-EPON RT can provide greater efficiency with respect to power budget, distance and user accommodation, cost per subscriber, and long-distance trunk fiber costs. However, to make up for the weak point above, we adopted quad-port architecture at the proposed 10/1G-EPON-RT.

## V. CONCLUSION

We proposed and experimentally demonstrated an efficient OEO-based 10/1G-EPON RT based on quad-port architecture to overcome the physical limitations of a legacy 10/1G-EPON system. We also confirmed that our proposed 10/1G-EPON RT can achieve a high power budget of 58 dB through 3R signal retiming using a legacy 10/1G-EPON PMD, and can be a cost-effective solution for a long-distance 10/1G-EPON system.

Our experimental results verified that the proposed RT can provide a distance of more than 40 km in a 1:64 split ratio, which many service providers desire. If 10/1G-EPON PMDs use the PRX30 power budget class, the 10/1G-EPON

 ISBN: 978-1-61208-205-9 

RT can be expected to support a reach of over 80 km in a 1:128 split ratio with no modifications of the legacy 10/1G-EPON standard.

In our future work, we will perform a feasibility test with either a commercialized 10/1G-EPON system or an evaluation system, and apply CWDM multiplexing to a trunk fiber with a 10/1G-EPON Central Office Terminal (COT) performing wavelength conversion between the EPON and CWDM.

## ACKNOWLEDGMENT

This research was supported by the KCC (Korea Communications Commission), Korea, under the R&D program supervised by the KCA (Korea Communications Agency) - (KCA-10913-05002).

## REFERENCES

[1] C. Chen, Z. Chair, and B. Velmurugan, "10G EPON: Next Generation Ethernet Passive Optical Networks," Proc. of OFC/NFOEC2009, March. 2009, pp. 1-3.

[2] IEEE Std 802.3av, "Carrier Sense Multiple Access With Collision Detection (CSMA/CD) Access Method and Physical Layer Specification, Amendment 1: Physical Layer Specifications and Management Parameters for 10 Gbit/s Passive Optical Networks," 2009.

[3] IEEE Std 802.3ah, "Carrier Sense Multiple Access with Collision Detection (CSMA/CD) Access Method and Physical Layer Specifications," 2004.

[4] IEEE Std 802.3ah, "Carrier Sense Multiple Access With Collision Detection (CSMA/CD) Access Method and Physical Layer Specifications, " 2008.

[5] M. Hajduczenia, "Call For Interest consensus building meeting: Extended EPON PMDs," IEEE802.3 Extended EPON Study Group, online presentations, available for download at: http://grouper.ieee.org/groups/802/3/EXTND_EPON/public/1107/index.html, July. 2011.

[6] FTTH Council, "The Adavantage of Fiber," 3rd ed., Spring 2009, 2009, pp. Sec2:1-32.

[7] B. Wang, J. Xu, and Z. Fu, "Proposal for Extended EPON PMD," IEEE802.3 Extended EPON study Group, http://grouper.ieee.org/groups/802/3/EXTND_EPON/public/1111/index.html, Nov. 2011.

[8] D. Piehler, Extending EPON link budget without new PMD definitions," IEEE802.3 Extended EPON Study Group, http://grouper.ieee.org/groups/802/3/EXTND_EPON/public/1111/index.html, Nov. 2011.

[9] E. Mallette, "Five Criteria Board Market Potential," IEEE802.3 Extended EPON Study Group, http://grouper.ieee.org/groups/802/3/EXTND_EPON/public/1111/index.html, Nov. 2011.

[10] M. Hajduczenia, "Project Objectives…hiw far, how long..," IEEE802.3 Extended EPON study Group, http://grouper.ieee.org/groups/802/3/EXTND_EPON/public/1111/index.html, Nov. 2011.

 ISBN: 978-1-61208-205-9 

# A Novel MIMO-OFDM Scheme Based on Modulation Diversity for IEEE 802.11ac Standard

Wu Zhanji, Gao Xiang, Li Yunzhoun
Beijing University of Post & Telecommunications, & Tsinghua University, Beijing, China
E-mail: wuzhanji@163.com, 381711574@qq.com, kutuzolv@163.com

***Abstract*—Wireless communications always strive for higher throughput and higher performance. The Multiple Inputs Multiple Outputs (MIMO)- Orthogonal Frequency Division Multiplexing (OFDM) scheme is the key Physical (PHY) layer feature of the next generation wireless local area networks (WLAN) IEEE 802.11ac standards. In this paper, we propose a novel MIMO-OFDM scheme based on modulation diversity for IEEE 802.11ac. This proposed scheme jointly optimizes the MIMO-OFDM and modulation diversity together, which makes full use of time diversity, frequency diversity and space diversity. It exhibits high spectral efficiency and low error rate in fading channels. The simulation results show that the proposed scheme outperforms the current MIMO-OFDM scheme based on Bit-Interleaved Coded Modulation (BICM) in the 802.11ac standard, which is up to 7dB SNR gain.**

***Keywords-WLAN; 802.11ac; modulation diversity; MIMO; OFDM***

## I. INTRODUCTION

In recent years, the applications of wireless local area networks (WLAN) have grown very fast in hot spots all over the world. Through the combination of Multiple Inputs Multiple Outputs (MIMO) and Orthogonal Frequency Division Multiplexing (OFDM), IEEE 802.11n significantly increases the maximum data rate up to 600 Mbit/s [1]. Although existing 802.11n can support data rate up to 600 Mbit/s, it cannot yet meet the growing demands for higher throughput and higher performance. Since 2008, IEEE 802.11ac Task Group (TG) has developed the next generation wireless local area networks (WLAN) IEEE 802.11ac standard in order to achieve 1 Gbit/s data throughput below 6 GHz to meet the fast-growing market demands [2]. It extends the air interface technologies in IEEE 802.11n [3]. The combination of OFDM and MIMO is still a key feature for high-throughput transmission in the IEEE 802.11ac standard.

OFDM is an orthogonal multi-carrier frequency-division multiplexing (FDM) modulation scheme. OFDM allocates its transmitted symbols into narrow-band sub-carriers and maintain its orthogonality between the sub-carriers, so that OFDM can avoid inter symbol interference (ISI) due to a frequency selective fading channel. MIMO systems have attracted much more attention in wireless communications, because it can obtain very high spectral efficiency. Thanks to these properties, MIMO-OFDM has become the foundation of advanced wireless transmission technologies in current WLAN 802.11standards.

The uncoded modulation diversity schemes based on multidimensional rotated constellations were proposed in [4][5] [6] for the conventional single-input single-output (SISO) scenario. The schemes are essentially uncoded and can achieve very high modulation diversity, which can approach to the additive white Gaussian noise (AWGN) error performance over fading channels. A rotated coding modulation OFDM system was put forward in [7], which extends the two-dimensional modulation diversity in coded OFDM systems. Through the combination of rotating the MPSK/MQAM constellation and interleaving the symbol-components, the performance of wireless communications systems can be significantly improved in flat fading channels without time-dispersion. Hence, a MIMO-OFDM system based on two-dimensional modulation diversity for IEEE 802.11ac is proposed, which jointly optimizes MIMO-OFDM and the rotated coding modulation. This scheme can take full advantage of the coding-gain of channel codes, the time and frequency diversity of OFDM system and the spatial diversity of MIMO all together. It is more suitable for space-time-frequency selective fading channels and exhibits the much better performance in wireless communications.

The rest of this paper is organized as follows. An improved MIMO-OFDM system based on modulation diversity for IEEE 802.11ac is proposed in Section II. Rotational modulation, the component interleaver and the detection algorithm in receiver are introduced in Sections III, IV and V, respectively. Simulation results are given in Section VI. Conclusions are reached in Section VII.

## II. MIMO-OFDM SYSTEMS BASED ON MODULATION DIVERSITY FOR 802.11AC

An improved MIMO-OFDM scheme based on modulation diversity is proposed, which is shown in Figure 1. The blocks drawn in dotted line are the additional proposed processing based on the conventional MIMO-OFDM system introduced in [8]. $N_T$ transmit and $N_R$ receive antennas are assumed.

In the transmitter, the number of encoders is determined by rate-dependent parameters [8]. Information bits are firstly divided between the encoders by sending bits to different encoders in a round robin manner, and then coded by binary convolutional codes (BCC) or low density parity codes (LDPC).

 ISBN: 978-1-61208-205-9

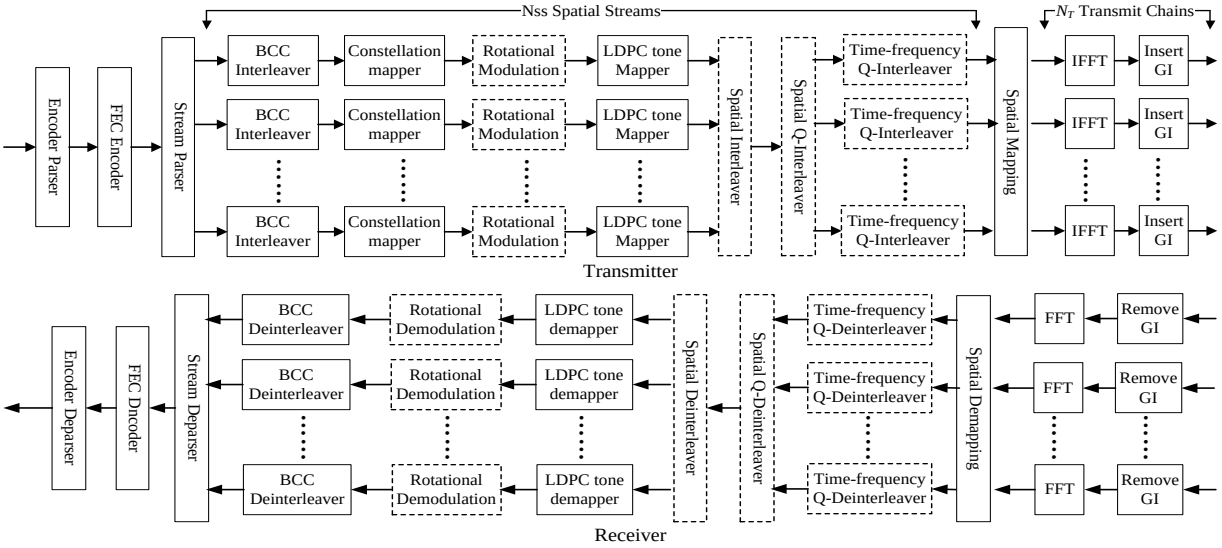


Fig. 1. Transmitter and receiver diagram of MIMO-OFDM system based on modulation diversity for 802.11ac

Afterwards, the coded bit stream is parsed into $N_{SS}$ spatial streams.

If BCC encoding is used, BCC interleaving is performed within each spatial stream according to a rule in [8]. For each of the encoded, parsed, and interleaved spatial stream, convert the bit group into complex-valued symbols according to the modulation encoding tables. And then, the rotational modulation mapper converts the conventional modulated symbols into new complex-valued rotated symbols which contain in-phase (I) components and Quadrature (Q) components. LDPC tone mapping is skipped in this case.

If LDPC is used, after the stream parsing, BCC interleaver is not used, and the coded bits on $N_{SS}$ spatial streams are converted into complex-valued symbols according to the modulation encoding tables. Based on the conventional modulated constellations, rotational modulation is carried out, and then the LDPC tone mapping shall be performed on all LDPC coded streams.

Afterwards, the spatial interleaving and spatial Q-interleaving are carried out over $N_{SS}$ spatial streams, which will be described in section V. The interleaved symbols are then mapped onto different time-frequency resource elements (REs) on each stream. For the Q-components, an additional time-frequency Q-interleaver is performed on each stream. In this paper, we consider that STBC is not used, so the number of space-time streams is the same as the number of spatial streams. After the spatial mapping, $N_{FFT}$ -point Inverse FFT (IFFT) and inserting guard interval (GI) are implemented for each group of subcarriers on each transmit antenna.

In the receiver, removing GI and $N_{FFT}$ -point FFT are carried out firstly. Afterwards, the spatial demapping is performed. And then, the received symbols of each spatial stream are obtained after time-frequency Q-component deinterleaving, spatial Q-deinterleaving and spatial deinterleaving.

If LDPC encoding is used, LDPC tone demapping is carried out after the above operations. For each symbol, the maximum likelihood (ML) rotational demodulation is used to produce the log-likelihood-ratios (LLRs) of encoded bits.

If BCC encoding is used, LDPC tone demapping is skipped. After the ML rotational demodulation, BCC deinterleaving is performed.

After the above operations, stream deparser is carried out, and then the channel decoder (BCC or LDPC) utilizes the LLRs to decode the information bits.

## III. ROTATIONAL MODULATION

Modulation diversity can be achieved via the rotational modulation, which provides an additional modulation diversity gain. Through the combination of rotating the conventional constellation and interleaving the components, the performance of wireless communications systems can be improved greatly in fading channels.

In the transmitter, coded bits $\mathbf{K} = (k_1, k_2, k_3 ... k_{N_{bit}})$ are modulated according to Gray-mapping constellation described in [8] to produce a sequence of complex-valued modulation symbols $\mathbf{D} = (d_1, d_2, d_3 ... d_{N_{Sym}})$.

Rotating the conventional constellation can be expressed as a complex-valued modulation symbol $d_i$ multiplied by a rotational matrix $\boldsymbol{R}$. The relationship between conventional modulated complex-valued symbol $d_i = I_i + jQ_i$ and the rotational complex-valued symbol $d_i' = X_i + jY_i$ is shown as follows.

$$\begin{pmatrix} X_i \\ Y_i \end{pmatrix} = \mathbf{R} \begin{pmatrix} I_i \\ Q_i \end{pmatrix} = \begin{pmatrix} \cos\theta & \sin\theta \\ -\sin\theta & \cos\theta \end{pmatrix} \begin{pmatrix} I_i \\ Q_i \end{pmatrix} \quad (1)$$

This processing can be illustrated in Figure 2. In the conventional square QPSK constellation, the I- component and Q-component of one complex-valued modulated symbol just carry one bit, respectively. In the rotational QPSK constellation,

 ISBN: 978-1-61208-205-9 

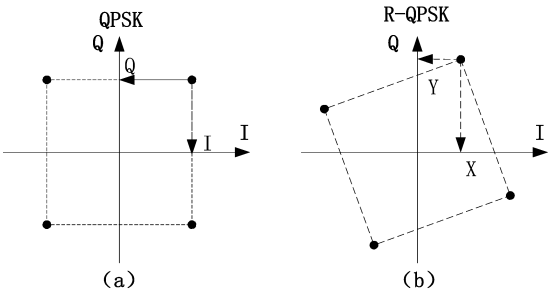

Fig. 2. conventional QPSK constellation (left) and Rotated QPSK constellation (right)

TABLE I. THE OPTIMAL ROTATION ANGLES FOR 802.11AC

| MCSs | Modulation | Code rate | Angle |
|---|---|---|---|
| MCS 2 | QPSK | 3/4 | arctan1/2 |
| MCS 4 | 16QAM | 3/4 | arctan1/3 |
| MCS 7 | 64QAM | 5/6 | arctan1/4 |
| MCS 8 | 256QAM | 3/4 | arctan1/7 |

two bit are carried by both components at the same time, which means the information of two bits is spread over the I-component and Q-component. After appropriate interleaving of the Q-components, the fading coefficients of the I- components and Q-components are uncorrelated. The modulation diversity order $L$ of a multidimensional signal set is the minimum number of distinct components between any two constellation points. Assuming independent Rayleigh fading channel and the maximum likelihood (ML) detection, multidimensional QAM constellation becomes insensitive to fading channel when the diversity $L$ is large [4].

The key of rotational modulation technique is finding an optimum rotational angle to minimize bit error rate (BER). J.Boutros studied the optimum criteria of the uncoded rotation modulation over the independent Rayleigh channel, and proposed that the diversity order $L$ and product distance should be maximized [4]. Simulation results indicate that the optimum rotation angle depends on the modulation order and code rate for coded modulation. The correlation between the code rate and optimum rotation angle is weak. Especially for the high code rates from 3/4 to 8/9, the optimal rotation angles keep almost the same value. However, it is strongly correlated to the modulation order. For the same code rate, the optimal rotation angle values are different for QPSK, 16QAM and 64QAM, and it decreases as the modulation order increases. Based on the above theoretical analysis and computer simulation, we obtain the optimal rotation angles that are suitable for IEEE 802.11ac, which are shown in Table I.

## IV. Q-COMPONENT INTERLEAVER

### A. Time-frequency Q-component interleaver

The Q-component interleaving is aimed to make the I-component and the Q-component in one modulated symbol as uncorrelated as possible in the time and frequency domain. We assume the OFDM system has $L$ subcarriers in frequency domain for each user and $N_{sym}$ OFDM symbols in time domain. One Q-component of a complex-valued modulated symbol is mapped onto one resource element $Q(f,t)$ , which at the $f^{th}$ subcarrier in the $t^{th}$ OFDM symbol. After time-frequency Q-component interleaving, the output is $Q(f',t')$ . The Q-component interleaving is defined as follows.

$$\begin{aligned} f' &= (f + L/2)\%L \\ t' &= (t + N_{sym}/2)\%N_{sym} \end{aligned} \tag{2}$$

where $f \in [0, L-1], t \in [0, N_{sym}-1]$ .Thus, the time interval between I-component and Q-component is $N_{sym}/2$ OFDM symbol duration. In frequency domain, the frequency interval is half of the bandwidth for each user. So, the time-frequency Q-component interleaver can make full use of the frequency diversity and the time diversity of OFDM system, and it can make the I-components and Q-components as uncorrelated as possible.

### B. Spatial interleaver and spatial Q-component interleaver

The spatial interleaving is the conventional spiral layer interleaving among all layers. Let $\mathrm{x}_t^i$ and $\overline{\mathrm{x}}_t^i$ denote the input-symbol and the output-symbol of the spatial interleaver on the $i^{th}$ spatial stream at the $t$ instant. The interleaving is defined as follows.

$$\overline{\mathrm{x}}_t^k = \mathrm{x}_t^i, k = (i+t) \bmod N_{SS} \tag{3}$$

where $k, i \in [0, N_{SS}-1]$ .The spatial Q-component interleaver is carried out after the spatial interleaving to ensure the independence of the I- components and Q-components. Let $\mathrm{Q}_t^i$ and $\overline{\mathrm{Q}}_t^i$ denote the input Q-component and the output Q-component of the Q-component interleaver on the $i^{th}$ spatial stream at the $t$ instant. The Q-component interleaving is defined as follows.

$$\overline{\mathrm{Q}}_t^k = \mathrm{Q}_t^i, k = N_{SS} - i - 1 \tag{4}$$

where $k, i \in [0, N_{SS}-1]$ .The achievable rate of the proposed scheme can increase via the spatial Q-component interleaver. For the sake of simplicity, a system with two transmit and two receive antennas is firstly considered, and the symbols are mapped to two spatial streams. That is to say, $N_T = N_R = N_{SS} = 2$ . We assume the total transmission power is $P$ and the bandwidth is W. Channel matrix $H_{2x2}$ is known at the transmitter, and the two singular values are $\sqrt{\lambda_1}$ and $\sqrt{\lambda_2}$ ( $\sqrt{\lambda_1} \geq \sqrt{\lambda_2}$ ). The total achievable rate is the sum of partial achievable rate on each singular-value-decomposition (SVD) spatial layer of the MIMO channel [11].

For the system without spatial Q-component interleaver, the fading coefficients of I- and Q-component in each symbol are identical. The achievable rate can be calculated as follows.

$$C_1 = W \cdot \log_2\left(1 + \frac{\lambda_1 P}{2\sigma^2}\right)\left(1 + \frac{\lambda_2 P}{2\sigma^2}\right) = W \cdot \log_2\left(1 + \frac{\lambda_1 + \lambda_2}{2\sigma^2}P + \frac{\lambda_1 \lambda_2}{4\sigma^4}P^2\right) \tag{5}$$

For the proposed system, thanks to the spatial Q-component interleaver, the fading coefficients of I- and Q-component in each symbol are $\sqrt{\lambda_1}$ and $\sqrt{\lambda_2}$ , respectively. Thus, the

 ISBN: 978-1-61208-205-9

achievable rate of the proposed system can be calculate as follows.

$$C_2 = W \cdot \log_2\left(1+\frac{(\lambda_1+\lambda_2)}{4\sigma^2}P\right)^2 = W \cdot \log_2\left(1+\frac{\lambda_1+\lambda_2}{2\sigma^2}P+\frac{(\lambda_1+\lambda_2)^2}{16\sigma^4}P^2\right) \quad (6)$$

It is easy to obtain $C_1 \le C_2$, because $(\lambda_1+\lambda_2)^2 \ge 4\lambda_1\lambda_2$.

## V. DETECTION AND DEMODULATION

Assuming perfect channel state information (CSI), the MIMO channel with $N_T \times N_R$ matrix $\mathbf{H}$ is well known to have the singular value decomposition (SVD) as

$$\mathbf{H} = \mathbf{U}\mathbf{D}\mathbf{V}^H \quad (7)$$

where the $N_R \times N_R$ matrix $\mathbf{U}$ and the $N_T \times N_T$ matrix $\mathbf{V}$ are unitary matrices and $\mathbf{D}$ is an $N_R \times N_T$ diagonal matrix of singular values $\{\sigma_i\}$ of $\mathbf{H}$. For the $i^{th}$ eigenvalue $\lambda_i$ of $\mathbf{H}\mathbf{H}^H$, $\sigma_i = \sqrt{\lambda_i}$. By using SVD, MIMO channel is divided into parallel independent spatial subchannels.

In the transmitter, the spatial mapping takes a vector $\mathbf{x}^p = \left[x^p_{(1)}, x^p_{(2)} \ldots x^p_{(N_{SS})}\right]^T$ on $N_{SS}$ space-time streams as input and generates a vectors $\mathbf{y}^p = \left[y^p_{(1)}, y^p_{(2)} \ldots y^p_{(N_T)}\right]^T$ to be mapped onto $N_T$ transmit chains at *p* symbol-instant, where $x^p_{(i)}$ represents the symbol *p* on space-time stream *i*, $y^p_{(i)}$ represents the symbol *p* on transmit chain *i*, where *i*=1, 2 for $N_T = N_{SS} = 2$. The input to the transmit chain $\mathbf{y}^p$ is the output of a linear transformation on input vector $\mathbf{x}^p$ as $\mathbf{y}^p = \mathbf{V} \cdot \mathbf{x}^p$.

In the receiver, let $\mathbf{r}^p = \left[r^p_{(1)}, r^p_{(2)} \ldots r^p_{(N_R)}\right]^T$ denote the received signal vector on $N_R$ antenna ports, which can be expressed for $N_T = N_R = N_{SS} = 2$ as follows.

$$\mathbf{r}^p = \mathbf{H} \cdot \mathbf{y}^p + \mathbf{n} \quad (8)$$

where, $\mathbf{n}^p = \left[n^p_{(1)}, n^p_{(2)} \ldots n^p_{(N_R)}\right]^T$ denote a white noise vector on $N_R$ antenna ports. The white noise variance is $\sigma^2$.

Receiver shaping performs a similar operation at the receiver by multiplying the channel output $\mathbf{r}^p$ with $\mathbf{U}^H$, as shown in (9).

$$\begin{aligned} \tilde{\mathbf{y}}^p &= \mathbf{U}^H \cdot \mathbf{r}^p \\ &= \mathbf{U}^H \cdot \mathbf{H} \cdot \mathbf{y}^p + \mathbf{U}^H\mathbf{n} \\ &= \mathbf{U}^H\mathbf{U}\mathbf{D}\mathbf{V}^H\mathbf{V} \cdot \mathbf{x}^p + \mathbf{U}^H\mathbf{n} \\ &= \mathbf{D} \cdot \mathbf{x}^p + \mathbf{n}' \end{aligned} \quad (9)$$

where $\mathbf{n}' = \mathbf{U}^H\mathbf{n}$. Note that multiplication by a unitary matrix does not change the distribution of the noise, so $\mathbf{n}'$ and $\mathbf{n}$ are identical Gaussian distribution. Thus, the transmit precoding and receiver shaping transform the MIMO channel into parallel independent channels. The received symbol after detection on each stream is

$$\tilde{\mathbf{y}}^p_{(i)} = \sigma_i \cdot \mathbf{x}^p_{(i)} + \mathbf{n}'^p_{(i)} \quad (10)$$

After the spatial demapping and space-time-frequency deinterleaving, the rotational demodulation is carried out on each antenna. We assume the $i^{th}$ rotated constellation point in the transmitter is $S^i = (S_I{}^i, S_Q{}^i)$, and the corresponding received constellation point after the above operations is $R^i = (R_I{}^i, R_Q{}^i)$. Thanks to the above Q-component interleaving, the fading coefficient of I-component $H_I$ and that of Q-component $H_Q$ in each symbol are different, as shown in Figure 3. For the $i^{th}$ symbol, the relationship between $S^i$ and $R^i$ is shown as follow,

$$(R_I^i, R_Q^i) = (H_I \cdot S_I^i + n_I, H_Q \cdot S_Q^i + n_Q) \quad (11)$$

Where $n_I$ and $n_Q$ are the additive Gaussian noise of I-component and that of Q-component, respectively. Rotational demodulation produces the LLRs of encoded bits $\mathbf{K}^i = (k_1^i, k_2^i, \ldots, k_m^i)$ as follows.

$$LLR(k_x^i) = \ln\frac{P(k_x^i = 0)}{P(k_x^i = 1)} \quad (12)$$

where $k_x^i$ denotes the $x^{th}$ bit of symbol *i*, $m = \log_2 M$. Assuming equal *apriо*r probabilities, *P* is calculated as follows.

$$P = \frac{1}{\sqrt{2\pi}\sigma}\exp\left(-\frac{(R_I^i - H_I^i S_I^i)^2}{2\sigma^2}\right) \cdot \exp\left(-\frac{(R_Q^i - H_Q^i S_Q^i)^2}{2\sigma^2}\right) \quad (13)$$

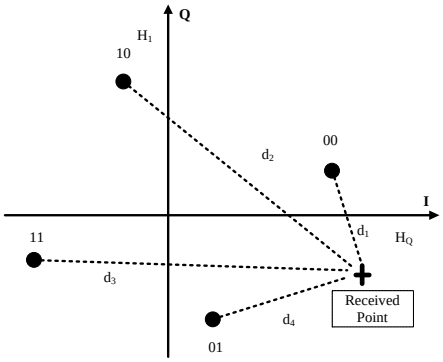


Fig. 3. Received constellation points for R-QPSK

## VI. SIMULATION RESULTS

To validate the advantages of the proposed scheme, an IEEE 802.11ac link level simulation platform is programmed by using Microsoft Visual Studio 2005 (VS2005). Computer simulations are carried out to compare the proposed scheme with the conventional MIMO-OFMD scheme in current 802.11ac standard draft. The frame structure, physical resource elements of OFDM system, channel model and coding are all based on 802.11ac standard draft [8][9], which are given in Table II.

Figure 4 and Figure 5 depict frame error rate (FER) performance comparison in NLOS channel for BCC coding and LDPC coding, respectively. The solid line shows the FER performance of our proposed scheme, while the dotted line is

 ISBN: 978-1-61208-205-9 

that of the conventional MIMO-OFMD scheme in current 802.11ac standard draft. From these figures, the proposed scheme can obtain obvious SNR gain as compared with the current 802.11ac MIMO-OFDM scheme. In NLOS channel, for BCC coding, SNR gains are about 7 dB and 4.8 dB at FER=0.01 for QPSK and 16QAM modulation, respectively. For LDPC coding, SNR gains are about 6.8 dB and 4.5 dB at FER=0.01 for QPSK and 16QAM modulation, respectively. Therefore, the proposed scheme obviously outperforms the current MIMO-OFDM system in 802.11ac. For higher code rate or lower modulation order, the SNR gain becomes more significant.

## VII. CONCLUSION

An improved MIMO-OFDM scheme based on modulation diversity is proposed. A simple and effective space-time-frequency component interleaver is designed to make the best use of space-time-frequency diversities. An efficient demodulation method is also put forward for it. This scheme can take full advantage of the coding-gain of channel codes (BCC and LDPC), the time and frequency diversity of OFDM system and the spatial diversity of MIMO all together. Simulation results turn out that it can obtain obvious SNR gain as compared with the current MIMO-OFDM scheme in IEEE 802.11ac standard. In the future, more theoretical analysis and simulations are still required to research for the impact of channel estimation to our proposed scheme. In a word, our proposed scheme is simple, efficient and robust for the next generation WLAN standard.

## ACKNOWLEDGMENT

This work is sponsored by National Natural Science Fund (61171101) and National Great Science Specific Projects (2009ZX03003-011-03 & 2010ZX03005-001-02) of P.R. China.

TABLE II SIMULATIONS PARAMETERS

| Parameters | Value |
|---|---|
| $N_T$ | 2 |
| $N_R$ | 2 |
| Carrier frequency | 5 GHz |
| Bandwidth | 20.0 MHz |
| Subcarrier Number | 52 |
| Useful Subcarrier Number | 56 |
| FFT Size | 64 |
| Coding | BCC, LDPC |
| MCSs | MCS2, MCS4, MCS7, MCS8 |
| sub-carrier bandwidth | 312.5 kHz |
| Channel Models | TGac Channel Model case E |
| Mobile Speed | 3km/h |
| Coherent Time | 1/0.4326=2.427s |
| Coherent Bandwidth | $B_{CLOS}$ =1.7 MHz, $B_{CNLOS}$ =1.6 MHz |
| Channel estimation | perfect CSI |

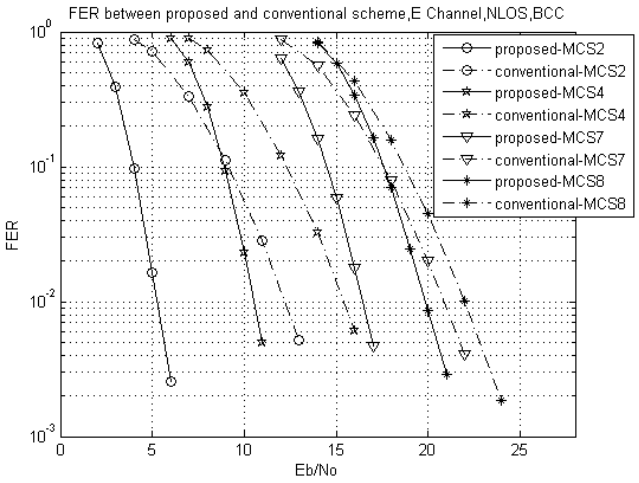


Fig. 4. FER performance of proposed scheme vs conventional MIMO-OFDM for different MCSs, BCC coding, AC case E Channel, NLOS

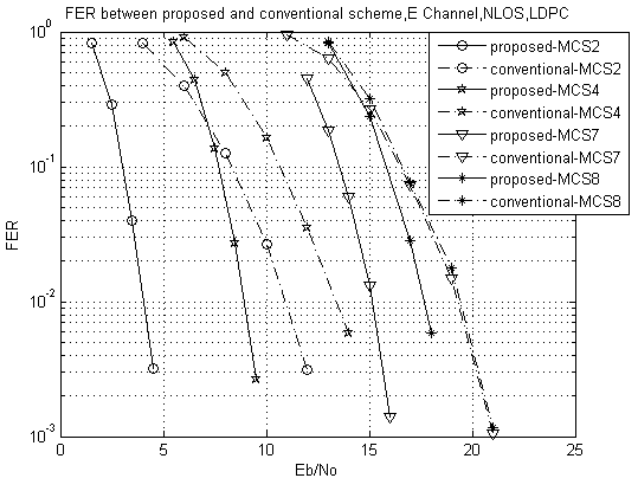


Fig. 5. FER performance of proposed scheme vs conventional MIMO-OFDM for different MCSs, LDPC coding, AC case E Channel, NLOS

## REFERENCES

[1] E.Perahi, "IEEE 802.11n Development: History, Process, and Technology," *IEEE Communications Magazine*, vol. 46, no. 7, pp. 48–55, July 2008.

[2] E.H.Ong, K.Jarkko, A.Olli, C.Zheng, H.Toni, and N.Timo, "IEEE 802.11ac: Enhancements for very high throughput WLANs," *2011 IEEE 22nd International Symposium on Personal, Indoor and Mobile Radio Communications*, pp. 38–45, Sept. 2011.

[3] E. Perahia and R. Stacey, "Next Generation Wireless LANs: Throughput, Robustness, and Reliability in 802.11n," Cambridge University Press, The Edinburg Building, Cambridge, UK, pp. 12-186, 2008.

[4] J.Boutros and E.Viterbo, "Signal Space Diversity: a power and bandwidth efficient diversity technique for the Rayleigh fading channel", *IEEE Trans. Inform. Theory*, vol. 44, pp. 1453-1467, July1998.

[5] A.Chindapol and J.A.Ritcey, "Bit-Interleaved Coded Modulation with Signal Space Diversity in Rayleigh Fading", *1999 ASILOMAR conference*, pp. 1003-1007, 1999.

[6] A.Chindapol and J.A.Ritcey, "Design, Analysis, and Performance Evaluation for BICM-ID with Square QAM Constellations in Rayleigh Fading Channels", *IEEE Journal on Selected Areas in Communications*, vol. 19, no. 5, pp. 944-957, May 2001.

[7] Z.Wu and W.Wang, "A novel Joint-Coding-Modulation-Diversity OFDM System," *Global Mobile Congress 2010*, pp. 1-6, 2010.10.

[8] IEEE P802.11ac/D2.0, Draft STANDARD for Information Technology-

 ISBN: 978-1-61208-205-9 

Telecommunications and information exchange between systems-Local and metropolitan area networks-Specific requirements, Part 11: Wireless LAN Medium Access Control (MAC) and Physical Layer (PHY) specifications, Amendment 4: Enhancements for Very High Throughput for Operation in Bands below 6 GHz, IEEE 802.11-D2.0, January 2012.

[9] IEEE P802.11ac. TGac Channel Model Addendum. IEEE 802.11-09/0308r12. March 2010.

[10] Z.Wu, T.T.Fu, X.Wang, L.L.Zhang, Y.Gao, C.Ma, and W.Wang, "A novel Coding-Rotated-Modulation OFDM scheme," *International Conference on Communication Technology and Application 2009, ICCTA 2009*, pp. 517-520, 2009.10.

[11] A.Goldsmith, "Wireless Communications," Cambridge University Press. pp. 299-309, August 8, 2005.

[12] Theodore S.Rappaport, "Wireless Communications Principles and Practice, Second Edition," Publishing House of Electronics Industry. pp. 177-289, 2006.7.

 ISBN: 978-1-61208-205-9 

# Experimental 20 Gbit/s Absolute Polar Duty Cycle Division Multiplexing - Polarization Division Multiplexing (AP-DCDM-PolDM) Transmission

Amin Malekmohamadi
Dept. of Electrical and Electronic Engineering
The University of Nottingham, Malaysia Campus
Malaysia
Aminmalek_m@ieee.org

Mohamad Khazani Abdullah
Dept. Research and Development
Significant Technologies, Sdn, Bhd
Malaysia
khazani@sigtech.com.my

***Abstract* - 20 Gbit/s ( 2 × 2 × 5 Gbit/s) Absolute Polar Duty Cycle Division Multiplexing (AP-DCDM)-Polarization Division Multiplexing (PolDM) over 180 km standard single-mode fiber has been experimentally demonstrated in order to double the capacity of PolDM and increase the maximum dispersion uncompensated reach. The AP-DCDM-POLDM performance is examined utilizing a polarization stabilizer. By increasing the length from 0 km (back-to-back) to 180 km the 10 Gbit/s single AP-DCDM channel without SOP stabilizer experienced ~1 dB penalty as compared to around 2 dB penalty when the SOP stabilizer is active.**

***Keywords- Optical Communication; Absolute Polar Duty Cycle Division Multiplexing (AP-DCDM); PolDM.***

## I. INTRODUCTION

Absolute polar duty cycle division multiplexing (AP-DCDM) appears promising for its spectral width and its chromatic dispersion tolerance [1-3]. The small spectrum of AP-DCDM system reduces the inter channel coherent crosstalk in AP-DCDM-WDM systems. The possibility of setting channel spacing as narrow as 62.5 GHz (0.5 nm) for 40 Gbit/s AP-DCDM signals over WDM was confirmed [3]. As reported in [3], a capacity of 1.28 Tbit/s (32 x 40 Gbit/s) was packed into ~ 15.5 nm (1550-1565.5 nm) EDFA gain-band with 0.64 bit/s/Hz spectral efficiency by using 10 Gbit/s transmitter and receiver. Good dispersion tolerance makes AP-DCDM very attractive for uncompensated optical links [1-3].

Transmission capacity enhancement is a key issue for network for today's telecommunication. Polarization division multiplexing (PolDM) is well known technique for doubling the spectral efficiency [4].

In PolDM systems, two signals are transmitted at the same wavelength with orthogonal states of polarization (SOP).

At the receiving end, the polarization channels are demultiplexed at polarization beam splitter and detected independently. In PolDM applications, due to external distraction factors an automatic state of polarization stabilization is actually desirable. Because of coherent cross talk between the two orthogonally polarized channels, SOP stabilizers cause impairments in PolDM applications [8, 9].

We have already discussed the implementation issues and advantages of AP-DCDM over a single wavelength, Wave length division multiplexing (WDM) and PolDM based on the simulation results [1-3].

In this paper, for the first time to the best of our knowledge, the AP-DCDM system has been exploited experimentally together with PolDM using a SOP in order to transmit over 180 km at an aggregated bitrate of 20 Gbit/s (2 × 2 × 5 Gbit/s), without dispersion compensation.

The polarization stabilizer which is used in this experiment is described in [8]. Bit-Error Rate (BER) versus Optical Signal Noise Ratio for various standard single mode fiber lengths is measured in a case of AP-DCDM over PolDM system utilizing a SOP stabilizer. In a case of single AP-DCDM channel, the BER versus OSNR is measured for both with and without the SOP stabilizer.

The experimental study shows the capabilities of AP-DCDM format to double the capacity of PolDM in dispersion uncompensated condition and evaluates the effect of the SOP stabilizer on propagation penalties.

This paper is organized as follows. Section II describes the experimental setup for a 2-channel AP-DCDM system over PolDM. Section III shows the performance of AP-DCDM over PolDM System. Section IV concludes our paper.

## II. EXPERIMENTAL SETUP

Figure 1 illustrates the experimental setup of AP-DCDM over PolDM. As shown in Figure 1a, the evaluation starts with two AP-DCDM channels (2 x 5 Gbit/s) with PRBS of $2^{31}$-1 and followed by 2 PolDM channels (2 x 10 Gbit/s) (Figure 1b). In this setup, each PolDM channel contains two users that were already multiplexed by using AP-DCDM, which means each PolDM channel contains 2 x 5 Gbit/s that can offer a possible transmission rate of 20 Gbit/s (2 x 2 x 5 Gbit/s) for PolDM system. Channel 1 and Channel 2, each at 5 Gbit/s with PRBS $2^{31}$ -1 are carved with one electrical RZ pulse carvers at 50% of duty cycle and NRZ pulse carver, respectively. The voltages for both users at the multiplexer input are identical. Both users' data are multiplexed via AP-DCDM multiplexer [1-3]. Subsequently, the rectifier circuit (REC) is used to produce an absolute signal [1-3]. The signals are used to modulate a distributed feedback laser (DFB), which operates at 1548.51 nm wavelengths using a

Mach-Zehnder-Modulator (MZM). The modulated AP-DCDM signal is divided into 2 uncorrelated copes using a fiber spoil, which has a delay of about 20 μs. Power for 2 signals is identical, two signals orthogonally polarized using a fiber polarization controller (PC) and combined using a polarization beam combiner (PBC).

Using an electro absorption modulator (EAM) one of the signals is marked with a pilot tone at one Megahertz.

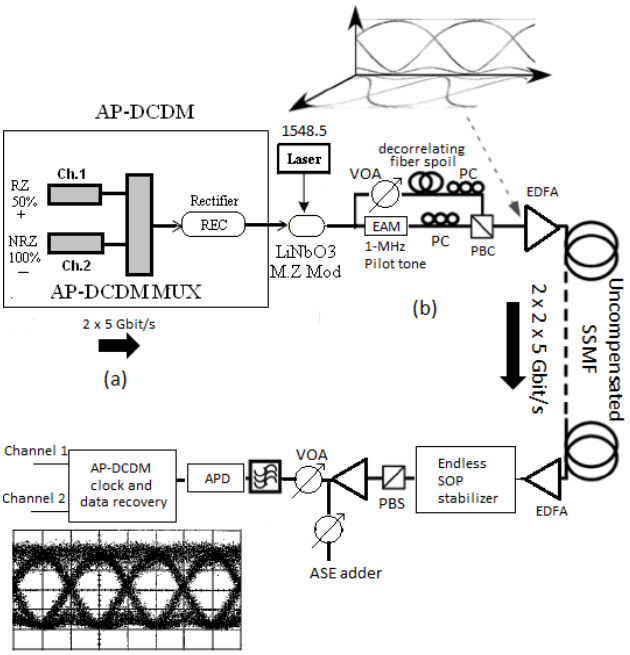


Figure 1. AP-DCDM-PolDM setup. (a) 2 x 5 Gbit/s AP-DCDM setup (b) 2 x 10 Gbit/s AP-DCDM signal over PolDM. The eye-diagram was taken for the 180 km link while transmitting both SOPs

A polarization multiplexed signal at an overall bit-rate of 20 Gbit/s is generated and launched in an uncompensated single mode fiber (SMF) link.

After transmitted over the fiber, by using a fiber polarization beam splitter, the 2 AP-DCDM- PolDM channels at the same wavelength are de-multiplexed.

In order to indemnify the random polarization fluctuations, we used a SOP stabilizer before the polarization beam splitter.

The SOP of both channels are checked and stabilized. The root-mean-square pilot tone is extracted and fed back to the electronic controller of the polarization stabilizer [8].

A single demultiplexed channel (which contains 2 AP-DCDM channels) is detected by an avalanche photodiode (APD) and passed through the AP-DCDM Clock-and-Data-Recovery (CDR) unit to extract the AP-DCDM channel 1 and channel 2 [1, 2].

As shown in Figure 1, by using a filtered amplified spontaneous emission (ASE) source and variable optical attenuator (VOA) a variable amount of ASE noise is added to the demultiplexed signal in order to change the optical signal to noise ratio (OSNR). For this measurement, we used Optical Spectrum Analyzer with resolution of 0.5 nm.

The performance of 20 Gbit/s AP-DCDM-PolDM is examined over fiber lengths from 0 km to 180 km.

Due to low lunch power the effect of nonlinearities are negligibly small.

## III. RESULT AND DISCUSSION

The PolDM-AP-DCDM system at aggregated bit rate of 20 Gbit/s with the SOP stabilizer is evaluated. We have measured the BER as a function of the single demultiplexed channel OSNR, which is detected after polarization demultiplexing.

Note that the input power to avalanche photodiode is fixed to -19 dBm. The performance of single channel transmission system is compared with the PolDM-AP-DCDM signal in the present and absence of SOP stabilizer.

Figure 2 reports the bit error rate curves versus optical signal noise ratio over back to back, 125 km and 180 km SSMF length. The 20 Gbit/s AP-DCDM-PolDM results (PolDM-APDCDM_SOP Stabilizer ON) refer to the channel tagged using a pilot tone, which has a worse performance than another channel. These BER curves are compared with 10 Gbit/s single user, when stabilizer is on (1CH-APDCDM_SOP Stabilizer On), off (1CH-APDCDM_SOP Stabilizer Off) and the pilot tone.

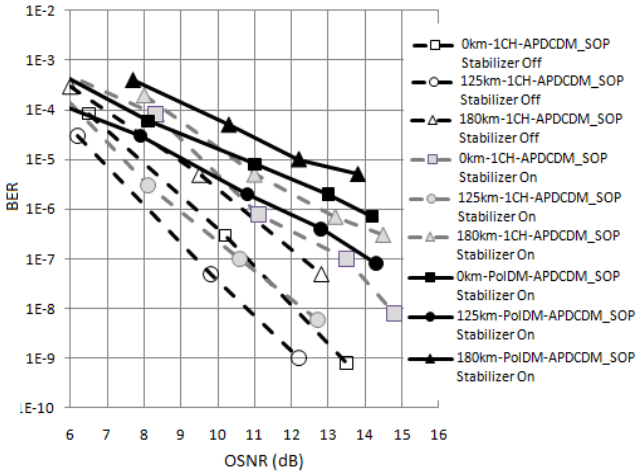


Figure 2. Bit Error Rate versus Optical Signal Noise Ratio for different lengths of standard single mode fiber. Measures are performed for PolDM-AP-DCDM system at 20 Gbit/s when the SOP stabilizer is on (black marker) and for single channel system at 10 Gbit/s (no SOP stabilizer) (open markers) and for single channel system at 10Gbit/s with a SOP stabilizer (gray market)

To realize a SOP stabilizer effect on the AP-DCDM-PolDM performance. Figure 3 shows the effect of propagation length on OSNR at BER of $10^{-6}$ for single-channel system at 10 Gbit/s in a presence and absence of SOP stabilizer and for AP-DCDM-PolDM transmission at 20 Gbit/s in presence of stabilizer.

The penalty of ~ 1 dB is experienced by increasing the length from 0 km (back-to-back) to 180 km for the 10 Gbit/s single channel transmission when the SOP stabilizer is off. And a penalty of around 2 dB is experienced when the SOP stabilizer is active.

A penalty increases to around 2.8 dB when both orthogonally polarized channels are propagating. The penalty increases because of the non ideal performances of optical components in SOP stabilizer which cause the inter-channel crosstalk because of the limited polarization extinction ratio (~ 14 dB) of the SOP stabilizer.

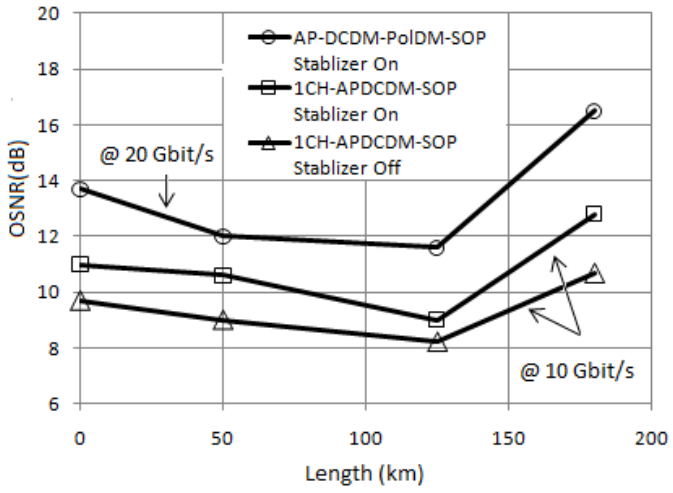


Figure 3. Optical Signal Noise Ratio for Bit Error Rate of $10^{-6}$ versus different standard single mode fiber length. Measures are performed for Polarization division multiplexing system at 20 Gbit/s when the SOP stabilizer is active, single-user system at 10 Gbit/s when the SOP stabilizer is off and single user system at 10 Gbit/s when the SOP stabilizer is on.

## IV. CONCLUSION

Absolute Polar Duty Cycle Division Multiplexing over Polarization Division Multiplexing has been shown an alternative technique to double the bitrate, while preserving the 10 Gbit/s dispersion tolerance of the AP-DCDM format. The experimental performance demonstrate the capability of AP-DCDM-PolDM to provide transmission over 180 km of SSMF uncompensated fiber at an overall capacity of 20 Gbit/s. We have shown the effectiveness of an SOP stabilizer in an APDCDM-PolDM system.

Despite of coherent crosstalk between channels, a BER of less than $10^{-6}$ with tolerable penalties is achieved up to 180 km transmission length of SSMF without using any dispersion compensation techniques.

Based on the experimental results, it can be concluded that using AP-DCDM technique, more than one user can be carried over the same PolDM channel. Consequently, the capacity utilization of the PolDM channels can be increased.

## REFERENCES


[1] A. Malekmohammadi, M.K. Abdullah, A.F., Abas and M. Mokhtar, "Analysis of RZ-OOK over Absolute Polar Duty Cycle Division Multiplexing in Dispersive Transmission Medium", *IET journal of Optoelectronics*, vol. 3, pp. 197–206, 2009

[2] A. Malekmohammadi, G. A. Mahdiraji , A. F.Abas, M. K. Abdullah, M. Mokhtar and M. F. A. Rasid, " Realization of High Capacity Transmission in Fiber Optic Communication Systems Using Absolute Polar Duty Cycle Division Multiplexing (AP-DCDM) Technique", *Optical Fiber Technology*, vol. 15, pp. 337-343, 2009

[3] A. Malekmohammadi, "20 Gbit/s Absolute Polar Duty Cycle Division Multiplexing-Polarization Division Multiplexing (AP-DCDM-PolDM) Transmission System" Proc. The Sixth International Conference on Systems and Networks Communications (ICED 2011), Aug.2011

[4] P. Boffi, M. Ferrario, P. Martelli, P. Parolari, A. Righetti and R. Siano, "20-Gb/s PolDM Duobinary transmission over 350-km ssmf supported by a polarization stabilizer and an optical dispersion compensator," *IEEE Photon.Technol. Lett.*, vol. 20, pp. 1118–1120, Jul. 2008.

[5] M. I. Hayee, M. C. Cardakli, A. B. Sahin, and A. E.Willner, "Doubling of bandwidth utilization using two orthogonal polarizations and power unbalancing in a polarization-division-multiplexing scheme," *IEEE Photon.Technol. Lett.*, vol. 13, no. 8, pp. 881–883, Aug. 2001.

[6] J. Toulouse, " Optical Nonlinearities in Fibers: Review, Recent Examples, and System Applications" *Journal of Lightwave Technologies*, vol. 23, no. 11, pp. 3625-3639, 2005.

[7] H. Kim and R.-J. Essiambre, "Transmission of 8 × 20 Gb/s DQPSK signals over 310-km SMF with 0.8-b/s/Hz spectral efficiency," *IEEE Photon. Technol. Lett.*, vol. 15, no. 5, pp. 769–771, May 2003.

[8] M. I. Hayeei, M. C. Cardakli, "Doubling of Bandwidth Utilization Using Two Orthogonal Polarizations and Power Unbalancing in a PolDM Scheme,"IEEE Photonic Technology Letter , Vol. 13, No. 8, pp/ 881-883, 2001.

[9] P. Winzer and R. Jean, Advance modulation formats for high-capacity optical transport networks, *J. Lightwave Technol*. vol. 24, pp. 4711–4728, 2006.

# Optical Access Network Migration from GPON to XG-PON

Bostjan Batagelj, Vesna Erzen,
Jurij Tratnik, Luka Naglic
University of Ljubljana
Faculty of Electrical Engineering
Ljubljana, Slovenia
e-mail: bostjan.batagelj@fe.uni-lj.si
e-mail: vesna.erzen@fe.uni-lj.si
e-mail: jurij.tratnik@fe.uni-lj.si
e-mail: luka.naglic@fe.uni-lj.si

Vitalii Bagan, Yury Ignatov, Maxim Antonenko
Moscow Institute for Physics and Technology
Department of Radio-Electronics
and Applied Informatics
Moscow, Russia
e-mail: VBagan@gmail.com
e-mail: yury.ignatov@gmail.com
e-mail: maxim.antonenko@gmail.com

***Abstract*—The purpose of this paper is to give an introduction into the new standard base of next-generation Passive Optical Network (NG-PON). Study and analysis of future trends in the development of next-generation fixed broadband optical network is performed. The main intention of this paper is to describe migration from Gigabit-capable Passive Optical Network (GPON) to Ten-Gigabit-Capable Passive Optical Networks (XG-PON). Paper answers the question of what extent active and passive GPON elements need to be replaced and what needs to be added when migrating to XG-PON. Special focus is also pointed on the coexistence of GPON and XG-PON.**

***Keywords-passive optical network; Gigabit PON; XG-PON; fiber to the home; optical access network***

## I. INTRODUCTION

With new services like three-dimensional high-definition television, cloud computing, more and more internet based applications the required bandwidth to the end user is increasing constantly (approx. 50% per year by Nielsen's law [1]). This gives the infrastructure providers an opportunity to offer new services and consequently increases average revenue per user, and thus they need to make smart decision about the investment into Fiber to the x (FTTx) technology, where x stands for node, cabinet, curb, cell, building, premises or even home as an ultimate and final solution.

It is the common fact that running fiber to the end customer (to the home) is the best possible option. After making the decision for FTTH there are two basic architectures possible. One is point-to-point (P2P) [2] and another is point-to-multipoint (P2MP) typically seen on the market as PON (Passive Optical Network) technology.

Most of the recent deployment in Europe and America is based on GPON system standardized by ITU-T series G.984 [3]. It offers downstream speed of 2.4 Gbit/s typically for up to 64 users and upstream speed of 1.2 Gbit/s. Since fiber as a media can transport much more, operators are expecting more from FTTH technology.

Present Gigabit-capable Passive Optical Network (GPON) as a future safe investment new standard for first generation of Ten-Gigabit-Capable Passive Optical Networks (XG-PON1) has been published in 2010 by ITU-T [4]. This standard will offer 10 Gbit/s downstream and 2.5 Gbit/s upstream speed; but, target distance and split ratio did not increase much. Research in this area continues the job to bring even better P2MP technology. Most of them are today known under the term second generation of next-generation Passive Optical Network (NG-PON2). Incorporating the Wavelength-Division Multiplexing (WDM) technology is mandatory to go beyond XG-PON data rates, splits and reach. The main difference between XG-PON1 and NG-PON2 from operator point of view will be the migration strategy. Since the NG-PON2 will use brand new technology, coexistence of GPON and NG-PON2 will be difficult.

This paper presents the migration from GPON to XG-PON. As an enhancement to GPON, XG-PON1 inherits the framing and management from GPON. XG-PON1 provides full-service operations via 4x higher rate and 2x larger split to support a PON network structure. In Section 2 of this paper basic technology and up-to-date standards status are described. Section 3 contains main points in the XG-PONs deployment and development: general description, co-existence with previous standards, physical layer capability, etc. Some information on the RF CATV co-existence inside XG-PON is also described. Section 4 contains information on the examples of products for WDM filters that are planned to use in XG-PON1, possible candidates for OLT filters and also information on the tunable lasers, their possible applications for NG-PONs systems, advantages and disadvantages. Section 5 summarizes the overall conclusions.

## II. BASIC TECHNOLOGY DESCRIPTION

### A. Gigabit PON

Efforts to standardize PON networks operating at above 1 Gbit/s were initiated in 2001 as the ITU-T G.984 series of recommendations [3]. GPON attempts to preserve as many

 ISBN: 978-1-61208-205-9 

characteristics of the G.983 series [5] of recommendations as possible, however, due to technical issues related to providing the higher line rates, the BPON and GPON systems are not interoperable.

At the moment, GPON standards have seven transmission-speed combinations (line rates): symmetric 1.2 or 2.4 Gbit/s; or asymmetric 1.2 or 2.4 Gbit/s downstream with 155 Mbit/s, 622 Mbit/s, or 1.2 Gbit/s in the upstream. But in fact there is the only one useful standard, which is 2.4 Gbit/s downstream and 1.2 Gbit/s or 2.4 Gbit/s upstream.

As with BPON, the network may be either a one or two-fiber system from the Optical Line Terminal (OLT). In the downstream direction, GPON is also a broadcast protocol with all Optical Network Terminals (ONTs) or Optical Network Units (ONUs) receiving all frames and discarding those not intended for them (Figure 1). Upstream transmission is via the Time Division Multiple Access (TDMA) and is controlled by an upstream bandwidth map that is sent as part of the downstream frame.

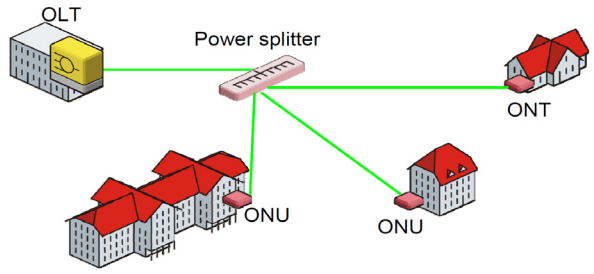


Figure 1. GPON consists of Optical Line Terminal (OLT), Passive Optical Splitter, Optical Network Units (ONU) or Optical Network Terminals (ONTs).

Up-to date GPON OLTs are able to support split ratios of 16, 32, or 64 users per fiber. ITU-T G.984.2 includes future ratios of up to 128 users per fiber and accounts for this in the transmission-convergence layer. According to G.983.3 (Figure 2), for a single-fiber system, the operating wavelength is in the 1480 nm to 1500 nm band in the downstream and in the 1260 nm to 1360 nm band in the upstream. This leaves the 1550 nm to 1560 nm band free for RF overlay video services. For a two-fiber system: in the 1260 nm to 1360 nm band in both the downstream and the upstream directions.

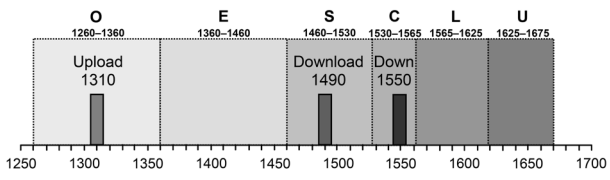


Figure 2. ITU-T definition of telecommunication wavelength bands with three operating windows. 1310 nm is used for upstream. 1490 nm and 1550 nm are used for downstream.

## B. *XG-PON1*

General XG-PON1 physical layer specifications were finalized in October 2009 and published by ITU-T in March 2010. XG-PON1 wavelength plan was a problem discussed in FSAN/ITU-T by vendors and operators. Driven by the optical transceivers market, FSAN/ITU-T selected the narrow downstream wavelength range of 1575 nm to 1580 nm, because it is the only wavelength band that is left in the system crowded with RF overlay video services. This choice has advantage that it also matches the downstream wavelength selection included in 10G-EPON draft standard.

The overall XG-PON and GPON optical spectrum is illustrated in Figure 3. C-, L-, and O- bands were compared in the selection of upstream wavelength. The first option of C band overlapping with the RF overlay video channel was eliminated. The L band was also eliminated due to the insufficient guard band between upstream and downstream wavelengths. After all, the candidate wavelength was narrowed down to O- band and O+ band. Comparing the pros and cons (such as complexity and costs), O- band was selected because O+ band has higher requirements on filters and is more expensive. Wavelength for upstream is 1260 nm to 1280 nm.

The downstream rate of XG-PON1 was defined as 10 Gbit/s, which was mainly driven by the well-established and low-cost 10 Gbit/s continuous transmission technology in the industry. The exact rate is 9.95328 Gbit/s that keeps the consistency with typical ITU-T rates. This is different from the rate of the IEEE 10GE-PON, which is 10.3125 Gbit/s. There were 2.5 Gbit/s and 10 Gbit/s proposals for the XG-PON1 upstream rate. 2.5 Gbit/s upstream rate was selected for specification after careful studying of application scenarios and component cost. The 10 Gbit/s upstream system is still considered as a high cost system with limited application scenarios in the near future.

As an enhancement to GPON, XG-PON1 inherits the framing and management from GPON [6]. XG-PON1 provides full-service operations via higher rate and larger split to support a PON network structure. The baseline XG-PON1 standards have been completed. In June 2010, the transmission convergence (TC) layer and optical network termination management and control interface (OMCI) standards for XGPON1 were consented in the general meeting of ITU-T SG15.

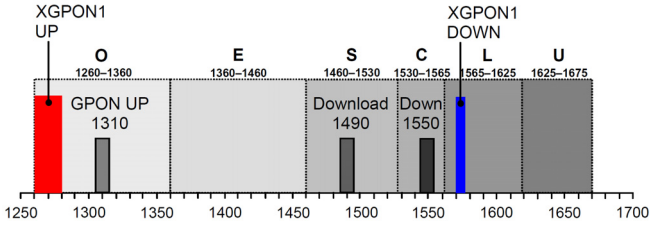


Figure 3. GPON and XG-PON wavelength allocation (video overlay band is supposed to be reused for WDM PON in the future).

 ISBN: 978-1-61208-205-9 

Since the downstream window is only 5 nm wide, it will require cooled laser sources and thus should be quite expensive [7]. It is conceivable that this downstream band could be extended beyond 1580 nm for systems that operate on more modern Optical Distribution Network (ODN) infrastructures, and this could enable optical line termination (OLT) optics suitable for outdoor deployment or uncooled operation in an indoor deployment. Such extension must be small, otherwise it will complicate ONU filter design. The upstream wavelength is 1270 nm and window is 20 nm wide, enabling the use of uncooled laser sources under all circumstances, saving on ONU optics costs.

### C. XG-PON2

The FSAN/ITU-T community has still not achieved a consensus concerning the direction for XG-PON2 development. Some experts see a natural progression from G-PON to XG-PON1 and to XG-PON2 with minimal changes in the framing, TC, and management protocols. Others see the 10 Gbit/s upstream as a point for transition to the 10G-EPON standard. This is a subject of ongoing study.

The obvious solution is to retain the 10 Gbit/s downstream paths as implemented in XG-PON1 and to extend the framing structures for the TC layer specified in the XG-PON1 section to support 10 Gbit/s upstream. This would allow for XG-PON1, XG-PON2 and G-PON co-existence on the same PON and would allow the reuse of all of the basic data structures. However, this solution suffers from grave shortcomings. Firstly, it is not clear if fragmentation should be supported in the upstream at these rates and what impacts that would have on the DBA algorithm could be proposed for NG-PON1 systems. In addition, separate ranging windows may be required for XG-PON1 and XG-PON2 to allow the dual rate receiver at the OLT to prepare for the reception of a specific burst at the correct bit rate.

If XG-PON2 follows the 10G-EPON system in some fashion, we then must address the notable gaps in this standard. The XG-PON2 work in the ITU would attempt to fill them. These uncovered topics include: activation, security, protection switching, dynamic bandwidth allocation, and management.

### D. Ethernet PON

EPON standards are being developed in the Institute of Electrical and Electronics Engineers (IEEE) 802.3ah Task Force [8]. The Ethernet in the first mile (EFM) task force of the IEEE 802.3 standards committee published standards that included a passive optical network (PON) variant in 2004. The protocol used in EPON is an extension of IEEE 802.3 and operates at 1 Gbit/s with a reach of 10 or 20 km between the central office and the customer. The architecture is a single shared fiber with an optical splitter. The supported split ratio is 16 users per PON. The system operates in the 1480 nm to 1500 nm band in the downstream direction, and in the 1260 nm to 1360 nm band in the upstream direction. As with 1 Gbit/s EFM Fiber, while not specifically mentioning the wavelength for broadcast video service, EPON allocates its wavelengths to leave the 1550 nm to 1560 nm band open and is capable of supporting a broadcast video wavelength in that band.

Since Ethernet does not utilize a P2MP topology, EPON required the development of a control protocol to make the P2MP topology appear as a P2P topology. This protocol is called the multipoint control protocol (MPCP). Like all PONs, in the downstream direction EPON is a broadcast protocol. Every ONT receives all packets, extracts the Ethernet frames intended for that customer, and discards the rest. As with APON and GPON, transmission in the upstream direction is regulated by TDMA.

### E. 10G-EPON

The 10 Gbit/s Ethernet Passive Optical Network standard (10G-EPON) supports two configurations: symmetric, operating at 10 Gbit/s data rate in both directions, and asymmetric, operating at 10 Gbit/s in the downstream (provider to customer) direction and 1 Gbit/s in the upstream direction. It was approved as IEEE 802.3av standard in 2009 [8].

The main driver for 10/10G-EPON symmetric configuration was to provide proper downstream and upstream bandwidth to support multi-family residential building (known in the standard as Multi Dwelling Unit (MDU)) customers. When deployed in the MDU configuration, one EPON ONU may be connected to up to a thousand subscribers.

The 10/10G-EPON employs a number of functions that are common to other P2P Ethernet standards. For example, such functions as 64B/66B line coding, self-synchronizing scrambler or gearbox are also used in optical fiber types of 10 Gigabit Ethernet links.

## III. OVERVIEW ON TECHNOLOGY DEVELOPMENT

PONs seems to be the most attractive solutions for optical access technologies. All signals are distributed through the optical network from the optical line terminal (OLT) to every end user's optical network termination unit (ONT), which are connected on the same PON branch.

The next-generation (NG) PON should satisfy demands for increasing traffic and higher bandwidths. All future strategies for NG-PON evolution are expected to deploy wavelength division multiplexing (WDM). .

Generally, NG-PON technologies are used to subdivide into two categories [9]:

- Evolutionary growth (the so-called NG-PON1). They are supposed to provide improved performance, such as higher data rates, with legacy optical distribution networks and co-exist with legacy PONs.
- Revolutionary change (NG-PON2). Such as WDM-PON, optical code division multiplexing (OCDM), etc., they are supposed to provide enhanced services on new distribution networks.

Current GPONs systems are intended to migrate to NG-PON1 applying identical colorless ONTs. The migration would occur in the same optical distribution network which implies coexistence. The advantage appears in cost saving, easier planning, maintaining and expanding of this network. Here, we mainly focus on evolutionary NG-PON

 ISBN: 978-1-61208-205-9 

technologies, XG-PON1 and XG-PON2, that are expected to replace current GPON and EPON solutions in the near- to midterm.

### A. Deployment Scenarios of XG-PON

A general requirement of NG-PON1 is to provide higher data transmission rates than GPON. On the other hand, it should be done with minimized costs. Thus operators expect NG-PON1 to leverage existing optical deployments. Hence, FSAN/ITU-T specified the NG-PON1 backward compatibility with legacy GPON deployments to protect the initial GPON investments of operators [7][10][11]. The specified NG-PON1 system is called XG-PON1. In an XG-PON1 system, the upstream rate is 2.5 Gbit/s and the downstream rate is 10 Gbit/s (asymmetric line-rate upgrade). In other words the downstream bandwidth of XG-PON1 is four times of that of GPON, while the upstream bandwidth of XG-PON1 is only twice as that of GPON. Since we have a very important result as the ODN in XG-PON1 entirely inherits that of GPON, implying that optical fibers and splitters in legacy GPON systems can be reused in XG-PON1. XG-PON1 also inherits the P2MP architecture of GPON. As indicated in XG-PON1 physical layer specifications, the upstream/downstream wavelength of XG-PON1 is different from that of GPON. Compatibility between XG-PON1 and GPON is achieved by implementing WDM splitter in the downstream at the central office (CO) and a Wavelength Blocking Filter (WBF) at the user side (could be located inside an ONU, between an ONU and an optical splitter, or on an optical splitter) to multiplex or demultiplex wavelengths on multiple signals in downstream and upstream directions. FSAN/ITU-T has proposed two evolution XG-PON1 deployment scenarios to greenfield and brownfield depending on the network maturity:

- Greenfield scenarios can use XG-PON1 to replace legacy copper line systems since they do not have any pre-existing optical fiber deployments. Greenfield scenarios require the deployment of new PON systems, which are straight-forward.
- Brownfield scenarios use coexistence of XG-PON1 with the pre-existing GPON deployments. When migrating to XG-PON1 operators can upgrade ONUs over the ODN batch by batch or all at once. The selection between these two types of upgrades is decided by how long GPON and XG-PON1 will coexist in the same ODN. To achieve a successful GPON-to-XG-PON1 upgrade, the OLT and each ONU must support [ITU-T G.984.5 AMD 1] compliant wavelength plans.

### B. Coexistence of GPON and XG-PON

FSAN/ITU-T standards are intended to provide the coexistence of GPON and XG-PON and define reserved wavelength plans. The wavelength allocation meets this standard and synergies with IEEE standardization [12].

The wavelength band allocations for GPON are: 1260 nm to 1360 nm for upstream and 1480 nm to 1500 nm for downstream. The neighboring bands are referred to as guard bands separating basic and enhancement bands and preventing interference. G.984.5 standard recommends pre-installing commercially available low-cost WBFs in GPON ONTs to obtain the required isolation outside the guard bands and to decrease the migration costs. In Figure 4, we propose the coexistence of GPON and XG-PON by implementing two super-separating WBFs in the GPON ONTs. WBFs of steep spectral characteristics should be able to separate the allocated passbands to avoid the interference and moreover to narrow the guard bands. An ideal band-pass has a completely flat passband and thus completely rejects all wavelengths outside the widths of the passband.

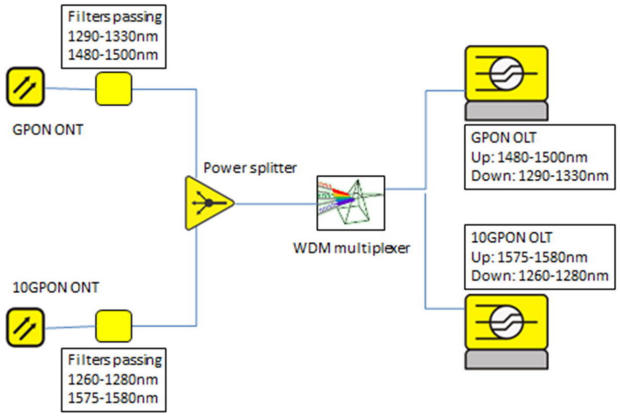


Figure 4. Coexistence of GPON and XG-PON using original ONTs supplemented by WBFs.

Accordingly, the FSAN/ITU-T requirements for the performance of the optical band super-separation filters are:

- at least 32 dB (according to 984.2) insertion loss outside the required passband width and maximum 5 dB insertion loss within the required pass band width of 1290 nm to 1330 nm for WBF upstream and 1480 nm to 1500 nm for WBF downstream,
- guarantee of the filter contrast factor (dB/nm) as high as possible (qualitatively) achieved by steep transmission curves in the vicinity of cut-on/cut-off wavelengths of 1290 nm / 1330 nm and 1480 nm / 1500 nm,
- minimizing severity of production by designing both band-pass WBFs as combinations of short-pass and a long-pass filters in series to achieve the required passbands and to minimize production costs.

## IV. NEW DEVICES FOR XG-PON DEPLOYMENTS

The evolutionary growth under NG-PON1 is based on the demand of the minimal equipment investments. Thus NG-PON1 should operate with the same infrastructure as GPON. However, current GPON and NG-PON1 coexistence requires wavelength separation of signals to avoid interferences between downstream and upstream channels. Low-cost WBF seems to be able to provide the wavelength band separation to ensure that GPON ONTs can operate undisturbed alongside NG-PON1 deployments. Passive filters based on thin film filter (TFF) technology seems to be the most suitable to use in the NG-PON system configuration with wavelength blocking filters [12].

When deploying XG-PON systems some devices needed to be replaced as shown on Figure 5.

 ISBN: 978-1-61208-205-9

Regarding the comparison of application of WDM filters and tunable lasers for NG-PONs deployment one can suppose that in relatively short-term period the usage of WDM filters seems to be more promising because of smaller costs and more developed technological basis. On the other hand, tunable lasers for NG-PONs are still developing meeting few problems on the temperature control and higher costs. With the lack of a cooling requirement and the electrical power requirements that accompanied by CWDM filters usage, the installation of DFBs-based devices is made possible for outdoor pedestal and strand mount as well as homes [13]. On the other hand, the usage of DWDM filters meets the same problems with high costs on temperature control systems as a configuration with tunable lasers [14].

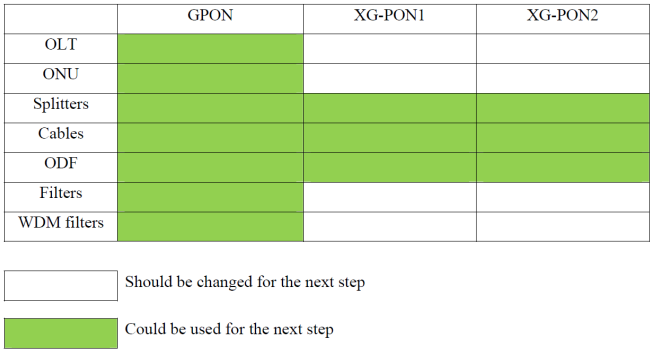


Figure 5. GPON, XG-PON1 and XG-PON2 backward compatibility.

We also consider different technologies and a number of solutions for the realization of integrated wavelength selective devices for WDM communication systems. Silicon nanowire based technology is a good example of this. This is an attractive way towards highly integrated systems with the capacity for wafer scale mass production compatible with microelectronics. The parameters of the fabricated devices are in many cases not sufficient for practical applications, but the technological improvements are still possible that should allow matching the market demands.

### *A. WDM multiplexer*

WDM multiplexer is the optical device, which is required at the central office (CO) under XG-PON deployment [15]. This device combines the GPON, XG-PON, and RF video downstream wavelengths for transmission over a common fiber between the WDM multiplexer and the splitter at the fiber distribution hub. In the upstream direction, the RF video, GPON and XG-PON upstream wavelengths are combined over a common fiber at the splitter hub and de-multiplexed at the WDM multiplexer for transmission to the RF translator, GPON and XG-PON OLT respectively.

WDM multiplexers are specified in ITU-T G.984.5. They allow signals from different wavelength channels to be multiplexed into one optical fiber, transmitted together and demultiplexed.

There are several kinds of WDM multiplexer components, which are available nowadays. The first class of such elements based on TFF or fiber Bragg gratings consists usually of discrete components for each wavelength. The second class is Planar Light wave Circuits (PLCs) also called Photonic Integrated Circuits (PICs) represented mainly by arrayed waveguide gratings (AWGs), but including also more seldom used etched diffraction grating-based multiplexers (EDGs). This is the class that can manage large numbers of channels and treat them in a parallel way and could be considered from aspect of the XG-PON2 deployment long-term prospects. This class can also be integrated with other passive and active components on a common platform.

During the last decade, PLC-based components have greatly improved core network solutions and capacity and are expected to have similar influence on NG access networks. Photonic integration based on silicon platform is now under a very intensive development and due to its compatibility to standard CMOS electronics promises low cost mass production allowing for deployment of FTTx infrastructures more cost effectively than ever before.

### *B. Wavelength Blocking Filter design*

As it was already discussed the TFF are suitable low-cost, ONT independent and simple operation candidates for WBFs [12]. TFF is usually made of a sequence of non-absorbing thin films of the thickness that is comparable to the wavelength of light and of materials of high and low refractive index. They should have optical characteristics resistant against temperature changes. The interference of light entering a multilayer structure of a specific number of alternating thin films causes the spectral dependent transfer characteristics of the filter (transmittance or reflectance of optical signal). The number of layers, layer materials, optical properties and thicknesses influence significantly TFF transmission characteristics. Therefore, the spectral transmittance or reflectance of a desired filter can be tailored for a specific application by the number and optical properties of layer used in the design.

## V. SUMMARY

In addition to the PON and BPON technologies developed by the ITU-T in the past, one can define three important stages in the technology development for the past and the next decades:

- 1 Gbit/s PON era. EPON and GPON concepts proposed in the beginning of 2000s by the IEEE and FSAN/ITU correspondingly were successfully adopted and already emerged as market leaders.
- 10 Gbit/s PON era. The IEEE and FSAN/ITU-T began researching 10G PON technology in 2008 as it was considered to be the beginning of the 10 Gbit/s optical access era. The IEEE released the 10G EPON standard in September 2009. Soon after, the ITU-T launched an initiative to set 10G GPON inheriting the Optical Distribution Frames (ODF) of current GPON and the main standards for XG-PON1 were approved and published in mid-2010. Driven by the growing demand for bandwidth and increasing market competition and given a combination of industry maturity and cost, 10G

 ISBN: 978-1-61208-205-9 

PON technology is expected to be commercialized on a small scale in 2013 at the earliest.

- Post-10G PON era. This area is not covered by the leading standards developers and still exists as some concepts and prototypes. The IEEE and FSAN/ITU-T have explored the topic but has not yet arrived at any concrete conclusions, because of large costs and weak relevancy to the market demands. WDM and hybrid WDM/TDM-based technologies may represent the trend, but OFDM, OCDMA and coherent technologies are the likely candidates in the future PON area.

Deployment of new PONs should be optimized by choosing of the correct passive splitting arrangement to decrease the costs on the active infrastructure implementation. Generally, several considerations need to be taken into account when designing the network:

- optimal use of active equipment
- coexistence with current technologies and flexibility to be able to adapt it easily to a future customer distribution
- regulatory needs for unbundling the next-generation access (NGA) networks
- optimizing operational cost due to field interventions

These considerations will result in a number of design rules.

Co-existence of XG-PON1 with current GPON system seems to be the most reasonable to provide with WBFs filters based on TFF technology (on the ONTs side) accompanied by WDM filters to distinguish the signals from different OLTs (on the CO side). WDM systems seem to be the most natural way to interconnect RF CATV and the migrating networks [16]. Physical layer capability of XG-PONs is quite well-known [7][10][11] and could be used as a real guideline for the new networks deployment.

A multi-level splitting system can help to solve the problem of split ratio demands increase corresponding to XG-PON1 deployment. Moreover, XG-PON1 inherits the framing and management from GPON. This is a good advantage of the technology that helps to decrease the deployment costs. Other network elements should be in general changed, replaced, introduced or developed with new network deployment.

In the present paper, we also regarded such technologies as XG-PON2 and tunable lasers that are not considered as a short-term perspective, but also supposed to be an important part of the network deployment in the future. Tunable lasers seem to be a luxury at the moment because of great costs on cooling systems and technological base development. On the other hand, XG-PON2 still does not correspond to the market demands on the upstream channel speed ratio with its also great costs taking into account. Another interesting possibility to improve upstream speeds with less costs using Non-Return-to-Zero (NRZ) coding is still under consideration. This could deliver 5 Gbit/s for not much more cost than the current 2.5Gbit/s optics, and it would of course coexist with the 2.5Gbit/s system (and G-PON) [6].

## ACKNOWLEDGMENT

The work reported in this paper was supported by bilateral project of Slovenian Research Agency and Russian Federation under the title: “NG-PON2 based on WDM technology”. Project is Co-financed by Rostelecom and Iskratel.

## REFERENCES

[1] J. Nielsen, "Nielsen's Law of Internet Bandwidth". http://www.useit.com/alertbox/980405.html, Retrieved: April 2012.

[2] B. Batagelj, “Implementation concepts of an optical access network by point–to–point architecture,” Electrotechnical Review, Ljubljana, Slovenija, Phil., pp. 259–266, 2010.

[3] ITU-T Rec. G.984 series: “Gigabit-capable passive optical networks (G-PON)”.

[4] ITU-T Rec. G.987 series: “10-Gibabit-capable passive optical networks (XG-PON)”.

[5] ITU-T Rec. G.983 series: “Broadband optical access systems based on passive optical networks”.

[6] Frank J. Effenberger, “The XG-PON System: Cost Effective 10 Gb/S Access”, Journal of Lightwave Technology, Vol. 29, Issue 4, pp. 403-409, 2011.

[7] F. J. Effenberger, H. Mukai, J.-I. Kani, and M. Rasztovits-Wiech, “Next-generation PON part III—System specifications for XG-PON,” IEEE Commun. Mag., vol. 47, no. 11, pp. 58–64, Nov. 2009.

[8] K. Tanaka, A. Agata, and Y. Horiuchi, “IEEE 802.3av 10G-EPON Standardization and Its Research and Development Status”, IEEE/OSA Journal of Lightwave Technology, vol. 28, no. 4, pp. 651-661, 2010.

[9] M.D. Andrade, G. Kramer, L. Wosinska, Jiajia Chen, S. Sallent, and B. Mukherjee, “Evaluating strategies for evolution of passive optical networks”, IEEE Communications Magazine, vol. 49, pp. 176-184, 2011.

[10] J.-I. Kani, F. Bourgart, A. Cui, A. Rafel, M. Campbell, R. Davey, and S. Rodrigues, “Next-generation PON part I—Technology roadmap and general requirements,” IEEE Commun. Mag., vol. 47, no. 11, pp. 43–49, Nov. 2009.

[11] F. J. Effenberger, H. Mukai, S. Park, and T. Pfeiffer, “Next-generation PON part II—Candidate systems for next generation PON,” IEEE Commun. Mag., vol. 47, no. 11, pp. 50–57, Nov. 2009.

[12] J. Mullerova and D. Korcek, “Super-separation thin film filtering for coexistence-type colorless WDM-PON networks,” 13th International Conference on Transparent Optical Networks (ICTON), pp. 1-4, 26-30 June 2011.

[13] C. Bouchat, C. Dessauvages, F. Fredricx, C. Hardalov, R. Schoop, and P. Vetter, “WDM-upgrade PONs for FTTH and FTTBusiness” in Proc. Int Workshop Opt. Hybrid Access Netw., Florence, Italy, pp. 231-238, Jun. 2002.

[14] L. G. Kazovsky, N. Cheng, W.-T. Shaw, D. Gutierrez, and S.-W. Wong, “Broadband optical access networks”, John Wiley & Sons, Inc., Hoboken, New Jersey, 2011.

[15] L. Wosinski, N. Zhu, and Z. Wang, “Wavelength selective devices for WDM communication systems”, 2009 IEEE 3rd International Symposium on Advanced Networks and Telecommunication Systems (ANTS), pp. 1-3, New Delhi, 14-16 Dec. 2009.

[16] J. D. Farina, “Coarse Wavelength Division Multiplexing”, Chapter 9. “CWDM in CATV/HFC Networks”, pp. 269-283, CRC Press 2007.

 ISBN: 978-1-61208-205-9 